



Deposited via The University of Sheffield.

White Rose Research Online URL for this paper:

<https://eprints.whiterose.ac.uk/id/eprint/193041/>

Version: Published Version

Article:

Aad, G, Abbott, B, Abbott, DC et al. (2022) Search for type-III seesaw heavy leptons in leptonic final states in pp collisions at $\sqrt{s}=13$ TeV with the ATLAS detector. The European Physical Journal C, 82 (11). 988. ISSN: 1434-6044

<https://doi.org/10.1140/epjc/s10052-022-10785-0>

Reuse

This article is distributed under the terms of the Creative Commons Attribution (CC BY) licence. This licence allows you to distribute, remix, tweak, and build upon the work, even commercially, as long as you credit the authors for the original work. More information and the full terms of the licence here:

<https://creativecommons.org/licenses/>

Takedown

If you consider content in White Rose Research Online to be in breach of UK law, please notify us by emailing eprints@whiterose.ac.uk including the URL of the record and the reason for the withdrawal request.



Search for type-III seesaw heavy leptons in leptonic final states in pp collisions at $\sqrt{s} = 13$ TeV with the ATLAS detector

ATLAS Collaboration*

CERN, 1211 Geneva 23, Switzerland

Received: 7 February 2022 / Accepted: 5 September 2022
© CERN for the benefit of the ATLAS Collaboration 2022

Abstract A search for the pair production of heavy leptons as predicted by the type-III seesaw mechanism is presented. The search uses proton–proton collision data at a centre-of-mass energy of 13 TeV, corresponding to 139 fb^{-1} of integrated luminosity recorded by the ATLAS detector during Run 2 of the Large Hadron Collider. The analysis focuses on final states with three or four electrons or muons from the possible decays of new heavy leptons via intermediate electroweak bosons. No significant deviations above the Standard Model expectation are observed; upper and lower limits on the heavy lepton production cross-section and masses are derived respectively. These results are then combined for the first time with the ones already published by ATLAS using the channel with two leptons in the final state. The observed lower limit on the mass of the type-III seesaw heavy leptons combining two, three and four lepton channels together is 910 GeV at the 95% confidence level.

1 Introduction

Neutrino physics presents one of the biggest puzzles yet to be addressed in modern particle physics. The extremely small values of the neutrino masses compared to the masses of the other fermions appear unnatural in the Standard Model (SM) [1]. The seesaw mechanism [2–6] provides an elegant way to give a very small mass m_ν to each of the SM neutrinos by introducing a heavy Majorana neutrino with mass M . The spontaneously broken electroweak (EW) symmetry explains the neutrino mass as a Yukawa coupling. Three types of seesaw mechanisms have been proposed and their phenomenology can be tested at collider experiments. The type-III seesaw [7] introduces at least one extra fermionic $SU(2)_L$ triplet field coupled to EW gauge bosons. These heavy charged and neutral leptons can in principle be produced by EW processes at the Large Hadron Collider (LHC).

Type-III seesaw heavy-lepton searches have already been performed in various decay channels by both the ATLAS and CMS collaborations. In Run 1, ATLAS excluded heavy leptons with masses below 335 GeV [8] using final states containing two light leptons (electrons or muons) and two jets. This mass limit was then improved to 470 GeV, still using Run 1 data, by adding the three-lepton channel [9] as suggested in Ref. [10]. Using the full Run 2 data sample of proton–proton collisions at $\sqrt{s} = 13$ TeV, the CMS Collaboration has excluded heavy-lepton masses up to 880 GeV [11] by analysing three- and four-lepton final states, while ATLAS has excluded heavy-lepton masses up to 790 GeV [12] by using only the two-lepton-plus-jets final state. The analysis presented in this paper searches for a type-III seesaw heavy lepton in three- and four-lepton final states. For the first time, a combination with the two-lepton-plus-jets final state is performed, giving a significant improvement in the sensitivity of the analysis.

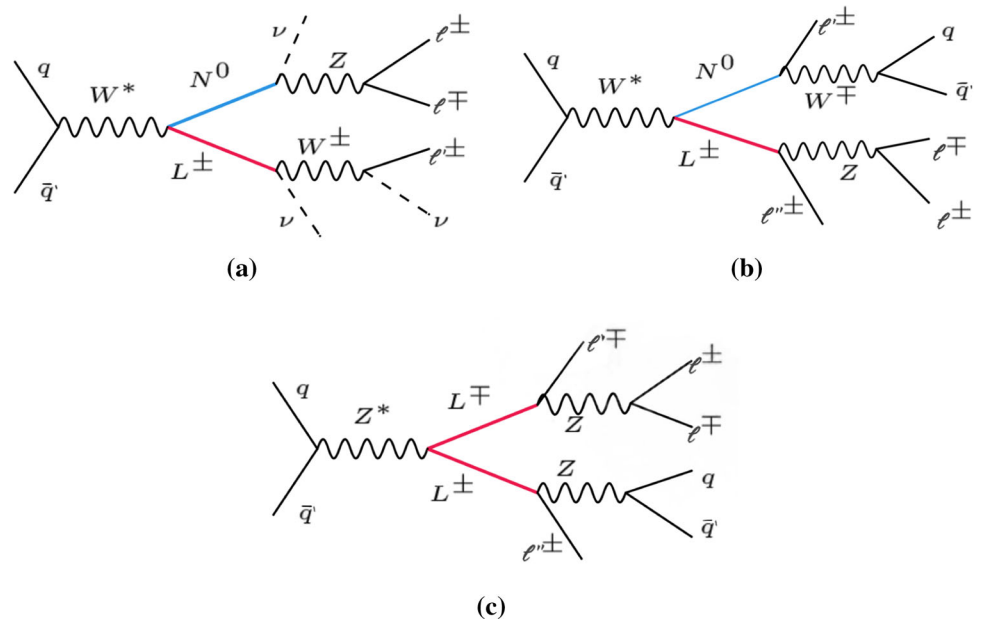
The type-III seesaw model targeted in this search is described in Ref. [13]. It assumes the pair production of the neutral Majorana (N^0) and charged (L^\pm) heavy leptons proceeds via the s -channel production of virtual EW

Contents

1	Introduction
2	ATLAS detector
3	Data and simulated events
4	Event reconstruction
5	Analysis strategy
5.1	Three-lepton channel
5.2	Four-lepton channel
6	Background composition and estimation
7	Systematic uncertainties
8	Statistical analysis and results
9	Conclusion
	References

* e-mail: atlas.publications@cern.ch

Fig. 1 Examples of Feynman diagrams for the considered type-III seesaw model [13] producing three- and four-lepton final states



gauge bosons. N^0 pairs are not produced because N^0 has $T_3 = Y = 0$ and thus does not couple to the Z [10,14]. The production cross-section depends only on the masses of the N^0 and L^\pm , which are assumed to be degenerate as the mass splitting due to electroweak radiative corrections is expected to be smaller than ~ 200 MeV [15]. The decays allowed in this model are $L^\pm \rightarrow H\ell^\pm, Z\ell^\pm, W^\pm\nu$ and $N^0 \rightarrow Z\nu, H\nu, W^\pm\ell^\mp$, where the SM leptons can be of any flavour, i.e. $\ell = e, \mu, \tau$. The branching ratios \mathcal{B}_ℓ for the heavy-lepton decays into ℓ plus one SM boson are determined by the parameters V_ℓ which govern mixing between the new heavy leptons and the SM leptons. Current bounds on V_ℓ can be found in Ref. [16]. In this analysis, we assume the *democratic* scenario, where the three mixing parameters are equal, so that $\mathcal{B}_e = \mathcal{B}_\mu = \mathcal{B}_\tau = 1/3$. The branching ratios $\mathcal{B}_Z, \mathcal{B}_W, \mathcal{B}_H$ for heavy-lepton decays into any SM lepton plus Z, W or H , namely $L^\pm, N^0 \rightarrow Z, W^\pm, H$, are independent of the mixing parameters. For N^0 masses larger than a few times the H mass, as considered in this analysis, the decays into different SM bosons are independent of the heavy-lepton mass, and therefore $2\mathcal{B}_H \simeq 2\mathcal{B}_Z \simeq \mathcal{B}_W \simeq 1/2$. Examples of Feynman diagrams in three- and four-lepton final states are shown in Fig. 1. These events are characterised by the production of two SM bosons (VV, VH or HH , where $V = W, Z$) and two charged leptons or neutrinos in the final state. The Majorana nature of N^0 allows final states with four leptons and non null total lepton electrical charge as shown in Fig. 1b. This analysis focuses on events with high light-lepton multiplicity, including light leptons from τ -lepton decays.

This paper is structured as follows. The ATLAS detector is described in Sect. 2, the data and simulated events used in the analysis are outlined in Sect. 3, and the event reconstruction

procedure is detailed in Sect. 4. The analysis strategy and background estimation are presented in Sects. 5 and 6, respectively. The systematic uncertainties are described in Sect. 7. Finally, results and their statistical interpretation are presented in Sect. 8, followed by the conclusions in Sect. 9.

2 ATLAS detector

The ATLAS detector [17] at the LHC is a multipurpose particle detector with a near- 4π coverage in solid angle around the collision point and a cylindrical geometry¹ coaxial with the beam axis. It consists of an inner tracking detector surrounded by a thin superconducting solenoid providing a 2 T magnetic field, electromagnetic and hadronic calorimeters, and a muon spectrometer with superconducting toroidal magnets.

The inner detector (ID) provides charged-particle tracking in the range $|\eta| < 2.5$ and, going outwards from the beam pipe, is composed of a high-granularity silicon pixel detector that typically provides four measurements per track, the first hit normally being in the insertable B-layer installed before Run 2 [18,19], a silicon microstrip tracker, and a transition radiation tracker that covers the region up to $|\eta| = 2.0$.

¹ ATLAS uses a right-handed coordinate system with its origin at the nominal interaction point (IP) in the centre of the detector and the z -axis along the beam pipe. The x -axis points from the IP to the centre of the LHC ring, and the y -axis points upwards. Polar coordinates (r, ϕ) are used in the transverse plane, ϕ being the azimuthal angle around the z -axis. The pseudorapidity is defined in terms of the polar angle θ as $\eta = -\ln \tan(\theta/2)$. Angular distance is measured in units of $\Delta R \equiv \sqrt{(\Delta\eta)^2 + (\Delta\phi)^2}$.

The calorimeter system covers the pseudorapidity range $|\eta| < 4.9$. Within the region $|\eta| < 3.2$, electromagnetic calorimetry is provided by barrel and endcap high-granularity lead/liquid-argon (LAr) calorimeters, with an additional thin LAr presampler covering $|\eta| < 1.8$ to correct for energy loss in material upstream of the calorimeters. Hadron calorimetry is provided by the steel/scintillator-tile calorimeter, segmented into three barrel structures within $|\eta| < 1.7$, and two copper/LAr hadron endcap calorimeters. The solid angle coverage is completed with forward copper/LAr and tungsten/LAr calorimeter modules optimised for electromagnetic and hadronic energy measurements respectively.

The muon spectrometer (MS) instruments the outer part of the detector and is composed of high-precision tracking chambers up to $|\eta| = 2.7$ and fast detectors for triggering up to $|\eta| = 2.4$. The MS is immersed in a magnetic field produced by three large superconducting air-core toroidal magnets with eight coils each.

A two-level trigger system is used to select events that are of interest for the ATLAS physics programme [20]. The first-level trigger is implemented in hardware and reduces the event rate to below 100 kHz. A software-based trigger further reduces this to a recorded event rate of approximately 1 kHz.

An extensive software suite [21] is used in the reconstruction and analysis of real and simulated data, in detector operations, and in the trigger and data acquisition systems of the experiment.

3 Data and simulated events

This analysis uses data collected in proton–proton collisions at $\sqrt{s} = 13$ TeV with proton bunches colliding every 25 ns. After requiring that all ATLAS subdetectors collected high-quality data and were operating normally [22], the total integrated luminosity amounts to 139 fb^{-1} . The uncertainty in the combined 2015–2018 integrated luminosity is 1.7% [23], obtained using the LUCID-2 detector [24] for the primary luminosity measurements. Events were collected using dilepton triggers selecting pairs of electrons [25] or muons [26]. The transverse momentum (p_T) threshold of the unscaled dilepton trigger was raised during the data taking, due to the increasing luminosity of the colliding beams, but was never higher than 24 GeV for the leading electrons and 22 GeV for the leading muons.

Signal and background events were modelled using different Monte Carlo (MC) generators as listed in Table 1. The response of the ATLAS detector was simulated [27] using the GEANT4 toolkit [28] and simulated events were reconstructed with the same algorithms as those applied to data [21]. The type-III seesaw signal model was implemented in the MADGRAPH5_AMC@NLO [29] generator at leading

order (LO) using FEYNRULES [30] and the NNPDF3.0LO [31] parton distribution function (PDF) set. All decays of L^\pm and N^0 into the different leptonic flavours and subsequent decays of the W , Z and H are considered. Matrix element (ME) events were interfaced to PYTHIA 8.230 [32] for parton showering with the A14 set of tuned parameters [33] and the NNPDF2.3LO PDF set [34]. The signal cross-section and its uncertainty at next-to-leading-order (NLO) plus next-to-leading-logarithm (NLL) accuracy were calculated from SU(2) triplet production in an electroweak chargino–neutralino model [35,36]. The calculated cross-sections are compatible within uncertainties with the type-III seesaw NLO implementation [37,38]. Production cross-section for a 600, 800 and 1000 GeV type-III seesaw heavy lepton are 29.6 ± 3.0 , 7.0 ± 0.8 and $1.97 \pm 0.25 \text{ fb}$ respectively.

Simulated SM background samples include diboson processes, which are the dominant ones, followed by processes labelled *rare top quark* that include multi-top-quark production and top-quark production in association with EW bosons ($t\bar{t}V$, $t\bar{t}H$, tWZ). Other SM simulated samples are triboson (VVV), $t\bar{t}$, single top, and Drell–Yan ($q\bar{q} \rightarrow Z/\gamma^* \rightarrow \ell^+\ell^-$ ($\ell = e, \mu, \tau$)) production processes. They are mainly used for the estimation of reducible backgrounds as described in Sect. 6. The MEPS@NLO prescription [39] was used in the generation of Drell–Yan processes to match the ME to the parton shower. The generators used in the MC sample production and the cross-section calculations used for MC sample normalisations are listed in Table 1. The normalisation of the dominant backgrounds, diboson and rare top-quark processes, are extracted from the final likelihood fit, as described in Sect. 8.

Diboson VV and triboson VVV events were simulated with the SHERPA 2.2.1–2 generator [44]. Off-shell effects and Higgs boson contributions were included. ME calculations were matched and merged with the SHERPA parton shower based on the Catani–Seymour dipole factorisation [45,46] using the MEPS@NLO prescription [39,47–49]. The OPEN-LOOPS library [50,51] provided QCD corrections. Diboson samples were produced with different lepton multiplicities using MEs at NLO accuracy in QCD for up to one additional parton and at LO accuracy for up to three additional parton emissions. Loop-induced $gg \rightarrow VV$ processes were generated with LO MEs for emission of up to one additional parton for both the fully leptonic and semileptonic final states. Electroweak production of a diboson pair in association with two jets ($VVjj$) was also simulated at LO. The PDFs used for the nominal samples were CT14 [52] and MMHT2014 [53].

Samples of events from $t\bar{t} + V$ (where V stands for γ^* , W , Z and H) and tWZ processes were produced using MADGRAPH5_AMC@NLO [29] at NLO accuracy and were interfaced to the PYTHIA 8.230 parton shower with NNPDF3.0NLO [31] PDFs. The h_{damp} parameter, which controls the matching between the ME and the parton shower,

Table 1 Configurations used for event generation of signal and most-relevant background processes. For the cross-section, the order in the strong coupling constant is shown for the perturbative calculation. If only one parton distribution function is shown, the same one is used for both the ME and parton shower generators; if two are shown, the first is used for the ME calculation and the second for the parton shower. Tune refers to the set of tuned underlying-event parameters used by the parton shower generator. The masses of the top quark and SM Higgs boson were set to 172.5 GeV and 125 GeV, respectively. The samples with negligible impact are mentioned in the table but not discussed in the text

Process	Generator	Cross-section	Parton shower	PDF set	Tune
Type-III seesaw					
$L^+ L^-, L^\pm N^0$	MADGRAPH5_AMC@NLO[29]	NLO+NLL	PYTHIA 8.230 [32]	NNPDF3.0nLO [31] NNPDF2.3LO [34]	A14 [33]
Top quark					
$t\bar{t}$	POWHEG BOX v2 [40–43]	NNLO	PYTHIA 8.230	NNPDF3.0NNLO [31] NNPDF3.0NLO [31]	A14
Single t	POWHEG BOX v2	NNLO	PYTHIA 8.230	NNPDF3.0NNLO NNPDF3.0NLO	A14
Rare top quark					
$3t, 4t$	MADGRAPH5_AMC@NLO	LO	PYTHIA 8.230	NNPDF3.0LO	A14
$t\bar{t} + W/Z/H, tWZ$	MADGRAPH5_AMC@NLO	NNLO	PYTHIA 8.230	NNPDF3.0NLO	A14
Diboson					
ZZ, WZ	SHERPA 2.2.1 [44] and 2.2.2	NLO	SHERPA	NNPDF3.0NNLO	SHERPA default
Triboson					
WWW, WWZ, WZZ, ZZZ	SHERPA 2.2.1 and 2.2.2	NNLO	SHERPA	NNPDF3.0NNLO	SHERPA default
Drell–Yan					
$Z/\gamma^* \rightarrow e^+e^-/\mu^+\mu^-/\tau^+\tau^-$	SHERPA 2.2.1	NLO	SHERPA	NNPDF3.0NNLO	SHERPA default

was set to $1.5m_{\text{top}}$ [54], using a top quark mass of $m_{\text{top}} = 172.5$ GeV.

All simulated events were overlaid with a simulation of multiple pp interactions occurring in the same or neighbouring bunch crossings. These pp inelastic scattering events were generated by PYTHIA 8.186 using the NNPDF2.3LO set of PDFs and the A3 set of tuned parameters [55]. Their effects are referred to as *pile-up*. The simulated events were reweighted such that the distribution of the average number of interactions per bunch crossing is compatible with that observed in the data.

4 Event reconstruction

Events considered in this analysis are required to have at least one collision vertex reconstructed with at least two tracks with transverse momentum greater than 500 MeV. The primary vertex of the hard-scattering event is the one with the largest sum of the associated tracks’ squared transverse momenta. Events have to satisfy the quality criteria listed in Ref. [22], including rejection of events with a large amount of calorimeter noise or non-collision background.

Electrons are reconstructed by matching a charged-particle track in the ID with an energy deposit in the electromagnetic calorimeter. Electron candidates are required to satisfy a *Loose* likelihood-based identification selection [56] and to be in the fiducial volume of the inner detector, $|\eta| < 2.47$. The transition region between the barrel and end-cap calorimeters ($1.37 < |\eta| < 1.52$) is excluded because it is partially non-instrumented due to services infrastructure. The transverse impact parameter d_0 of the track associated with the candidate electron must have a significance satisfying $|d_0|/\sigma(d_0) < 5$. This is required in order to reduce the number of electrons originating from secondary decays. Similarly, the track’s longitudinal impact parameter z_0 relative to the primary vertex must satisfy $|z_0 \sin(\theta)| < 0.5$ mm, where θ is the track’s polar angle. The electron’s transverse energy E_T must exceed 10 GeV. After this preselection, to refine the electron quality, a *Tight* likelihood-based identification selection and a set of *Loose* isolation criteria based on both calorimetric and tracking information are applied to primarily select electrons coming from the decays of the heavy leptons or the EW bosons.

Track segments in the MS are matched with ID tracks to reconstruct muons if they are within the η coverage of the ID. Muon candidates with p_T lower than 300 GeV are required to satisfy the *Medium* muon identification requirements, while for high- p_T muons, a specific identification working point is applied [57]. Muon candidates are required to have $|\eta| < 2.5$, a transverse impact parameter significance of $|d_0|/\sigma(d_0) < 3$ and a longitudinal impact parameter value of $|z_0 \sin(\theta)| < 0.5$ mm. The minimum muon p_T is 10 GeV.

After this preselection, an isolation requirement based only on tracking information is applied.

In this analysis, particle-flow objects [58] are formed from energy-deposit clusters in the calorimeters and tracks measured in the ID but not matched to identified leptons. Particle-flow objects are then clustered into jets using the anti- k_t algorithm [59] with a radius parameter $R = 0.4$. The measured jet p_T is corrected for detector effects to measure the particle energy before interactions with the detector material [60]. Energy within jets that is due to pile-up is estimated and removed by subtracting an amount equal to the mean pile-up energy deposition density multiplied by the η - ϕ area of the jet. Pile-up can also produce additional jets that are identified and rejected by the jet-vertex tagger (JVT) algorithm [61], which distinguishes them from jets originating from the hard-scattering primary vertex. Only jets with transverse energy greater than 20 GeV and $|\eta| < 2.4$ are considered. Jets originating from heavy-flavour quarks are identified with the MV2c10 multivariate b -tagging algorithm using the 77% efficiency working point [62–64], with measured rejection factors of approximately 134, 6 and 22 for light-quark and gluon jets, c -jets, and hadronically decaying τ -leptons, respectively.

The missing transverse momentum \vec{p}_T^{miss} (with magnitude E_T^{miss}) is calculated as the negative vectorial sum of the p_T of reconstructed jets and leptons in the event. A ‘soft term’ taking into account tracks associated with the primary vertex but not with any hard object is then added to guarantee the best performance in a high pile-up environment [65]. The E_T^{miss} significance $\mathcal{S}(E_T^{\text{miss}})$, calculated with a maximum-likelihood ratio method, is used in Sect. 5 to define the various analysis regions, taking into account the direction of the \vec{p}_T^{miss} and calibrated objects as well as their respective resolutions.

Different objects reconstructed close together in the η - ϕ plane could in principle have originated from the same primary object. Possible overlaps are resolved by an algorithm that appropriately removes one of the two closely spaced objects to avoid double-counting. If a muon candidate is found to share an ID track with an electron candidate, the electron candidate is rejected. If two electron candidates share an ID track, the one with the lower p_T is rejected. Jets are rejected if they are within $\Delta R = 0.2$ of a lepton candidate, except if the candidate is a muon and three or more collinear tracks are found. Finally, lepton candidates that are within $\Delta R = 0.4$ of any remaining jet are removed.

5 Analysis strategy

Once events have been classified according to the presence of exactly either three or four light leptons,² the two lepton-

² Leptons are ordered going from the highest to the lowest momentum, ℓ_1 to ℓ_3 (ℓ_4 for four-lepton events).

multiplicity categories are refined with dedicated selections. Events with larger lepton multiplicities can be categorized in lower lepton multiplicities regions if one or more leptons escape detection. Signal regions (SRs) are defined so as to maximise the significance of the signal event count predicted by the targeted model relative to the expected number of SM background events. SM backgrounds are normalised by performing a simultaneous fit in the SRs and in dedicated control regions (CRs). The CRs are defined so as to be enriched in relevant background processes and depleted in events from signal processes. The fit uses a kinematic variable chosen to optimise the sensitivity to the small cross-sections expected for the signal processes. Validation regions (VRs), also depleted in signal events, are used to validate the extrapolation of the SM background expectations obtained from the background-only fit to independent regions kinematically close to the SRs. All CRs and VRs are characterised by a signal contamination below 2%.

Backgrounds are assigned to two broad categories: reducible and irreducible backgrounds. Reducible backgrounds include leptons from misreconstructed objects such as jets, or from light- or heavy-quark decays or, in the electron case, photon conversions. These are called *fake or non-prompt* (FNP) leptons, and events containing at least one such lepton are referred to as the FNP background. Its contribution is calculated using a data-driven method. Irreducible backgrounds are produced by SM processes with three or four prompt leptons in the final state. Prompt leptons are leptons produced in the decays of W bosons, Z bosons, and τ -leptons, as well as direct decays of the heavy leptons considered as signal in this analysis. The most important sources are diboson and rare top-quark processes, with the latter being primarily $t\bar{t}$ pairs produced in association with an EW or Higgs boson. For these processes, kinematic distributions are obtained from MC simulation and their normalisation is extracted from the fit. Because low-mass heavy leptons have been excluded by previous searches, this search focuses on higher masses, where signal events are characterised by objects having high momenta.

Details about the three- and four-lepton analysis regions are provided below, while details of the two-lepton analysis regions are given in Ref. [12]. The analysis regions are all orthogonal to one another.

5.1 Three-lepton channel

Table 2 summarises the selection criteria used to define the three-lepton SRs, CRs and VRs. The ZL SR is characterised by a leptonically decaying Z boson, and thus an opposite-sign, same-flavour (OSSF) lepton pair compatible with the Z boson mass is required. The SM boson from the decay of the other heavy lepton produced in the event, decays hadronically. Signal events are expected to have a large three-lepton

Table 2 Summary of the selection criteria used to define relevant regions in the three-lepton analysis. No selection is applied when a dash is present in the corresponding cell

	ZL					ZLVeto	JNLow		
	Fake-VR	CR	DB-VR	RT-VR	SR	SR	VR	SR	
		$p_T(\ell_1) > 40 \text{ GeV}$ $p_T(\ell_2) > 40 \text{ GeV}$ $p_T(\ell_3) > 15 \text{ GeV}$							
$S(E_T^{\text{miss}})$	< 5	≥ 5							
$N(\text{jet})$	-	≥ 2					≤ 1		
$N(b\text{-jet})$	-	-	0	≥ 1	-	-	-	-	
$m_{\ell\ell}$ (OSSF) [GeV]	-	80–100					≥ 115	≥ 80	
$H_T + E_T^{\text{miss}}$ [GeV]	-	-	-	-	-	≥ 600	-	-	
$m_{\ell\ell\ell}$ [GeV]	-	-	≥ 300			≥ 300	-	-	
$H_T(\text{SS})$ [GeV]	-	-	-	-	-	≥ 300	-	-	
m_{jj} [GeV]	-	-	-	-	-	< 300	-	-	
$H_T(\ell\ell\ell)$ [GeV]	-	-	-	-	-	-	≥ 230		
$m_T(\ell_1)$ [GeV]	-	-	≥ 200			-	< 240	≥ 240	
$m_T(\ell_2)$ [GeV]	-	< 200	≥ 200			-	≥ 150		
$\Delta R(\ell_1, \ell_2)$	-	-	< 1.2		1.2–3.5	-	≥ 1.3		

invariant mass ($m_{\ell\ell\ell}$), and the transverse masses of the two highest- p_T leptons, $m_T(\ell_1)$ and $m_T(\ell_2)$, are also expected to be large.³ An additional requirement is placed on the angular distance between the leading and subleading leptons to further increase the signal-to-background ratio in the SRs.

A complementary ZLVeto SR, targeting signals involving leptonic decays of W bosons and hadronic decays of Z bosons (including those from H bosons), is defined by vetoing events containing OSSF lepton pairs compatible with a leptonic decay of an on-shell Z boson requiring the invariant mass of the pair to be larger than 115 GeV. The H_T variable is defined as the scalar sum of the p_T of all selected objects in the event. In cases where the scalar sum of the p_T is restricted to only a subset of the objects, they are specified. Signal events are characterised by large H_T and E_T^{miss} values and by a large value of the scalar sum of the momenta of the same-sign leptons, denoted by $H_T(\text{SS})$. Since the presence of SS leptons in this region is mainly due to rare top events and FNP leptons, the H_T of this pair is used as discriminating variable looking for values $H_T(\text{SS}) \geq 300$ GeV. To account for possible hadronic decays of electroweak bosons from diboson background sources, an upper limit is placed on the two leading jets invariant mass m_{jj} .

Finally, the JNLow SR targets events where the electroweak bosons decay leptonically, and therefore events with low jet multiplicity, as in Fig. 1a, are selected. A lower bound

is imposed on the invariant mass of the OSSF lepton pair ($m_{\ell\ell}(\text{OSSF})$)⁴ and a large value of the scalar sum of the p_T of the three leptons, $H_T(\ell\ell\ell)$, is required. Fake-lepton background is further reduced by requiring $m_T(\ell_1)$ and $m_T(\ell_2)$ to exceed a minimum value. The angular separation $\Delta R(\ell_1, \ell_2)$ between the two leptons is required to exceed a minimum value to reduce the FNP contribution. Overall selection efficiencies for the production of a 800 GeV type-III seesaw heavy lepton are 0.29%, 0.57%, 0.41% for the ZL, ZLVeto and JNLow SR respectively.

SM backgrounds in the three-lepton SRs consist of diboson events, which contribute $\sim 60\%$, $\sim 80\%$ and $\sim 40\%$ in the ZL, JNLow and ZLVeto regions, respectively. Another background in the ZL and ZLVeto regions originates from rare top-quark processes involving one or more top quarks, which contribute $\sim 40\%$ and $\sim 50\%$ of the background in those regions, respectively. Therefore, a CR targeting the normalisation of the diboson background is defined by requiring at least two jets and a low transverse mass for the subleading lepton such that $m_T(\ell_2) \leq 200$ GeV.

Two VRs are defined in order to validate background estimates for events containing a Z boson decaying into leptons, both obtained by inverting the $\Delta R(\ell_1, \ell_2)$ selection of the ZL SR, and applying additional requirements. The DB-VR also requires a b -tag veto, while in the RT-VR the presence of at least one b -tagged jet is required. These VRs validate the

³ The generic transverse mass of one or multiple objects N_{obj} is defined as: $m_T^2(N_{\text{obj}}) = \left(\sum_i^{N_{\text{obj}}} E_{T,i} + E_T^{\text{miss}}\right)^2 - \left|\sum_i^{N_{\text{obj}}} \vec{p}_{T,i} + \vec{p}_T^{\text{miss}}\right|^2$.

⁴ If two OSSF lepton pairs are present, the requirement is applied to both pairs.

Table 3 Summary of the selection criteria used to define relevant regions in the four-lepton analysis. N_Z is the number of leptonically reconstructed Z bosons, using opposite-sign same-flavour leptons. No selection is applied when a dash is in the corresponding cell

	Q0					Q2	
	DB-CR	RT-CR	DB-VR	RT-VR	SR	VR	SR
	$p_T(\ell_{1,2}) > 40 \text{ GeV}$ $p_T(\ell_3) > 15 \text{ GeV}$ $p_T(\ell_4) > 10 \text{ GeV}$						
$ \sum q_\ell $	0					2	
$N(b\text{-jet})$	0	≥ 2	1	1	0	-	-
$m_{\ell\ell\ell\ell}$ [GeV]	170–300	< 500	170–300	300–500	≥ 300	< 200 OR < 300	≥ 300
$H_T + E_T^{\text{miss}}$ [GeV]	-	-	-	≥ 400	≥ 300	< 300	≥ 300
N_Z	-	-	-	-	≤ 1	-	-
$S(E_T^{\text{miss}})$	-	-	-	≥ 5	≥ 5	-	-

predictions and normalisation of diboson and rare top-quark processes respectively. An additional JNLow-VR is obtained from the JNLow SR by inverting the transverse mass requirement on the leading lepton, $m_T(\ell_1) \leq 240 \text{ GeV}$. Moreover, a Fake-VR is defined by inverting the $S(E_T^{\text{miss}})$ selection common to all the other regions without applying any additional requirement except for lepton p_T ones. This region is enriched in contributions from FNP backgrounds and is therefore used to validate them.

In the three-lepton channel SRs, the kinematic variable used as the final discriminant to the data is the transverse mass of the three-lepton system.

5.2 Four-lepton channel

In the four-lepton channel, the momentum requirement on the three leading leptons is the same as in the three-lepton channel; the momentum of the fourth lepton is required to be larger than 10 GeV. Events are classified using the sum of the charges of the four leptons in the final state: $\sum q_\ell$. The conditions $\sum q_\ell = 0$ and $|\sum q_\ell| = 2$ identify the *zero charge* (Q0) and *double charge* (Q2) regions, respectively. A summary of the selection criteria defining the four-lepton regions is shown in Table 3. Signal events are characterised by large H_T and large invariant mass $m_{\ell\ell\ell\ell}$ of the four-lepton system. The presence of possible neutrinos in the final state is taken into account using the $H_T + E_T^{\text{miss}}$ variable; therefore $m_{\ell\ell\ell\ell} \geq 300 \text{ GeV}$ and $H_T + E_T^{\text{miss}} \geq 300 \text{ GeV}$ are required in both the Q0 and Q2 signal regions. Apart from the common lepton p_T requirements, these are the only kinematic selections applied in the Q2 SR, which has less background than the Q0 SR since it is very rare for a SM process to produce a doubly charged final state. To reduce the ZZ^* contribution in the Q0 SR, no more than one OSSF lepton pair in an event is allowed to be compatible with a leptonic Z decay defined by

the invariant mass window 80–100 GeV. Background in the Q0 SR is further reduced by requiring $S(E_T^{\text{miss}}) \geq 5$. Overall selection efficiencies for the production of a 800 GeV type-III seesaw heavy lepton are 0.14% and 0.11% for the Q0 and Q2 SR respectively.

Two CRs and two VRs are defined in the zero-charge Q0 kinematic space. A DB-CR targeting diboson backgrounds is built by requiring a b -jet veto and defining an invariant mass window for the four-lepton system ($170 \text{ GeV} \leq m_{\ell\ell\ell\ell} < 300 \text{ GeV}$). A RT-CR targeting rare top-quark background is obtained by requiring at least two b -tagged jets and $m_{\ell\ell\ell\ell} < 500 \text{ GeV}$. To ensure orthogonality to the CRs, the VRs require events to have exactly one b -jet. To increase the contributions of diboson and rare top-quark backgrounds in the VRs, $m_{\ell\ell\ell\ell}$ must satisfy $170 \text{ GeV} \leq m_{\ell\ell\ell\ell} < 300 \text{ GeV}$ in DB-VR and $300 \text{ GeV} \leq m_{\ell\ell\ell\ell} < 500 \text{ GeV}$ in RT-VR. The RT-VR also requires $H_T + E_T^{\text{miss}} \geq 400 \text{ GeV}$ and $S(E_T^{\text{miss}}) \geq 5$.

The main sources of background in the Q2 signal region are diboson or rare top-quark events where the electric charge of one of the electrons is mismeasured. As mentioned above, the only additional kinematic selections used to define the Q2 SR are that both $H_T + E_T^{\text{miss}}$ and the four-lepton invariant mass must exceed 300 GeV. A dedicated Q2 VR is obtained by requiring $m_{\ell\ell\ell\ell} < 200 \text{ GeV}$ or $H_T + E_T^{\text{miss}} < 300 \text{ GeV}$ in order to validate both the diboson and FNP background estimates.

In the four-lepton channel SRs, the kinematic variable $H_T + E_T^{\text{miss}}$ is used as the final discriminant to fit to the data.

6 Background composition and estimation

The background estimation techniques used in the analysis, combining simulations and data-driven methods common to all channels, are discussed in this section.

Irreducible-background predictions are obtained directly from simulations, but normalisation of diboson and rare top-quark processes is obtained from the fit. To avoid double-counting between background estimates derived from MC simulation and the data-driven reducible-background predictions, a specific check is performed: events from irreducible-background MC samples are considered only if generator-level prompt leptons can be matched to their reconstructed counterparts.

There are two sources of reducible background: events in which at least one lepton charge is misidentified and FNP leptons. The former source is relevant only in the Q2 four-lepton signal region where an event in the Q0 category can migrate to the Q2 category if the charge of one of the leptons is mismeasured.

Charge misidentification for muons is well described by the simulation and occurs only for high-momentum muons where detector misalignments degrade the muon momentum resolution. However, electrons are more susceptible to charge misidentification, as a combination of effects from bremsstrahlung and photon conversions that might not be adequately described by the detector simulation. Correction factors (scale factors) accounting for charge misreconstruction are applied to the simulated background events. They are derived by comparing the charge misidentification probability measured in data with the one in simulations and are parameterised as function of p_T and η . The charge misidentification probability is extracted by performing a likelihood fit in a dedicated $Z \rightarrow ee$ data sample, as described in Ref. [56]. The charge misidentification probability increases from $\sim 10^{-4}$ to $\sim 10^{-1}$ with increasing p_T and $|\eta|$.

FNP leptons are produced by secondary decays of light- or heavy-flavour mesons into light leptons embedded within jets. Although the b -jet veto and lepton isolation significantly reduce the number of FNP leptons, a fraction still satisfy the selection requirements. Significant components of FNP electrons arise from photon conversions and from jets that are wrongly reconstructed as electrons. MC samples are not used to estimate these background sources because the simulation of jet production and hadronisation has large intrinsic uncertainties.

Instead, the FNP background is estimated with a data-driven approach, known as the *fake factor* (FF) method, as described in Ref. [66]. The FF is measured in dedicated FNP-enriched regions where the events satisfy single-lepton triggers without isolation requirements and have low E_T^{miss} , no b -jets, and only one reconstructed lepton that satisfies the lepton identification preselection described in Sect. 5. In these

regions, two kinds of leptons are identified, \mathcal{L} leptons satisfy looser object selection criteria than the ones used to identify the leptons considered in the analysis regions, which are here named \mathcal{T} leptons. Electron and muon FFs are then defined as the ratio of the number of \mathcal{T} leptons to the number of \mathcal{L} leptons, and are parameterised as functions of p_T and η . The FNP background is then estimated in the SRs by applying the FF as an event weight in a template region defined with the same selection criteria as the corresponding SRs, except that at least one of the leptons must be an \mathcal{L} lepton but not a \mathcal{T} one.

The prompt-lepton contribution is subtracted from the template region by using the irreducible-background MC samples to estimate the prompt-lepton contamination in the adjacent regions [56]. The Fake-VR, as defined in Table 2, is used to validate the data-driven FNP-lepton estimate.

7 Systematic uncertainties

Uncertainties affect several aspects of this analysis. Experimental uncertainties related to the trigger selection, lepton reconstruction, identification, momentum measurement and isolation selection affect both the global selection efficiency and the shape of the kinematic distributions used in the fit. The main contributions come from the electron selection efficiency and the sagitta resolution of the muon spectrometer. Uncertainties are estimated mainly from $Z \rightarrow \ell\ell$ and $J/\psi \rightarrow \ell\ell$ processes [56, 57]. Uncertainties in the jet energy scale and resolution are evaluated from MC simulations and data, using multi-jet, Z +jets and γ +jets events [67]; they are estimated to be less than 2% in the range of jet transverse momentum of interest and affect both the selection efficiency measurement and the kinematic distributions used in the fit. Uncertainties in the b -tagging efficiencies are evaluated from data using dileptonic $t\bar{t}$ events [68]. They are estimated to range from 8% at low momentum to 1% at high momentum. These uncertainties affect the analysis region selection efficiencies. The E_T^{miss} measurement uncertainties are estimated from data-to-MC comparison in $Z \rightarrow \mu\mu$ events without jets as described in Ref. [69]. The E_T^{miss} uncertainties affect both the selection efficiencies and the kinematic distributions used in the fit. The charge misidentification uncertainty affects only the Q2 analysis regions. The uncertainty in the charge-misidentification scale factor is estimated to be less than 10% from a comparison between same-sign dielectron data and MC events, with the same electron selection as used in this analysis, and with $|m_{ee} - m_Z| < 10$ GeV as described in Ref. [56]. The uncertainty in the pile-up simulation, derived from a comparison of data with simulation, is also taken into account [70]. The limited size of the MC samples is taken into account as an additional uncertainty.

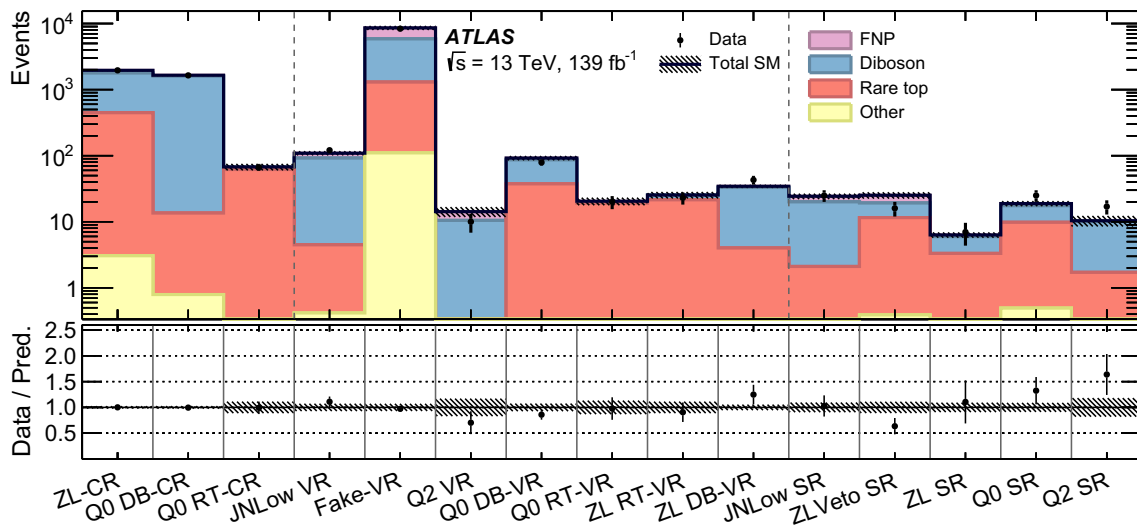


Fig. 2 Observed and expected event yields in the CRs, VRs and SRs for the three- and four-lepton channels after the fit procedure described in the text. *Diboson* indicates background from diboson processes. *Rare top* indicates background from $t\bar{t} + V$ and $t\bar{t}WZ$ processes. *FNP* includes the background from fake or non-prompt leptons. *Other* indicates all the

other considered backgrounds that contribute less than 2%. The hatched bands include systematic uncertainties with the correlations between various background sources taken into account. The lower panel shows the ratio of the observed data to the predicted SM background after the likelihood fit

The FNP background uncertainty comes from the modelling and normalisation of the prompt leptons subtracted in the FF estimation. The origin of the FNP background is then varied by selecting slightly modified FNP-enriched regions, where the FF is measured. Variations of the FNP-enriched regions are, for example, obtained by varying the jet multiplicity requirement and the E_T^{miss} selection. The resulting uncertainty of the FF depends on the lepton momentum and pseudorapidity and ranges from 5 to 40% for electrons and from 10 to 30% for muons.

Theoretical uncertainties affect both the signal and background predictions. For both, the uncertainties from missing higher orders are evaluated by independently varying the QCD factorisation and renormalisation scales in the matrix element by up to a factor of two [71]. The PDF uncertainties are evaluated using the LHAPDF toolkit [72] and the PDF4LHC prescription [73]. An additional uncertainty of 10% is added to the diboson cross-section to take into account variations in the level of data-to-MC agreement for VV processes in different jet multiplicity regions. For rare top-quark backgrounds, uncertainties in the $t\bar{t}W$ cross-section are evaluated to be $\pm 50\%$, while for the $t\bar{t}H$ cross-section the uncertainty from varying the QCD factorisation and renormalisation scales is $^{+5.8}_{-9.2}\%$, with another $\pm 3.6\%$ from PDF+ α_s variations. Since the yields of the rare top-quark and diboson backgrounds are derived from the likelihood fit to the data in the CRs, the systematic variations have little impact on the final yields of the background predictions in the CR and SR.

8 Statistical analysis and results

The HISTFITTER [74] statistical package is used to fit the predictions to the data in the CRs and SRs. The fit considers the $m_{T,3\ell}$ and $H_T + E_T^{\text{miss}}$ distributions for the three- and four-lepton channels, respectively, calculating lower limits on the heavy-lepton mass with a test statistic based on the binned profile likelihood in the asymptotic approximation [75], whose validity is tested using a pseudo-experiment approach. The lower limits on the mass are calculated at 95% confidence level (CL) and the binning is chosen to optimise the sensitivity to signal. The various components of the background predictions are validated in the corresponding VRs. Background and signal contributions are modelled by a product of independent Poisson probability density functions representing the likelihood of the fit. Systematic uncertainties are modelled by Gaussian probability density functions centred on the pre-fit prediction of the nuisance parameters, with widths that correspond to the magnitudes of these uncertainties. Four different fitting procedures are performed: the three-lepton channel on its own, the four-lepton channel on its own, the three- and four-lepton channels combined, and finally the two-, three- and four-lepton channels combined, where results for the two-lepton channel are taken from Ref. [12]. All the contributions from the experimental uncertainties in the lepton, jet and E_T^{miss} selections and reconstruction, pile-up simulation, background simulation, theoretical calculations and irreducible-background estimates are considered correlated among the different multiplicity channels in multi-channel fits.

Table 4 Observed data and background yields in the three- and four-lepton signal regions after the background-only fit in the combined three- and four-lepton regions; the combination of statistical and systematic uncertainties have been reported

	Three-lepton signal regions			Four-lepton signal regions	
	ZL SR	ZLVeto SR	JNLow SR	Q0 SR	Q2 SR
Data	7	16	25	25	17
Total background	6.25 ± 0.52	25.2 ± 2.8	24.4 ± 2.3	19.0 ± 1.6	10.3 ± 1.9
Diboson	2.62 ± 0.27	7.64 ± 0.95	18.0 ± 2.1	7.70 ± 0.78	8.5 ± 1.6
Rare top	3.2 ± 0.5	11.2 ± 1.7	1.82 ± 0.32	9.4 ± 1.4	1.63 ± 0.35
Fakes	0.29 ± 0.05	5.98 ± 0.85	4.3 ± 0.5	1.37 ± 0.36	0.07 ± 0.37
Other	0.113 ± 0.015	0.36 ± 0.12	0.33 ± 0.03	0.49 ± 0.04	0.1001 ± 0.0098

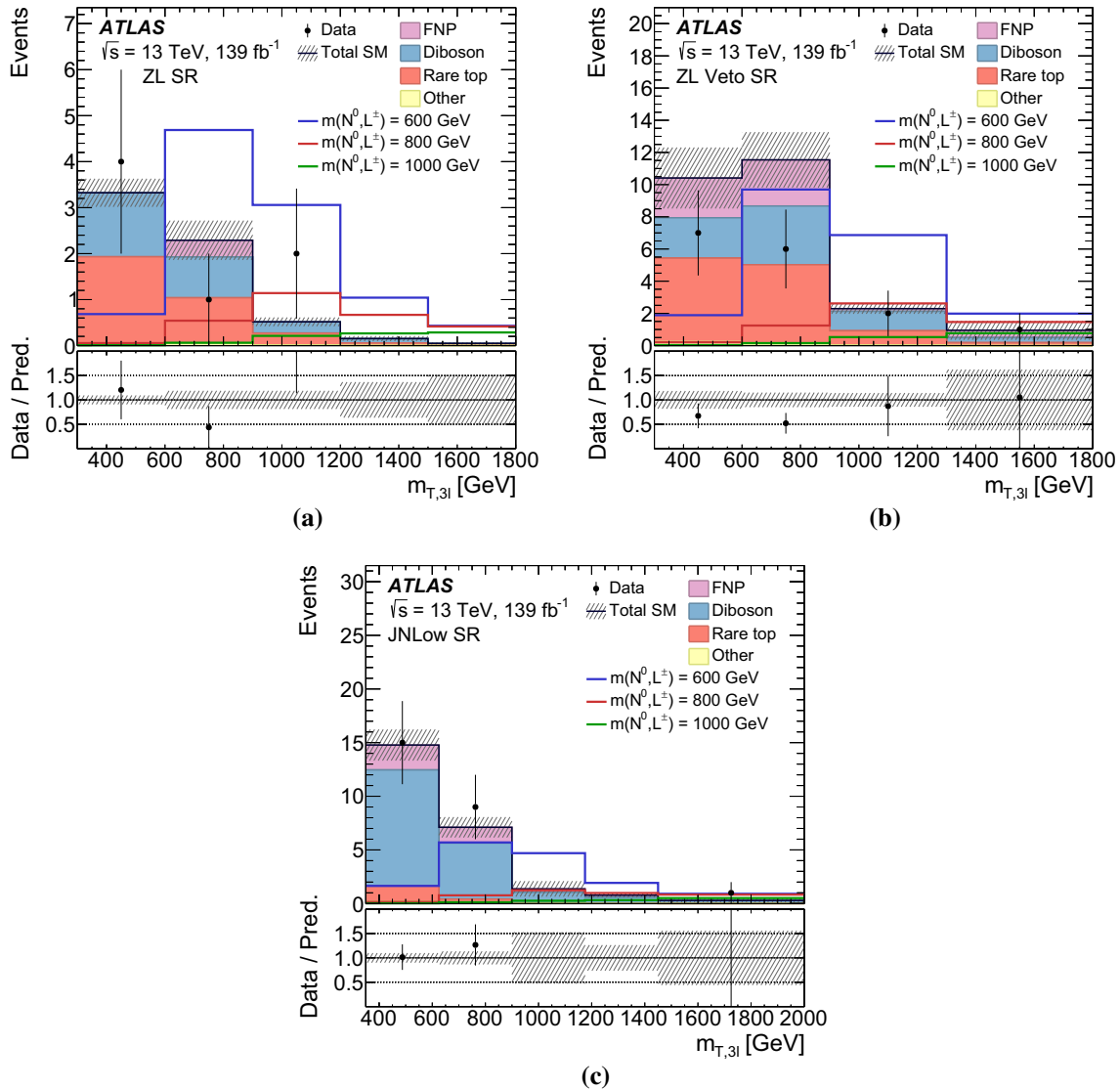


Fig. 3 Distributions of $m_{T,3\ell}$ in the three-lepton signal regions after the combined fit: **a** the ZL signal region, **b** the ZLVeto signal region and **c** the JNLow signal region. The coloured lines correspond to signal samples with the N^0 and L^\pm mass values stated in the legend. The hatched bands include all statistical and systematic post-fit uncertain-

ties with the correlations between various background sources taken into account. The lower panel shows the ratio of the observed data to the predicted SM background. The last bin in the distributions contains the overflows

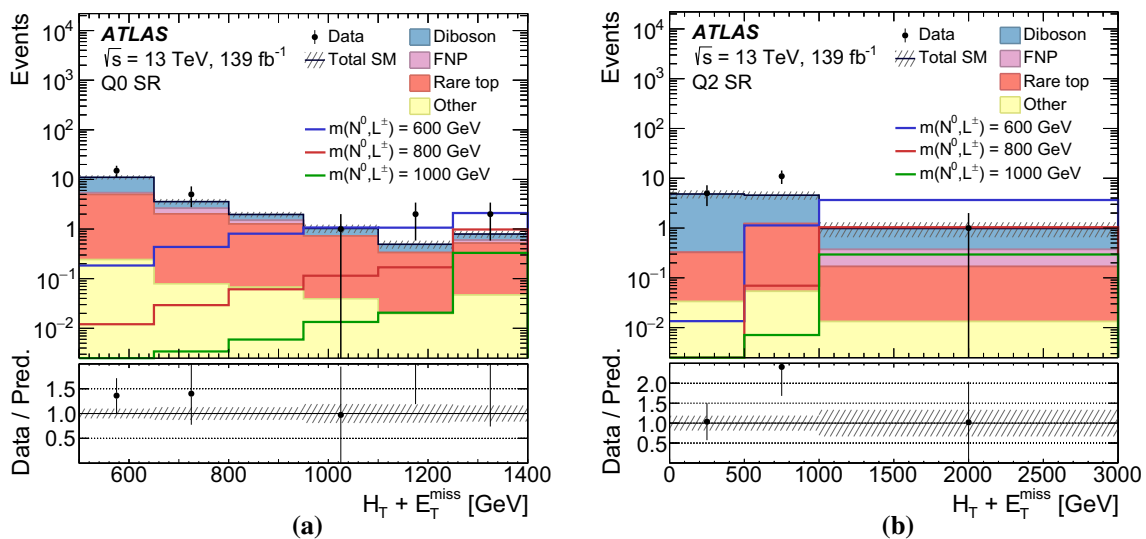


Fig. 4 Distributions of $H_T + E_T^{\text{miss}}$ in the four-lepton signal regions after the combined fit: **a** the Q0 signal region where the sum of lepton charges is zero and **b** the Q2 signal region where the sum of lepton charges is ± 2 . The coloured lines correspond to signal samples with the N^0 and L^\pm mass values stated in the legend. The hatched bands

include all statistical and systematic post-fit uncertainties with the correlations between various background sources taken into account. The lower panel shows the ratio of the observed data to the predicted SM background. The last bin in the distributions contains the overflows

After a background-only likelihood fit in the CRs, the three- and four-lepton channel diboson normalisation factors are found to be 0.80 ± 0.09 and 1.08 ± 0.03 , respectively. The normalisation and shape of the $m_{T,3\ell}$ and $H_T + E_T^{\text{miss}}$ distributions are validated in the ZL DB-VR and Q0 DB-VR, respectively, by comparing data and SM expectations after the fit. The rare top-quark contribution normalisation is estimated to be 1.3 ± 0.2 in the four-lepton channel Q0 RT-CR and is then extrapolated to all the SRs. The background modelling is validated in the ZL RT-VR and Q0 RT-VR for the three- and four-lepton channels, respectively.

Event yields after the likelihood fit for the analysis regions in the three- and four-lepton channels are shown in Fig. 2. Good agreement within statistical and systematic uncertainties between data and SM predictions is observed in all regions, demonstrating the validity of the background estimation procedure as shown in Table 4.

The post-fit distributions of the $m_{T,3\ell}$ and $H_T + E_T^{\text{miss}}$ variables used in the likelihood fit in the three- and four-lepton channels are shown in Figs. 3 and 4, respectively, for the signal regions, with the binning used in the fit. After the fit, the compatibility of the data and the expected background is assessed. Good agreement is observed. The p -values,⁵ evaluated using the distributions in Figs. 3 and 4, are 0.38, 0.090 and 0.25 for the three-, four- and the combined three-and-four lepton channels, respectively. Figure 5 shows the dis-

tributions of these discriminating variables in some of the control and validation regions.

The relative uncertainties in the background yield estimates are shown in Fig. 6 for all analysis regions in the three- and four-lepton channels. The dominant uncertainty in the SRs, and in most of the other regions, is the statistical uncertainty of the data, which varies from 20 to 37% depending on the signal region. The MC statistical uncertainty varies from 2 to 7% instead. In the Q2 SR an uncertainty contribution close to the data statistical uncertainty comes from the charge misidentification background, considered in the *Experimental* category.

In the absence of a significant deviation from SM expectations, 95% CL upper limits on the signal production cross-section are derived using the CL_s method [76]. The upper limits on the production cross-sections of the $pp \rightarrow W^* \rightarrow N^0 L^\pm$ and $pp \rightarrow Z^* \rightarrow L^\pm L^\mp$ processes are evaluated as a function of the heavy-lepton mass, using the three- and four-lepton channels with the democratic \mathcal{B}_ℓ scenario. By comparing the upper limits on the cross-section with the theoretical cross-section calculation as a function of the heavy-lepton mass, a lower limit on the mass of the type-III seesaw heavy leptons N^0 and L^\pm is derived. The observed (expected) exclusion limit is 870 GeV (900^{+80}_{-80} GeV).

The signal hypothesis in the three- and four-lepton channel result is also tested in a combined fit with the similar type-III seesaw search regions in the two-lepton channel [12]. All the CRs, VRs and SRs in the various lepton multiplicity regions are statistically independent. The reconstruction

⁵ The p -value is defined as the probability of observing an excess at least as large as the one observed in data, in the absence of signal.

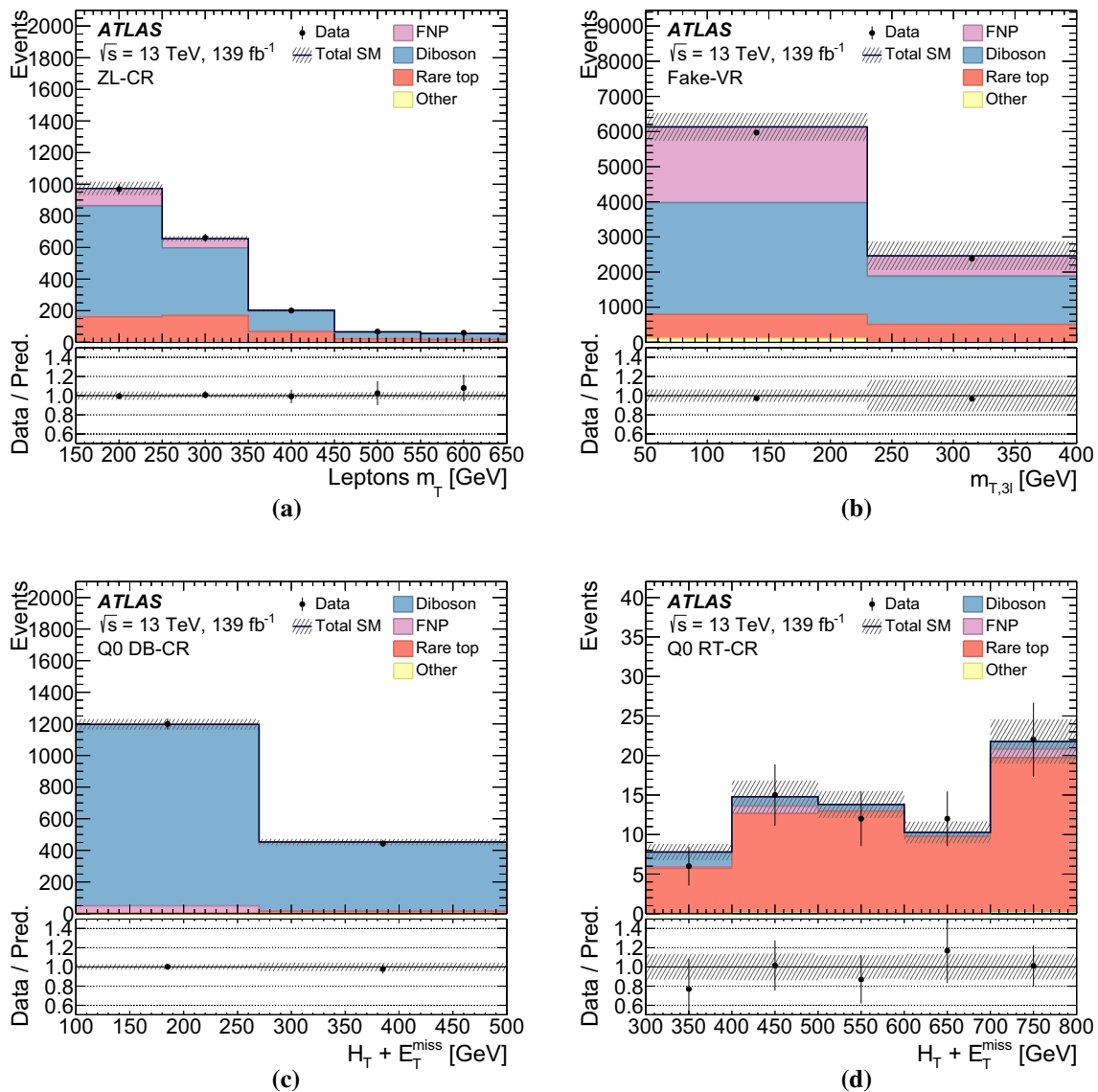


Fig. 5 Distributions of $m_{T,3\ell}$ in the three-lepton control and validation regions **a** ZL-CR and **b** fake-VR, and of $H_T + E_T^{\text{miss}}$ in the four-lepton control regions **c** Q0 DB-CR and **d** Q0 RT-CR after the combined fit. The simulated signal contribution was found to be below 2% and is not shown in the figure. The hatched bands include all statistical and

systematic post-fit uncertainties with the correlations between various background sources taken into account. The lower panel shows the ratio of the observed data to the predicted SM background. The last bin in the distributions contains the overflow

algorithms and working points are the same in all cases, and the FNP and lepton charge misidentification backgrounds are estimated using the same method. The parameter of interest, namely the number of signal events, and common systematic uncertainties are treated as correlated. Normalisations of the diboson, $t\bar{t}$ (for the two-lepton multiplicity region) and rare top-quark (for the three- and four-lepton multiplicity regions) backgrounds are treated as uncorrelated since they account for different physics processes and different acceptances in each final state. The three-lepton channel's limit dominates in the high heavy-lepton mass region, while

the two-lepton channel dominates in the lower mass region. The combined observed (expected) exclusion limits on the total cross-section are shown in Fig. 7, excluding heavy-lepton masses lower than 910 GeV (960^{+90}_{-80} GeV) at 95% CL. The combined observed (expected) exclusion limits on the total cross-section restraining to three-lepton and four-lepton channels are shown in Figs. 8 and 9 respectively.

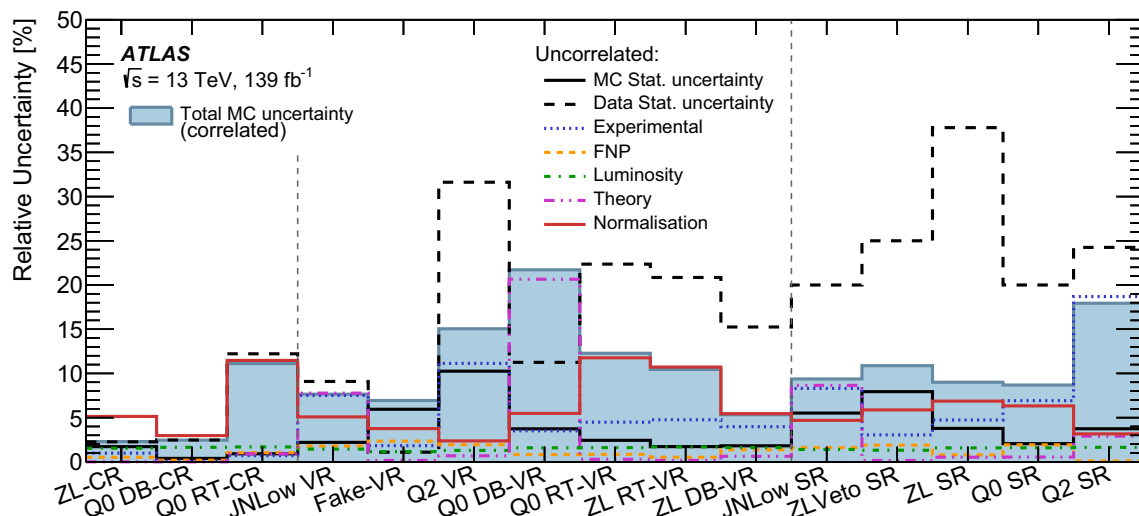


Fig. 6 Relative contributions from different sources of statistical and systematic uncertainty to the total background yield estimates after the fit. *Experimental* uncertainties are related to the lepton, jet and E_T^{miss} selection and reconstruction, and also to lepton charge misidentification. *FNP* includes the fake or non-prompt leptons contribution. *Luminosity* is related to the luminosity uncertainty that affects the background simulation yields. *Theory* includes theoretical uncertainties associated with the PDF, α_s , and renormalisation and factorisation scales. *Normalisation* is related to the diboson and rare top-quark normalisation factors

extracted by the likelihood fit. Systematic uncertainties are calculated by changing each nuisance parameter from its fit value by one standard deviation, keeping all the other parameters at their central values, and comparing the resulting event yield with the nominal yield. Individual uncertainties can be correlated within each region, and do not necessarily add in quadrature to the total background uncertainty, which is shown as *Total MC uncertainty (correlated)*. *Data Stat. uncertainty* refers to the statistical uncertainty of the collected data

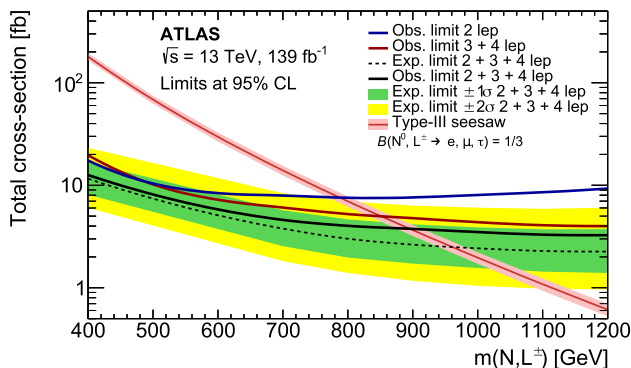


Fig. 7 Expected and observed exclusion limits in the two-lepton channel (from Ref. [12]), the three- and four-lepton channels, and the two-, three- and four-lepton channels for the type-III seesaw process with the corresponding one- and two-standard-deviation uncertainty bands, showing the 95% CL upper limit on the cross-section. The theoretical signal cross-section prediction, given by the NLO calculation [35,36], with its corresponding uncertainty band is also shown

9 Conclusion

ATLAS has searched for pair-produced heavy leptons predicted by the type-III seesaw model in 139 fb^{-1} of data from proton–proton collisions at $\sqrt{s} = 13 \text{ TeV}$, recorded during the 2015–2018 data-taking period. A lower limit on the mass of the type-III seesaw heavy leptons N^0 and L^\pm is derived for final states with three or four light leptons.

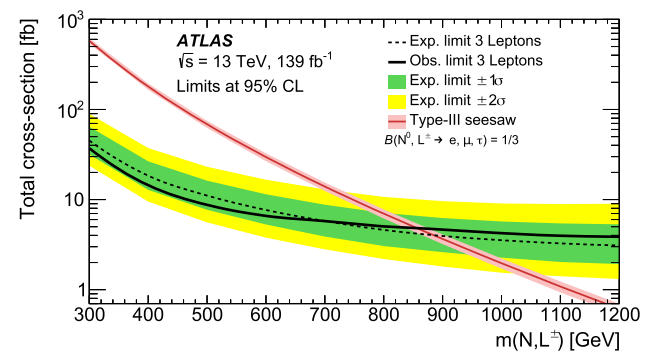


Fig. 8 Expected and observed 95% CL_s exclusion limits in the three lepton channel for the type-III seesaw process with the corresponding one- and two-standard-deviation bands, showing the 95% CL upper limit on the cross-section. The theoretical signal cross-section prediction, given by the NLO calculation [35,36], is shown with the corresponding uncertainty bands for the expected limit

No significant deviation from SM expectations is observed. The observed (expected) exclusion limit on the heavy-lepton mass is 870 GeV (900^{+80}_{-80} GeV) at the 95% CL. This result is combined with the result of the two-lepton analysis, which

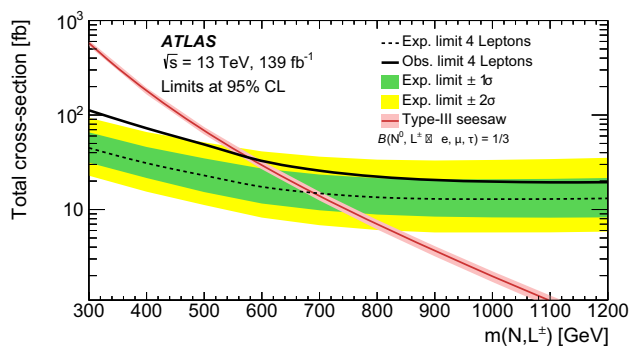


Fig. 9 Expected and observed 95% CL_s exclusion limits in the four lepton channel for the type-III seesaw process with the corresponding one- and two-standard-deviation bands, showing the 95% CL upper limit on the cross-section. The theoretical signal cross-section prediction, given by the NLO calculation [35,36], is shown with the corresponding uncertainty bands for the expected limit

used very similar experimental methodologies and treatment of statistics. In the full combination, heavy leptons with masses below 910 GeV are excluded at the 95% CL, while the expected lower limit on the mass is 960^{+90}_{-80} GeV. This is the most stringent limit to date on the type-III seesaw model from events with light leptons at LHC.

Acknowledgements We thank CERN for the very successful operation of the LHC, as well as the support staff from our institutions without whom ATLAS could not be operated efficiently. We acknowledge the support of ANPCyT, Argentina; YerPhI, Armenia; ARC, Australia; BMWFW and FWF, Austria; ANAS, Azerbaijan; SSTC, Belarus; CNPq and FAPESP, Brazil; NSERC, NRC and CFI, Canada; CERN; ANID, Chile; CAS, MOST and NSFC, China; Minciencias, Colombia; MEYS CR, Czech Republic; DNRF and DNSRC, Denmark; IN2P3-CNRS and CEA-DRF/IRFU, France; SRNSFG, Georgia; BMBF, HGF and MPG, Germany; GSRI, Greece; RGC and Hong Kong SAR, China; ISF and Benozziyo Center, Israel; INFN, Italy; MEXT and JSPS, Japan; CNRST, Morocco; NWO, Netherlands; RCN, Norway; MEiN, Poland; FCT, Portugal; MNE/IFA, Romania; JINR; MES of Russia and NRC KI, Russian Federation; MESTD, Serbia; MSSR, Slovakia; ARRS and MIZŠ, Slovenia; DSI/NRF, South Africa; MICINN, Spain; SRC and Wallenberg Foundation, Sweden; SERI, SNSF and Cantons of Bern and Geneva, Switzerland; MOST, Taiwan; TAEK, Turkey; STFC, UK; DOE and NSF, USA. In addition, individual groups and members have received support from BCKDF, CANARIE, Compute Canada and CRC, Canada; COST, ERC, ERDF, Horizon 2020 and Marie Skłodowska-Curie Actions, European Union; Investissements d’Avenir Labex, Investissements d’Avenir Idex and ANR, France; DFG and AvH Foundation, Germany; Herakleitos, Thales and Aristeia programmes co-financed by EU-ESF and the Greek NSRF, Greece; BSF-NSF and GIF, Israel; Norwegian Financial Mechanism 2014–2021, Norway; NCN and NAWA, Poland; La Caixa Banking Foundation, CERCA Programme Generalitat de Catalunya and PROMETEO and GenT Programmes Generalitat Valenciana, Spain; Göran Gustafssons Stiftelse, Sweden; The Royal Society and Leverhulme Trust, UK. The crucial computing support from all WLCG partners is acknowledged gratefully, in particular from CERN, the ATLAS Tier-1 facilities at TRIUMF (Canada), NDGF (Denmark, Norway, Sweden), CC-IN2P3 (France), KIT/GridKA (Germany), INFN-CNAF (Italy), NL-T1 (Netherlands), PIC (Spain), ASGC (Taiwan), RAL (UK) and BNL (USA), the Tier-2

facilities worldwide and large non-WLCG resource providers. Major contributors of computing resources are listed in Ref. [77].

Data Availability Statement This manuscript has no associated data or the data will not be deposited. [Authors’ comment: All ATLAS scientific output is published in journals, and preliminary results are made available in Conference Notes. All are openly available, without restriction on use by external parties beyond copyright law and the standard conditions agreed by CERN. Data associated with journal publications are also made available: tables and data from plots (e.g. cross section values, likelihood profiles, selection efficiencies, cross section limits, ...) are stored in appropriate repositories such as HEPDATA (<http://hepdata.cedar.ac.uk/>). ATLAS also strives to make additional material related to the paper available that allows a reinterpretation of the data in the context of new theoretical models. For example, an extended encapsulation of the analysis is often provided for measurements in the framework of RIVET (<http://rivet.hepforge.org/>). This information is taken from the ATLAS Data Access Policy, which is a public document that can be downloaded from <http://opendata.cern.ch/record/413> [opendata.cern.ch].

Open Access This article is licensed under a Creative Commons Attribution 4.0 International License, which permits use, sharing, adaptation, distribution and reproduction in any medium or format, as long as you give appropriate credit to the original author(s) and the source, provide a link to the Creative Commons licence, and indicate if changes were made. The images or other third party material in this article are included in the article’s Creative Commons licence, unless indicated otherwise in a credit line to the material. If material is not included in the article’s Creative Commons licence and your intended use is not permitted by statutory regulation or exceeds the permitted use, you will need to obtain permission directly from the copyright holder. To view a copy of this licence, visit <http://creativecommons.org/licenses/by/4.0/>.

Funded by SCOAP³. SCOAP³ supports the goals of the International Year of Basic Sciences for Sustainable Development.

References

1. I. Esteban, M.C. Gonzalez-Garcia, A. Hernandez-Cabezudo, M. Maltoni, T. Schwetz, Global analysis of three-flavour neutrino oscillations: synergies and tensions in the determination of θ_{23} , δ_{CP} , and the mass ordering. *JHEP* **01**, 106 (2019). [https://doi.org/10.1007/JHEP01\(2019\)106](https://doi.org/10.1007/JHEP01(2019)106). arXiv: 1811.05487 [hep-ph]
2. P. Minkowski, $\mu \rightarrow e\gamma$ at a rate of one out of 10^9 muon decays? *Phys. Lett. B* **67**, 421 (1977). [https://doi.org/10.1016/0370-2693\(77\)90435-X](https://doi.org/10.1016/0370-2693(77)90435-X)
3. T. Yanagida, in *Proceedings of the Workshop on Unified Theory and the Baryon Number in the Universe*, vol. 95, ed. by O. Sawada, A. Sugamoto. KEK Report No. 79-18 (1979)
4. S. Glashow, in *Quarks and Leptons, Proceedings of the 1979 Cargèse Summer Institute*, ed. By M. Levy et al. (NATO ASI Series, New York, 1980), p. 687. <https://doi.org/10.1007/978-1-4684-7197-7>
5. M. Gell-Mann, P. Ramond, R. Slansky, *Proceedings of Supergravity Workshop*, ed. By P. van Nieuwenhuizen & D.Z. Freedman (North Holland Publ. Co., Amsterdam, 1979) p. 315 arXiv:1306.4669 [hep-th]
6. R.N. Mohapatra, G. Senjanović, Neutrino mass and spontaneous parity nonconservation. *Phys. Rev. Lett.* **44**, 912 (1980). <https://doi.org/10.1103/PhysRevLett.44.912>
7. R. Foot, H. Lew, X.G. He, G.C. Joshi, See-saw neutrino masses induced by a triplet of leptons. *Z. Phys. C* **44**, 441 (1989). <https://doi.org/10.1007/BF01415558>

8. ATLAS Collaboration, Search for type-III seesaw heavy leptons in pp collisions at $\sqrt{s} = 8$ TeV with the ATLAS detector. Phys. Rev. D **92**, 032001 (2015). <https://doi.org/10.1103/PhysRevD.92.032001>. arXiv:1506.01839 [hep-ex]
9. ATLAS Collaboration, Search for heavy lepton resonances decaying to a Z boson and a lepton in pp collisions at $\sqrt{s} = 8$ TeV with the ATLAS detector. JHEP **09**, 108 (2015). [https://doi.org/10.1007/JHEP09\(2015\)108](https://doi.org/10.1007/JHEP09(2015)108). arXiv:1506.01291 [hep-ex]
10. F. del Aguila, J.A. Aguilar-Saavedra, Distinguishing seesaw models at LHC with multi-lepton signals. Nucl. Phys. B **813**, 22 (2009). <https://doi.org/10.1016/j.nuclphysb.2008.12.029>. arXiv:0808.2468 [hep-ph]
11. CMS Collaboration, Search for physics beyond the standard model in multilepton final states in proton-proton collisions at $\sqrt{s} = 13$ TeV. JHEP **03**, 051 (2020). [https://doi.org/10.1007/JHEP03\(2020\)051](https://doi.org/10.1007/JHEP03(2020)051). arXiv:1911.04968 [hep-ex]
12. ATLAS Collaboration, Search for type-III seesaw heavy leptons in dilepton final states in pp collisions at $\sqrt{s} = 13$ TeV with the ATLAS detector. Eur. Phys. J. C **81**, 218 (2021). <https://doi.org/10.1140/epjc/s10052-021-08929-9>. arXiv:2008.07949 [hep-ex]
13. C. Biggio, F. Bonnet, Implementation of the type III seesaw model in FeynRules/MadGraph and prospects for discovery with early LHC data. Eur. Phys. J. C **72**, 1899 (2012). <https://doi.org/10.1140/epjc/s10052-012-1899-z>. arXiv:1107.3463 [hep-ph]
14. A. Strumia and F. Vissani, Neutrino masses and mixings and..., (2006), arXiv:hep-ph/0606054
15. A. Arhrib et al., Collider signatures for the heavy lepton triplet in type I+III seesaw. Phys. Rev. D **82**, 053004 (2010). <https://doi.org/10.1103/PhysRevD.82.053004>. arXiv:0904.2390 [hep-ph]
16. A. Das, S. Mandal, Bounds on the triplet fermions in type-III seesaw and implications for collider searches. Nucl. Phys. B **966**, 115374 (2021). <https://doi.org/10.1016/j.nuclphysb.2021.115374>. arXiv:2006.04123 [hep-ph]
17. ATLAS Collaboration, The ATLAS experiment at the CERN large hadron collider. JINST **3**, S08003 (2008). <https://doi.org/10.1088/1748-0221/3/08/S08003>
18. ATLAS Collaboration, ATLAS insertable B-layer: technical design report, ATLAS-TDR-19; CERN-LHCC-2010-013 (2010). <https://cds.cern.ch/record/1291633> [Addendum: ATLAS-TDR-19-ADD-1; CERN-LHCC-2012-009 (2012). <https://cds.cern.ch/record/1451888>]
19. B. Abbott et al., Production and integration of the ATLAS insertable B-layer. JINST **13**, T05008 (2018). <https://doi.org/10.1088/1748-0221/13/05/T05008>. arXiv:1803.00844 [physics.ins-det]
20. ATLAS Collaboration, Performance of the ATLAS trigger system in 2015. Eur. Phys. J. C **77**, 317 (2017). <https://doi.org/10.1140/epjc/s10052-017-4852-3>. arXiv:1611.09661 [hep-ex]
21. ATLAS Collaboration, The ATLAS collaboration software and firmware. ATL-SOFT-PUB-2021-001 (2021). <https://cds.cern.ch/record/2767187>
22. ATLAS Collaboration, ATLAS data quality operations and performance for 2015–2018 data-taking. JINST **15**, P04003 (2020). <https://doi.org/10.1088/1748-0221/15/04/P04003>. arXiv:1911.04632 [physics.ins-det]
23. ATLAS Collaboration, Luminosity determination in pp collisions at $\sqrt{s} = 13$ TeV using the ATLAS detector at the LHC. ATLAS-CONF-2019-021 (2019). <https://cds.cern.ch/record/2677054>
24. G. Avoni et al., The new LUCID-2 detector for luminosity measurement and monitoring in ATLAS. JINST **13**, P07017 (2018). <https://doi.org/10.1088/1748-0221/13/07/P07017>
25. ATLAS Collaboration, Performance of electron and photon triggers in ATLAS during LHC Run 2. Eur. Phys. J. C **80**, 47 (2020). <https://doi.org/10.1140/epjc/s10052-019-7500-2>. arXiv:1909.00761 [hep-ex]
26. ATLAS Collaboration, Performance of the ATLAS muon triggers in Run 2. JINST **15**, P09015 (2020). <https://doi.org/10.1088/1748-0221/15/09/p09015>. arXiv:2004.13447 [hep-ex]
27. ATLAS Collaboration, The ATLAS simulation infrastructure. Eur. Phys. J. C **70**, 823 (2010). <https://doi.org/10.1140/epjc/s10052-010-1429-9>. arXiv:1005.4568 [physics.ins-det]
28. GEANT4 Collaboration, S. Agostinelli et al., GEANT4—a simulation toolkit. Nucl. Instrum. Methods A **506**, 250 (2003). [https://doi.org/10.1016/S0168-9002\(03\)01368-8](https://doi.org/10.1016/S0168-9002(03)01368-8)
29. J. Alwall et al., The automated computation of tree-level and next-to-leading order differential cross sections, and their matching to parton shower simulations. JHEP **07**, 079 (2014). [https://doi.org/10.1007/JHEP07\(2014\)079](https://doi.org/10.1007/JHEP07(2014)079). arXiv:1405.0301 [hep-ph]
30. A. Alloul, N.D. Christensen, C. Degrande, C. Duhr, B. Fuks, FeynRules 2.0—a complete toolbox for tree-level phenomenology. Comput. Phys. Commun. **185**, 2250 (2014). <https://doi.org/10.1016/j.cpc.2014.04.012>. arXiv:1310.1921 [hep-ph]
31. R.D. Ball et al., Parton distributions for the LHC run II. JHEP **04**, 040 (2015). [https://doi.org/10.1007/JHEP04\(2015\)040](https://doi.org/10.1007/JHEP04(2015)040). arXiv:1410.8849 [hep-ph]
32. T. Sjöstrand et al., An introduction to PYTHIA 8.2. Comput. Phys. Commun. **191**, 159 (2015). <https://doi.org/10.1016/j.cpc.2015.01.024>. arXiv:1410.3012 [hep-ph]
33. ATLAS Collaboration, ATLAS Pythia 8 tunes to 7 TeV data. ATL-PHYS-PUB-2014-021 (2014). <https://cds.cern.ch/record/1966419>
34. R.D. Ball et al., Parton distributions with LHC data. Nucl. Phys. B **867**, 244 (2013). <https://doi.org/10.1016/j.nuclphysb.2012.10.003>. arXiv:1207.1303 [hep-ph]
35. B. Fuks, M. Klasen, D.R. Lamprea, M. Rothering, Gaugino production in proton–proton collisions at a center-of-mass energy of 8 TeV. JHEP **10**, 081 (2012). [https://doi.org/10.1007/JHEP10\(2012\)081](https://doi.org/10.1007/JHEP10(2012)081). arXiv:1207.2159 [hep-ph]
36. B. Fuks, M. Klasen, D.R. Lamprea, M. Rothering, Precision predictions for electroweak superpartner production at hadron colliders with RESUMMINO. Eur. Phys. J. C **73**, 2480 (2013). <https://doi.org/10.1140/epjc/s10052-013-2480-0>. arXiv:1304.0790 [hep-ph]
37. R. Ruiz, QCD corrections to pair production of type III seesaw leptons at hadron colliders. JHEP **12**, 165 (2015). [https://doi.org/10.1007/JHEP12\(2015\)165](https://doi.org/10.1007/JHEP12(2015)165). arXiv:1509.05416 [hep-ph]
38. Y. Cai, T. Han, T. Li, R. Ruiz, Lepton number violation: seesaw models and their collider tests. Front. Phys. **6**, 40 (2018). <https://doi.org/10.3389/fphy.2018.00040>. arXiv:1711.02180 [hep-ph]
39. S. Höche, F. Krauss, M. Schönherr, F. Siegert, QCD matrix elements + parton showers. The NLO case. JHEP **04**, 027 (2013). [https://doi.org/10.1007/JHEP04\(2013\)027](https://doi.org/10.1007/JHEP04(2013)027). arXiv:1207.5030 [hep-ph]
40. S. Frixione, G. Ridolfi, P. Nason, A positive-weight next-to-leading-order Monte Carlo for heavy flavour hadroproduction. JHEP **09**, 126 (2007). <https://doi.org/10.1088/1126-6708/2007/09/126>. arXiv:0707.3088 [hep-ph]
41. P. Nason, A new method for combining NLO QCD with shower Monte Carlo algorithms. JHEP **11**, 040 (2004). <https://doi.org/10.1088/1126-6708/2004/11/040>. arXiv:hep-ph/0409146
42. S. Frixione, P. Nason, C. Oleari, Matching NLO QCD computations with parton shower simulations: the POWHEG method. JHEP **11**, 070 (2007). <https://doi.org/10.1088/1126-6708/2007/11/070>. arXiv:0709.2092 [hep-ph]
43. S. Alioli, P. Nason, C. Oleari, E. Re, A general framework for implementing NLO calculations in shower Monte Carlo programs: the POWHEG BOX. JHEP **06**, 043 (2010). [https://doi.org/10.1007/JHEP06\(2010\)043](https://doi.org/10.1007/JHEP06(2010)043). arXiv:1002.2581 [hep-ph]
44. E. Bothmann et al., Event generation with Sherpa 2.2. SciPost Phys. **7**, 034 (2019). <https://doi.org/10.21468/SciPostPhys.7.3.034>. arXiv:1905.09127 [hep-ph]



45. T. Gleisberg, S. Höche, Comix, a new matrix element generator. *JHEP* **12**, 039 (2008). <https://doi.org/10.1088/1126-6708/2008/12/039>. arXiv:0808.3674 [hep-ph]
46. S. Schumann, F. Krauss, A parton shower algorithm based on Catani–Seymour dipole factorisation. *JHEP* **03**, 038 (2008). <https://doi.org/10.1088/1126-6708/2008/03/038>. arXiv:0709.1027 [hep-ph]
47. S. Höche, F. Krauss, M. Schönherr, F. Siegert, A critical appraisal of NLO+PS matching methods. *JHEP* **09**, 049 (2012). [https://doi.org/10.1007/JHEP09\(2012\)049](https://doi.org/10.1007/JHEP09(2012)049). arXiv:1111.1220 [hep-ph]
48. S. Catani, F. Krauss, B.R. Webber, R. Kuhn, QCD matrix elements + parton showers. *JHEP* **11**, 063 (2001). <https://doi.org/10.1088/1126-6708/2001/11/063>. arXiv:hep-ph/0109231
49. S. Höche, F. Krauss, S. Schumann, F. Siegert, QCD matrix elements and truncated showers. *JHEP* **05**, 053 (2009). <https://doi.org/10.1088/1126-6708/2009/05/053>. arXiv:0903.1219 [hep-ph]
50. F. Cascioli, P. Maierhöfer, S. Pozzorini, Scattering amplitudes with open loops. *Phys. Rev. Lett.* **108**, 111601 (2012). <https://doi.org/10.1103/PhysRevLett.108.111601>. arXiv:1111.5206 [hep-ph]
51. A. Denner, S. Dittmaier, L. Hofer, COLLIER: a Fortran-based complex one-loop library in extended regularizations. *Comput. Phys. Commun.* **212**, 220 (2017). <https://doi.org/10.1016/j.cpc.2016.10.013>. arXiv:1604.06792 [hep-ph]
52. S. Dulat et al., New parton distribution functions from a global analysis of quantum chromodynamics. *Phys. Rev. D* **93**, 033006 (2016). <https://doi.org/10.1103/PhysRevD.93.033006>. arXiv:1506.07443 [hep-ph]
53. L. Harland-Lang, A. Martin, P. Motylinski, R. Thorne, Parton distributions in the LHC era: MMHT 2014 PDFs. *Eur. Phys. J. C* **75**, 204 (2015). <https://doi.org/10.1140/epjc/s10052-015-3397-6>. arXiv:1412.3989 [hep-ph]
54. ATLAS Collaboration, Studies on top-quark Monte Carlo modelling for Top2016, ATL-PHYS-PUB-2016-020 (2016). <https://cds.cern.ch/record/2216168>
55. ATLAS Collaboration, The Pythia 8 A3 tune description of ATLAS minimum bias and inelastic measurements incorporating the Donnachie–Landshoff diffractive model. ATL-PHYS-PUB-2016-017 (2016). <https://cds.cern.ch/record/2206965>
56. ATLAS Collaboration, Electron and photon performance measurements with the ATLAS detector using the 2015–2017 LHC proton–proton collision data. *JINST* **14**, P12006 (2019). <https://doi.org/10.1088/1748-0221/14/12/P12006>. arXiv:1908.00005 [hep-ex]
57. ATLAS Collaboration, Muon reconstruction and identification efficiency in ATLAS using the full Run 2 pp collision data set at $\sqrt{s} = 13$ TeV. *Eur. Phys. J. C* **81**, 578 (2021). <https://doi.org/10.1140/epjc/s10052-021-09233-2>. arXiv:2012.00578 [hep-ex]
58. ATLAS Collaboration, Jet reconstruction and performance using particle flow with the ATLAS detector. *Eur. Phys. J. C* **77**, 466 (2017). <https://doi.org/10.1140/epjc/s10052-017-5031-2>. arXiv:1703.10485 [hep-ex]
59. M. Cacciari, G.P. Salam, G. Soyez, The anti- k_r jet clustering algorithm. *JHEP* **04**, 063 (2008). <https://doi.org/10.1088/1126-6708/2008/04/063>. arXiv:0802.1189 [hep-ph]
60. ATLAS Collaboration, Jet energy scale measurements and their systematic uncertainties in proton–proton collisions at $\sqrt{s} = 13$ TeV with the ATLAS detector. *Phys. Rev. D* **96**, 072002 (2017). <https://doi.org/10.1103/PhysRevD.96.072002>. arXiv:1703.09665 [hep-ex]
61. ATLAS Collaboration, Performance of pile-up mitigation techniques for jets in pp collisions at $\sqrt{s} = 8$ TeV using the ATLAS detector. *Eur. Phys. J. C* **76**, 581 (2016). <https://doi.org/10.1140/epjc/s10052-016-4395-z>. arXiv:1510.03823 [hep-ex]
62. ATLAS Collaboration, Performance of b-jet identification in the ATLAS experiment. *JINST* **11**, P04008 (2016). <https://doi.org/10.1088/1748-0221/11/04/P04008>. arXiv:1512.01094 [hep-ex]
63. ATLAS Collaboration, Optimisation of the ATLAS b-tagging performance for the 2016 LHC Run, ATL-PHYS-PUB-2016-012 (2016). <https://cds.cern.ch/record/2160731>
64. ATLAS Collaboration, Optimisation and performance studies of the ATLAS b-tagging algorithms for the 2017–18 LHC run, ATL-PHYS-PUB-2017-013 (2017). <https://cds.cern.ch/record/2273281>
65. ATLAS Collaboration, Performance of missing transverse momentum reconstruction with the ATLAS detector using proton–proton collisions at $\sqrt{s} = 13$ TeV. *Eur. Phys. J. C* **78**, 903 (2018). <https://doi.org/10.1140/epjc/s10052-018-6288-9>. arXiv:1802.08168 [hep-ex]
66. ATLAS Collaboration, Search for anomalous production of prompt same-sign lepton pairs and pair-produced doubly charged Higgs bosons with $\sqrt{s} = 8$ TeV pp collisions using the ATLAS detector. *JHEP* **03**, 041 (2015). [https://doi.org/10.1007/JHEP03\(2015\)041](https://doi.org/10.1007/JHEP03(2015)041). arXiv:1412.0237 [hep-ex]
67. G. Aad et al., Jet energy scale and resolution measured in proton–proton collisions at $\sqrt{s} = 13$ TeV with the ATLAS detector. *Eur. Phys. J. C* **81**, 689 (2021). <https://doi.org/10.1140/epjc/s10052-021-09402-3>. arXiv:2007.02645 [hep-ex]
68. ATLAS Collaboration, ATLAS b-jet identification performance and efficiency measurement with $t\bar{t}$ events in pp collisions at $\sqrt{s} = 13$ TeV. *Eur. Phys. J. C* **79**, 970 (2019). <https://doi.org/10.1140/epjc/s10052-019-7450-8>. arXiv:1907.05120 [hep-ex]
69. ATLAS Collaboration, E_T^{miss} performance in the ATLAS detector using 2015–2016 LHC pp collisions, ATLAS-CONF-2018-023 (2018). <https://cds.cern.ch/record/2625233>
70. ATLAS Collaboration, Tagging and suppression of pileup jets with the ATLAS detector, ATLAS-CONF-2014-018 (2014). <https://cds.cern.ch/record/1700870>
71. E. Bothmann, M. Schönherr, S. Schumann, Reweighting QCD matrix-element and parton-shower calculations. *Eur. Phys. J. C* **76**, 590 (2016). <https://doi.org/10.1140/epjc/s10052-016-4430-0>. arXiv:1606.08753 [hep-ph]
72. A. Buckley et al., LHAPDF6: parton density access in the LHC precision era. *Eur. Phys. J. C* **75**, 132 (2015). <https://doi.org/10.1140/epjc/s10052-015-3318-8>. arXiv:1412.7420 [hep-ph]
73. J. Butterworth et al., PDF4LHC recommendations for LHC Run II. *J. Phys. G* **43**, 023001 (2016). <https://doi.org/10.1088/0954-3899/43/2/023001>. arXiv:1510.03865 [hep-ph]
74. M. Baak et al., HistFitter software framework for statistical data analysis. *Eur. Phys. J. C* **75**, 153 (2015). <https://doi.org/10.1140/epjc/s10052-015-3327-7>. arXiv:1410.1280 [hep-ex]
75. G. Cowan, K. Cranmer, E. Gross, O. Vitells, Asymptotic formulae for likelihood-based tests of new physics. *Eur. Phys. J. C* **71**, 1554 (2011). <https://doi.org/10.1140/epjc/s10052-011-1554-0>. arXiv:1007.1727 [physics.data-an]. [Erratum: *Eur. Phys. J. C* **73**, 2501 (2013). <https://doi.org/10.1140/epjc/s10052-013-2501-z>]
76. A.L. Read, Presentation of search results: the CL_S technique. *J. Phys. G* **28**, 2693 (2002). <https://doi.org/10.1088/0954-3899/28/10/313>
77. ATLAS Collaboration, ATLAS Computing Acknowledgements, ATL-SOFT-PUB-2021-003. <https://cds.cern.ch/record/2776662>

ATLAS Collaboration*

G. Aad⁹⁹, B. Abbott¹²⁴, D. C. Abbott¹⁰⁰, A. Abed Abud³⁴, K. Abeling⁵¹, D. K. Abhayasinghe⁹¹, S. H. Abidi²⁷, H. Abramowicz¹⁵⁷, H. Abreu¹⁵⁶, Y. Abulaiti⁵, A. C. Abusleme Hoffman^{142a}, B. S. Acharya^{64a,64b,p}, B. Achkar⁵¹, L. Adam⁹⁷, C. Adam Bourdarios⁴, L. Adamczyk^{81a}, L. Adamek¹⁶², S. V. Addepalli²⁴, J. Adelman¹¹⁷, A. Adiguzel^{11c,ae}, S. Adorni⁵², T. Adye¹³⁹, A. A. Affolder¹⁴¹, Y. Afik¹⁵⁶, C. Agapopoulou⁶², M. N. Agaras¹², J. Agarwala^{68a,68b}, A. Aggarwal¹¹⁵, C. Agheorghiesei^{25c}, J. A. Aguilar-Saavedra^{135a,135f,ad}, A. Ahmad³⁴, F. Ahmadov^{77,ab}, W. S. Ahmed¹⁰¹, X. Ai⁴⁴, G. Aielli^{71a,71b}, I. Aizenberg¹⁷⁵, S. Akatsuka⁸³, M. Akbiyik⁹⁷, T. P. A. Åkesson⁹⁴, A. V. Akimov¹⁰⁸, K. Al Khoury³⁷, G. L. Alberghi^{21b}, J. Albert¹⁷¹, P. Albicocco⁴⁹, M. J. Alconada Verzini⁸⁶, S. Alderweireldt⁴⁸, M. Aleksa³⁴, I. N. Aleksandrov⁷⁷, C. Alexa^{25b}, T. Alexopoulos⁹, A. Alfonsi¹¹⁶, F. Alfonsi^{21b}, M. Alhroob¹²⁴, B. Ali¹³⁷, S. Ali¹⁵⁴, M. Aliev¹⁶¹, G. Alimonti^{66a}, C. Allaire³⁴, B. M. M. Allbrooke¹⁵², P. P. Allport¹⁹, A. Aloisio^{67a,67b}, F. Alonso⁸⁶, C. Alpigiani¹⁴⁴, E. Alunno Camelia^{71a,71b}, M. Alvarez Estevez⁹⁶, M. G. Alvigi^{67a,67b}, Y. Amaral Coutinho^{78b}, A. Ambler¹⁰¹, L. Ambroz¹³⁰, C. Amelung³⁴, D. Amidei¹⁰³, S. P. Amor Dos Santos^{135a}, S. Amoroso⁴⁴, C. S. Amrouche⁵², C. Anastopoulos¹⁴⁵, N. Andari¹⁴⁰, T. Andeen¹⁰, J. K. Anders¹⁸, S. Y. Andrean^{43a,43b}, A. Andreazza^{66a,66b}, S. Angelidakis⁸, A. Angerami³⁷, A. V. Anisenkov^{118a,118b}, A. Annovi^{69a}, C. Antel⁵², M. T. Anthony¹⁴⁵, E. Antipov¹²⁵, M. Antonelli⁴⁹, D. J. A. Antrim¹⁶, F. Anulli^{70a}, M. Aoki⁷⁹, J. A. Aparisi Pozo¹⁶⁹, M. A. Aparo¹⁵², L. Aperio Bella⁴⁴, N. Aranzabal³⁴, V. Araujo Ferraz^{78a}, C. Arcangeletti⁴⁹, A. T. H. Arce⁴⁷, E. Arena⁸⁸, J-F. Arguin¹⁰⁷, S. Argyropoulos⁵⁰, J.-H. Arling⁴⁴, A. J. Armbruster³⁴, A. Armstrong¹⁶⁶, O. Arnaez¹⁶², H. Arnold³⁴, Z. P. Arrubarrena Tame¹¹¹, G. Artoni¹³⁰, H. Asada¹¹³, K. Asai¹²², S. Asai¹⁵⁹, N. A. Asbah⁵⁷, E. M. Asimakopoulou¹⁶⁷, L. Asquith¹⁵², J. Assahsah^{33d}, K. Assamagan²⁷, R. Astalos^{26a}, R. J. Atkin^{31a}, M. Atkinson¹⁶⁸, N. B. Atlay¹⁷, H. Atmani^{58b}, P. A. Atlasiddha¹⁰³, K. Augsten¹³⁷, S. Auricchio^{67a,67b}, V. A. Austrup¹⁷⁷, G. Avner¹⁵⁶, G. Avolio³⁴, M. K. Ayoub^{13c}, G. Azuelos^{107,al}, D. Babal^{26a}, H. Bachacou¹⁴⁰, K. Bachas¹⁵⁸, A. Bachiu³², F. Backman^{43a,43b}, A. Badae⁵⁷, P. Bagnaia^{70a,70b}, H. Bahrasemani¹⁴⁸, A. J. Bailey¹⁶⁹, V. R. Bailey¹⁶⁸, J. T. Baines¹³⁹, C. Bakalis⁹, O. K. Baker¹⁷⁸, P. J. Bakker¹¹⁶, E. Bakos¹⁴, D. Bakshi Gupta⁷, S. Balaji¹⁵³, R. Balasubramanian¹¹⁶, E. M. Baldin^{118a,118b}, P. Balek¹³⁸, E. Ballabene^{66a,66b}, F. Balli¹⁴⁰, W. K. Balunas¹³⁰, J. Balz⁹⁷, E. Banas⁸², M. Bandieramonte¹³⁴, A. Bandyopadhyay¹⁷, S. Bansal²², L. Barak¹⁵⁷, E. L. Barberio¹⁰², D. Barberis^{53a,53b}, M. Barbero⁹⁹, G. Barbour⁹², K. N. Barends^{31a}, T. Barillari¹¹², M-S. Barisits³⁴, J. Barkeloo¹²⁷, T. Barklow¹⁴⁹, B. M. Barnett¹³⁹, R. M. Barnett¹⁶, A. Baroncelli^{58a}, G. Barone²⁷, A. J. Barr¹³⁰, L. Barranco Navarro^{43a,43b}, F. Barreiro⁹⁶, J. Barreiro Guimarães da Costa^{13a}, U. Barron¹⁵⁷, S. Barsov¹³³, F. Bartels^{59a}, R. Bartoldus¹⁴⁹, G. Bartolini⁹⁹, A. E. Barton⁸⁷, P. Bartos^{26a}, A. Basalae⁴⁴, A. Basan⁹⁷, I. Bashta^{72a,72b}, A. Bassalat^{62,ai}, M. J. Basso¹⁶², C. R. Basson⁹⁸, R. L. Bates⁵⁵, S. Batlamous^{33e}, J. R. Batley³⁰, B. Batool¹⁴⁷, M. Battaglia¹⁴¹, M. Bauce^{70a,70b}, F. Bauer^{140,*}, P. Bauer²², H. S. Bawa²⁹, A. Bayirli^{11c}, J. B. Beacham⁴⁷, T. Beau¹³¹, P. H. Beauchemin¹⁶⁵, F. Becherer⁵⁰, P. Bechtel²², H. P. Beck^{18,r}, K. Becker¹⁷³, C. Becot⁴⁴, A. J. Beddall^{11a}, V. A. Bednyakov⁷⁷, C. P. Bee¹⁵¹, T. A. Beermann¹⁷⁷, M. Begalli^{78b}, M. Begel²⁷, A. Behera¹⁵¹, J. K. Behr⁴⁴, C. Beirao Da Cruz E Silva³⁴, J. F. Beirer^{34,51}, F. Beisiegel²², M. Belfkir⁴, G. Bella¹⁵⁷, L. Bellagamba^{21b}, A. Bellerive³², P. Bellos¹⁹, K. Beloborodov^{118a,118b}, K. Belotskiy¹⁰⁹, N. L. Belyaev¹⁰⁹, D. Bencheikroun^{33a}, Y. Benhammou¹⁵⁷, D. P. Benjamin²⁷, M. Benoit²⁷, J. R. Bensinger²⁴, S. Bentvelsen¹¹⁶, L. Beresford³⁴, M. Beretta⁴⁹, D. Berge¹⁷, E. Bergeas Kuutmann¹⁶⁷, N. Berger⁴, B. Bergmann¹³⁷, L. J. Bergsten²⁴, J. Beringer¹⁶, S. Berlendis⁶, G. Bernardi¹³¹, C. Bernius¹⁴⁹, F. U. Bernlochner²², T. Berry⁹¹, P. Berta¹³⁸, A. Berthold⁴⁶, I. A. Bertram⁸⁷, O. Bessidskaia Bylund¹⁷⁷, S. Bethke¹¹², A. Betti⁴⁰, A. J. Bevan⁹⁰, S. Bhatta¹⁵¹, D. S. Bhattacharya¹⁷², P. Bhattarai²⁴, V. S. Bhopatkar⁵, R. Bi¹³⁴, R. M. Bianchi¹³⁴, O. Biebel¹¹¹, R. Bielski¹²⁷, N. V. Biesuz^{69a,69b}, M. Biglietti^{72a}, T. R. V. Billoud¹³⁷, M. Bindi⁵¹, A. Bingul^{11d}, C. Bini^{70a,70b}, S. Biondi^{21a,21b}, A. Biondini⁸⁸, C. J. Birch-sykes⁹⁸, G. A. Bird^{19,139}, M. Birman¹⁷⁵, T. Bisanz³⁴, J. P. Biswal², D. Biswas^{176,k}, A. Bitadze⁹⁸, C. Bittrich⁴⁶, K. Björke¹²⁹, I. Bloch⁴⁴, C. Blocker²⁴, A. Blue⁵⁵, U. Blumenschein⁹⁰, J. Blumenthal⁹⁷, G. J. Bobbink¹¹⁶, V. S. Bobrovnikov^{118a,118b}, M. Boehler⁵⁰, D. Bogavac¹², A. G. Bogdanchikov^{118a,118b}, C. Bohm^{43a}, V. Boisvert⁹¹, P. Bokan⁴⁴, T. Bold^{81a}, M. Bomben¹³¹, M. Bona⁹⁰, M. Boonekamp¹⁴⁰, C. D. Booth⁹¹, A. G. Borbély⁵⁵, H. M. Borecka-Bielska¹⁰⁷, L. S. Borgna⁹², G. Borissov⁸⁷, D. Bortoletto¹³⁰, D. Boscherini^{21b}, M. Bosman¹², J. D. Bossio Sola³⁴, K. Bouaouda^{33a}, J. Boudreau¹³⁴, E. V. Bouhova-Thacker⁸⁷, D. Boumediene³⁶, R. Bouquet¹³¹, A. Boveia¹²³, J. Boyd³⁴, D. Boye²⁷, I. R. Boyko⁷⁷, A. J. Bozson⁹¹, J. Bracinik¹⁹, N. Brahimi^{58c,58d}, G. Brandt¹⁷⁷





















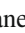
















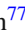







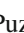






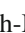


















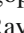





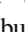







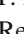




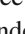









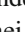

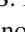


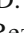




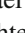

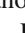


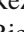


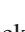
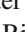

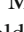



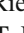


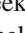










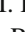
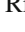

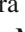


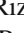



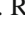


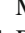




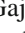

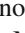

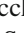
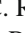




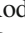









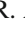


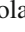
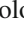




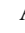
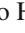

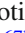

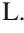

















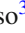


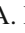



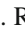

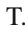



























































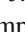




O. Brandt³⁰, F. Braren⁴⁴, B. Brau¹⁰⁰, J. E. Brau¹²⁷, W. D. Breaden Madden⁵⁵, K. Brendlinger⁴⁴, R. Brenner¹⁷⁵, L. Brenner³⁴, R. Brenner¹⁶⁷, S. Bressler¹⁷⁵, B. Brickwedde⁹⁷, D. L. Briglin¹⁹, D. Britton⁵⁵, D. Britzger¹¹², I. Brock²², R. Brock¹⁰⁴, G. Brooijmans³⁷, W. K. Brooks^{142d}, E. Brost²⁷, P. A. Bruckman de Renstrom⁸², B. Brüers⁴⁴, D. Bruncko^{26b}, A. Bruni^{21b}, G. Bruni^{21b}, M. Bruschi^{21b}, N. Bruscinò^{70a,70b}, L. Bryngemark¹⁴⁹, T. Buanes¹⁵, Q. Buat¹⁵¹, P. Buchholz¹⁴⁷, A. G. Buckley⁵⁵, I. A. Budagov⁷⁷, M. K. Bugge¹²⁹, O. Bulekov¹⁰⁹, B. A. Bullard⁵⁷, T. J. Burch¹¹⁷, S. Burdin⁸⁸, C. D. Burgard⁴⁴, A. M. Burger¹²⁵, B. Burghgrave⁷, J. T. P. Burr⁴⁴, C. D. Burton¹⁰, J. C. Burzynski¹⁰⁰, V. Büscher⁹⁷, P. J. Bussey⁵⁵, J. M. Butler²³, C. M. Buttar⁵⁵, J. M. Butterworth⁹², W. Buttinger¹³⁹, C. J. Buxo Vazquez¹⁰⁴, A. R. Buzykaev^{118a,118b}, G. Cabras^{21b}, S. Cabrera Urbán¹⁶⁹, D. Caforio⁵⁴, H. Cai¹³⁴, V. M. M. Cairo¹⁴⁹, O. Cakir^{3a}, N. Calace³⁴, P. Calafiura¹⁶, G. Calderini¹³¹, P. Calfayan⁶³, G. Callea⁵⁵, L. P. Caloba^{78b}, S. Calvente Lopez⁹⁶, D. Calvet³⁶, S. Calvet³⁶, T. P. Calvet⁹⁹, M. Calvetti^{69a,69b}, R. Camacho Toro¹³¹, S. Camarda³⁴, D. Camarero Munoz⁹⁶, P. Camarri^{71a,71b}, M. T. Camerlingo^{72a,72b}, D. Cameron¹²⁹, C. Camincher¹⁷¹, M. Campanelli⁹², A. Camplani³⁸, V. Canale^{67a,67b}, A. Canesse¹⁰¹, M. Cano Bret⁷⁵, J. Cantero¹²⁵, Y. Cao¹⁶⁸, F. Capocasa²⁴, M. Capua^{39a,39b}, A. Carbone^{66a,66b}, R. Cardarelli^{71a}, J. C. J. Cardenas⁷, F. Cardillo¹⁶⁹, G. Carducci^{39a,39b}, T. Carli³⁴, G. Carlino^{67a}, B. T. Carlson¹³⁴, E. M. Carlson^{163a,171}, L. Carminati^{66a,66b}, M. Carnesale^{70a,70b}, R. M. D. Carney¹⁴⁹, S. Caron¹¹⁵, E. Carquin^{142d}, S. Carrá⁴⁴, G. Carratta^{21a,21b}, J. W. S. Carter¹⁶², T. M. Carter⁴⁸, D. Casadei^{31c}, M. P. Casado^{12h}, A. F. Casha¹⁶², E. G. Castiglia¹⁷⁸, F. L. Castillo^{59a}, L. Castillo Garcia¹², V. Castillo Gimenez¹⁶⁹, N. F. Castro^{135a,135c}, A. Catinaccio³⁴, J. R. Catmore¹²⁹, A. Cattai³⁴, V. Cavaliere²⁷, N. Cavalli^{21a,21b}, V. Cavasinni^{69a,69b}, E. Celebi^{11b}, F. Celli¹³⁰, M. S. Centonze^{65a,65b}, K. Cerny¹²⁶, A. S. Cerqueira^{78a}, A. Cerri¹⁵², L. Cerrito^{71a,71b}, F. Cerutti¹⁶, A. Cervelli^{21b}, S. A. Cetin^{11b}, Z. Chadi^{33a}, D. Chakraborty¹¹⁷, M. Chala^{135f}, J. Chan¹⁷⁶, W. S. Chan¹¹⁶, W. Y. Chan⁸⁸, J. D. Chapman³⁰, B. Chargeishvili^{155b}, D. G. Charlton¹⁹, T. P. Charman⁹⁰, M. Chatterjee¹⁸, S. Chekanov⁵, S. V. Chekulaev^{163a}, G. A. Chelkov^{77,ag}, A. Chen¹⁰³, B. Chen¹⁵⁷, C. Chen^{58a}, C. H. Chen⁷⁶, H. Chen^{13c}, H. Chen²⁷, J. Chen^{58c}, J. Chen²⁴, S. Chen¹³², S. J. Chen^{13c}, X. Chen^{58c}, X. Chen^{13b}, Y. Chen^{58a}, Y-H. Chen⁴⁴, C. L. Cheng¹⁷⁶, H. C. Cheng^{60a}, A. Cheplakov⁷⁷, E. Cheremushkina⁴⁴, E. Cherepanova⁷⁷, R. Cherkaoui El Moursli^{33e}, E. Cheu⁶, K. Cheung⁶¹, L. Chevalier¹⁴⁰, V. Chiarella⁴⁹, G. Chiarelli^{69a}, G. Chiodini^{65a}, A. S. Chisholm¹⁹, A. Chitan^{25b}, Y. H. Chiu¹⁷¹, M. V. Chizhov^{77,t}, K. Choi¹⁰, A. R. Chomont^{70a,70b}, Y. Chou¹⁰⁰, E. Y. S. Chow¹¹⁶, L. D. Christopher^{31f}, M. C. Chu^{60a}, X. Chu^{13a,13d}, J. Chudoba¹³⁶, J. J. Chwastowski⁸², D. Cieri¹¹², K. M. Ciesla⁸², V. Cindro⁸⁹, I. A. Cioară^{25b}, A. Ciocio¹⁶, F. Ciroto^{67a,67b}, Z. H. Citron^{175,l}, M. Citterio^{66a}, D. A. Ciubotaru^{25b}, B. M. Ciungu¹⁶², A. Clark⁵², P. J. Clark⁴⁸, J. M. Clavijo Columbie⁴⁴, S. E. Clawson⁹⁸, C. Clement^{43a,43b}, L. Clissa^{21a,21b}, Y. Coadou⁹⁹, M. Cobal^{64a,64c}, A. Coccaro^{53b}, J. Cochran⁷⁶, R. F. Coelho Barrue^{135a}, R. Coelho Lopes De Sa¹⁰⁰, S. Coelli^{66a}, H. Cohen¹⁵⁷, A. E. C. Coimbra³⁴, B. Cole³⁷, J. Collot⁵⁶, P. Conde Muñio^{135a,135h}, S. H. Connell^{31c}, I. A. Connelly⁵⁵, E. I. Conroy¹³⁰, F. Conventi^{67a,am}, H. G. Cooke¹⁹, A. M. Cooper-Sarkar¹³⁰, F. Cormier¹⁷⁰, L. D. Corpe³⁴, M. Corradi^{70a,70b}, E. E. Corrigan⁹⁴, F. Corriveau^{101,aa}, M. J. Costa¹⁶⁹, F. Costanza⁴, D. Costanzo¹⁴⁵, B. M. Cote¹²³, G. Cowan⁹¹, J. W. Cowley³⁰, K. Cranmer¹²¹, S. Crépe-Renaudin⁵⁶, F. Crescioli¹³¹, M. Cristinziani¹⁴⁷, M. Cristoforetti^{73a,73b,b}, V. Croft¹⁶⁵, G. Crosetti^{39a,39b}, A. Cueto³⁴, T. Cuhadar Donszelmann¹⁶⁶, H. Cui^{13a,13d}, A. R. Cukierman¹⁴⁹, W. R. Cunningham⁵⁵, P. Czodrowski³⁴, M. M. Czurylo^{59b}, M. J. Da Cunha Sargedas De Sousa^{58a}, J. V. Da Fonseca Pinto^{78b}, C. Da Via⁹⁸, W. Dabrowski^{81a}, T. Dado⁴⁵, S. Dabhi^{31f}, T. Dai¹⁰³, C. Dallapiccola¹⁰⁰, M. Dam³⁸, G. D'amen²⁷, V. D'Amico^{72a,72b}, J. Damp⁹⁷, J. R. Dandoy¹³², M. F. Daneri²⁸, M. Danninger¹⁴⁸, V. Dao³⁴, G. Darbo^{53b}, S. Darmora⁵, A. Dattagupta¹²⁷, S. D'Auria^{66a,66b}, C. David^{163b}, T. Davidek¹³⁸, D. R. Davis⁴⁷, B. Davis-Purcell³², I. Dawson⁹⁰, K. De⁷, R. De Asmundis^{67a}, M. De Beurs¹¹⁶, S. De Castro^{21a,21b}, N. De Groot¹¹⁵, P. de Jong¹¹⁶, H. De la Torre¹⁰⁴, A. De Maria^{13c}, D. De Pedis^{70a}, A. De Salvo^{70a}, U. De Sanctis^{71a,71b}, M. De Santis^{71a,71b}, A. De Santo¹⁵², J. B. De Vivie De Regie⁵⁶, D. V. Dedovich⁷⁷, J. Degens¹¹⁶, A. M. Deiana⁴⁰, J. Del Peso⁹⁶, Y. Delabat Diaz⁴⁴, F. Deliot¹⁴⁰, C. M. Delitzsch⁶, M. Della Pietra^{67a,67b}, D. Della Volpe⁵², A. Dell'Acqua³⁴, L. Dell'Asta^{66a,66b}, M. Delmastro⁴, P. A. Delsart⁵⁶, S. Demers¹⁷⁸, M. Demichev⁷⁷, S. P. Denisov¹¹⁹, L. D'Eramo¹¹⁷, D. Derendarz⁸², J. E. Derkaoui^{33d}, F. Derue¹³¹, P. Dervan⁸⁸, K. Desch²², K. Dette¹⁶², C. Deutsch²², P. O. Deviveiros³⁴, F. A. Di Bello^{70a,70b}, A. Di Ciaccio^{71a,71b}, L. Di Ciaccio⁴, C. Di Donato^{67a,67b}, A. Di Girolamo³⁴, G. Di Gregorio^{69a,69b}, A. Di Luca^{73a,73b}, B. Di Micco^{72a,72b}, R. Di Nardo^{72a,72b}, C. Diaconu⁹⁹, F. A. Dias¹¹⁶, T. Dias Do Vale^{135a}, M. A. Diaz^{142a}, F. G. Diaz Capriles²², J. Dickinson¹⁶, M. Didenko¹⁶⁹, E. B. Diehl¹⁰³, J. Dietrich¹⁷, S. Díez Cornell⁴⁴, C. Díez Pardos¹⁴⁷, A. Dimitrievska¹⁶, W. Ding^{13b}, J. Dingfelder²², I-M. Dinu^{25b}



S. J. Dittmeier^{59b}, F. Dittus³⁴, F. Djama⁹⁹, T. Djobava^{155b}, J. I. Djuvsland¹⁵, M. A. B. Do Vale¹⁴³, D. Dodsworth²⁴, C. Doglioni⁹⁴, J. Dolejsi¹³⁸, Z. Dolezal¹³⁸, M. Donadelli^{78c}, B. Dong^{58c}, J. Donini³⁶, A. D'onofrio^{13c}, M. D'Onofrio⁸⁸, J. Dopke¹³⁹, A. Doria^{67a}, M. T. Dova⁸⁶, A. T. Doyle⁵⁵, E. Drechsler¹⁴⁸, E. Dreyer¹⁴⁸, T. Dreyer⁵¹, A. S. Drobac¹⁶⁵, D. Du^{58b}, T. A. du Pree¹¹⁶, F. Dubinin¹⁰⁸, M. Dubovsky^{26a}, A. Dubreuil⁵², E. Duchovni¹⁷⁵, G. Duckeck¹¹¹, O. A. Ducu^{25b,34}, D. Duda¹¹², A. Dudarev³⁴, M. D'uffizi⁹⁸, L. Dufflot⁶², M. Dührssen³⁴, C. Dülsen¹⁷⁷, A. E. Dumitriu^{25b}, M. Dunford^{59a}, S. Dungs⁴⁵, K. Dunne^{43a,43b}, A. Duperrin⁹⁹, H. Duran Yildiz^{3a}, M. Düren⁵⁴, A. Durglishvili^{155b}, B. Dutta⁴⁴, B. L. Dwyer¹¹⁷, G. I. Dyckes¹³², M. Dyndal^{81a}, S. Dysch⁹⁸, B. S. Dziedzic⁸², B. Eckerova^{26a}, M. G. Eggleston⁴⁷, E. Egidio Purcino De Souza^{78b}, L. F. Ehrke⁵², T. Eifert⁷, G. Eigen¹⁵, K. Einsweiler¹⁶, T. Ekelof¹⁶⁷, Y. El Ghazali^{33b}, H. El Jarrari^{33e}, A. El Moussaouy^{33a}, V. Ellajosyula¹⁶⁷, M. Ellert¹⁶⁷, F. Ellinghaus¹⁷⁷, A. A. Elliot⁹⁰, N. Ellis³⁴, J. Elmsheuser²⁷, M. Elsing³⁴, D. Emelianov¹³⁹, A. Emerman³⁷, Y. Enari¹⁵⁹, J. Erdmann⁴⁵, A. Ereditato¹⁸, P. A. Erland⁸², M. Errenst¹⁷⁷, M. Escalier⁶², C. Escobar¹⁶⁹, O. Estrada Pastor¹⁶⁹, E. Etzion¹⁵⁷, G. Evans^{135a}, H. Evans⁶³, M. O. Evans¹⁵², A. Ezhilov¹³³, F. Fabbri⁵⁵, L. Fabbri^{21a,21b}, V. Fabiani¹¹⁵, G. Facini¹⁷³, V. Fadeyev¹⁴¹, R. M. Fakhruddinov¹¹⁹, S. Falciano^{70a}, P. J. Falke²², S. Falke³⁴, J. Faltova¹³⁸, Y. Fan^{13a}, Y. Fang^{13a}, Y. Fang^{13a}, G. Fanourakis⁴², M. Fanti^{66a,66b}, M. Faraj^{58c}, A. Farbin⁷, A. Farilla^{72a}, E. M. Farina^{68a,68b}, T. Farooque¹⁰⁴, S. M. Farrington⁴⁸, P. Farthouat³⁴, F. Fassi^{33c}, D. Fassouliotis⁸, M. Fauci Giannelli^{71a,71b}, W. J. Fawcett³⁰, L. Fayard⁶², O. L. Fedin^{133,q}, M. Feickert¹⁶⁸, L. Feligioni⁹⁹, A. Fell¹⁴⁵, C. Feng^{58b}, M. Feng^{13b}, M. J. Fenton¹⁶⁶, A. B. Fenyuk¹¹⁹, S. W. Ferguson⁴¹, J. Ferrando⁴⁴, A. Ferrari¹⁶⁷, P. Ferrari¹¹⁶, R. Ferrari^{68a}, D. Ferrere⁵², C. Ferretti¹⁰³, F. Fiedler⁹⁷, A. Filipčić⁸⁹, F. Filthaut¹¹⁵, M. C. N. Fiolhais^{135a,135c,a}, L. Fiorini¹⁶⁹, F. Fischer¹⁴⁷, W. C. Fisher¹⁰⁴, T. Fitschen¹⁹, I. Fleck¹⁴⁷, P. Fleischmann¹⁰³, T. Flick¹⁷⁷, B. M. Flierl¹¹¹, L. Flores¹³², L. R. Flores Castillo^{60a}, F. M. Follega^{73a,73b}, N. Fomin¹⁵, J. H. Foo¹⁶², B. C. Forland⁶³, A. Formica¹⁴⁰, F. A. Förster¹², A. C. Forti⁹⁸, E. Fortin⁹⁹, M. G. Foti¹³⁰, L. Fountas⁸, D. Fournier⁶², H. Fox⁸⁷, P. Francavilla^{69a,69b}, S. Francescato⁵⁷, M. Franchini^{21a,21b}, S. Franchino^{59a}, D. Francis³⁴, L. Franco⁴, L. Franconi¹⁸, M. Franklin⁵⁷, G. Frattari^{70a,70b}, A. C. Freegard⁹⁰, P. M. Freeman¹⁹, W. S. Freund^{78b}, E. M. Freundlich⁴⁵, D. Froidevaux³⁴, J. A. Frost¹³⁰, Y. Fu^{58a}, M. Fujimoto¹²², E. Fullana Torregrosa¹⁶⁹, J. Fuster¹⁶⁹, A. Gabrielli^{21a,21b}, A. Gabrielli³⁴, P. Gadow⁴⁴, G. Gagliardi^{53a,53b}, L. G. Gagnon¹⁶, G. E. Gallardo¹³⁰, E. J. Gallas¹³⁰, B. J. Gallop¹³⁹, R. Gamboa Goni⁹⁰, K. K. Gan¹²³, S. Ganguly¹⁷⁵, J. Gao^{58a}, Y. Gao⁴⁸, Y. S. Gao^{29,n}, F. M. Garay Walls^{142a}, C. García¹⁶⁹, J. E. García Navarro¹⁶⁹, J. A. García Pascual^{13a}, M. Garcia-Sciveres¹⁶, R. W. Gardner³⁵, D. Garg⁷⁵, S. Gargiulo⁵⁰, C. A. Garner¹⁶², V. Garonne¹²⁹, S. J. Gasiorowski¹⁴⁴, P. Gaspar^{78b}, G. Gaudio^{68a}, P. Gauzzi^{70a,70b}, I. L. Gavrilenko¹⁰⁸, A. Gavriilyuk¹²⁰, C. Gay¹⁷⁰, G. Gaycken⁴⁴, E. N. Gazis⁹, A. A. Geanta^{25b}, C. M. Gee¹⁴¹, C. N. P. Gee¹³⁹, J. Geisen⁹⁴, M. Geisen⁹⁷, C. Gemme^{53b}, M. H. Genest⁵⁶, S. Gentile^{70a,70b}, S. George⁹¹, W. F. George¹⁹, T. Gerialis⁴², L. O. Gerlach⁵¹, P. Gessinger-Befurt³⁴, M. Ghasemi Bostanabad¹⁷¹, M. Ghneimat¹⁴⁷, A. Ghosh¹⁶⁶, A. Ghosh⁷⁵, B. Giacobbe^{21b}, S. Giagu^{70a,70b}, N. Giangiacomi¹⁶², P. Giannetti^{69a}, A. Giannini^{67a,67b}, S. M. Gibson⁹¹, M. Gignac¹⁴¹, D. T. Gil^{81b}, B. J. Gilbert³⁷, D. Gillberg³², G. Gilles¹¹⁶, N. E. K. Gillwald⁴⁴, D. M. Gingrich^{2,al}, M. P. Giordani^{64a,64c}, P. F. Giraud¹⁴⁰, G. Giugliarelli^{64a,64c}, D. Giugni^{66a}, F. Giuli^{71a,71b}, I. Gkialas^{8,i}, P. Gkoutoumis⁹, L. K. Gladilin¹¹⁰, C. Glasman⁹⁶, G. R. Gledhill¹²⁷, M. Glisic¹²⁷, I. Gnesi^{39b,d}, M. Goblirsch-Kolb²⁴, D. Godin¹⁰⁷, S. Goldfarb¹⁰², T. Golling⁵², D. Golubkov¹¹⁹, J. P. Gombas¹⁰⁴, A. Gomes^{135a,135b}, R. Goncalves Gama⁵¹, R. Gonçalves^{135a,135c}, G. Gonella¹²⁷, L. Gonella¹⁹, A. Gongadze⁷⁷, F. Gonnella¹⁹, J. L. Gonski³⁷, S. González de la Hoz¹⁶⁹, S. Gonzalez Fernandez¹², R. Gonzalez Lopez⁸⁸, C. Gonzalez Renteria¹⁶, R. Gonzalez Suarez¹⁶⁷, S. Gonzalez-Sevilla⁵², G. R. Gonzalvo Rodriguez¹⁶⁹, R. Y. González Andana^{142a}, L. Goossens³⁴, N. A. Gorasia¹⁹, P. A. Gorbounov¹²⁰, H. A. Gordon²⁷, B. Gorini³⁴, E. Gorini^{65a,65b}, A. Gorišek⁸⁹, A. T. Goshaw⁴⁷, M. I. Gostkin⁷⁷, C. A. Gottardo¹¹⁵, M. Goughri^{33b}, V. Goumarre⁴⁴, A. G. Goussiou¹⁴⁴, N. Govender^{31c}, C. Goy⁴, I. Grabowska-Bold^{81a}, K. Graham³², E. Gramstad¹²⁹, S. Grancagnolo¹⁷, M. Grandi¹⁵², V. Gratchev¹³³, P. M. Gravila^{25f}, F. G. Gravili^{65a,65b}, H. M. Gray¹⁶, C. Grefe²², I. M. Gregor⁴⁴, P. Grenier¹⁴⁹, K. Grevtsov⁴⁴, C. Grieco¹², N. A. Grieser¹²⁴, A. A. Grillo¹⁴¹, K. Grimm^{29,m}, S. Grinstein^{12,x}, J.-F. Grivaz⁶², S. Groh⁹⁷, E. Gross¹⁷⁵, J. Grosse-Knetter⁵¹, C. Grud¹⁰³, A. Grummer¹¹⁴, J. C. Grundy¹³⁰, L. Guan¹⁰³, W. Guan¹⁷⁶, C. Gubbels¹⁷⁰, J. Guenther³⁴, J. G. R. Guerrero Rojas¹⁶⁹, F. Guescini¹¹², D. Guest¹⁷, R. Gugel⁹⁷, A. Guida⁴⁴, T. Guillemain⁴, S. Guindon³⁴, J. Guo^{58c}, L. Guo⁶², Y. Guo¹⁰³, R. Gupta⁴⁴, S. Gurbuz²², G. Gustavino¹²⁴, M. Guth⁵², P. Gutierrez¹²⁴, L. F. Gutierrez Zagazeta¹³², C. Gutschow⁹², C. Guyot¹⁴⁰, C. Gwenlan¹³⁰, C. B. Gwilliam⁸⁸, E. S. Haaland¹²⁹, A. Haas¹²¹, M. Habedank¹⁷, C. Haber¹⁶, H. K. Hadavand⁷


A. Hadeef⁹⁷ , S. Hadzic¹¹² , M. Haleem¹⁷² , J. Haley¹²⁵ , J. J. Hall¹⁴⁵ , G. Halladjian¹⁰⁴ , G. D. Hallowell⁹⁹ , L. Halser¹⁸ , K. Hamano¹⁷¹ , H. Hamdaoui^{33c} , M. Hamer²² , G. N. Hamity⁴⁸ , K. Han^{58a} , L. Han^{13c} , L. Han^{58a} , S. Han¹⁶ , Y. F. Han¹⁶² , K. Hanagaki^{79.v} , M. Hance¹⁴¹ , M. D. Hank³⁵ , R. Hankache⁹⁸ , E. Hansen⁹⁴ , J. B. Hansen³⁸ , J. D. Hansen³⁸ , M. C. Hansen²² , P. H. Hansen³⁸ , K. Hara¹⁶⁴ , T. Harenberg¹⁷⁷ , S. Harkusha¹⁰⁵ , Y. T. Harris¹³⁰ , P. F. Harrison¹⁷³ , N. M. Hartman¹⁴⁹ , N. M. Hartmann¹¹¹ , Y. Hasegawa¹⁴⁶ , A. Hasib⁴⁸ , S. Hassani¹⁴⁰ , S. Haug¹⁸ , R. Hauser¹⁰⁴ , M. Havranek¹³⁷ , C. M. Hawkes¹⁹ , R. J. Hawkins³⁴ , S. Hayashida¹¹³ , D. Hayden¹⁰⁴ , C. Hayes¹⁰³ , R. L. Hayes¹⁷⁰ , C. P. Hays¹³⁰ , J. M. Hays⁹⁰ , H. S. Hayward⁸⁸ , S. J. Haywood¹³⁹ , F. He^{58a} , Y. He¹⁶⁰ , Y. He¹³¹ , M. P. Heath⁴⁸ , V. Hedberg⁹⁴ , A. L. Heggelund¹²⁹ , N. D. Hehir⁹⁰ , C. Heidegger⁵⁰ , K. K. Heidegger⁵⁰ , W. D. Heidorn⁷⁶ , J. Heilman³² , S. Heim⁴⁴ , T. Heim¹⁶ , B. Heinemann^{44.aj} , J. G. Heinlein¹³² , J. J. Heinrich¹²⁷ , L. Heinrich³⁴ , J. Hejbal¹³⁶ , L. Helary⁴⁴ , A. Held¹²¹ , S. Hellesund¹²⁹ , C. M. Helling¹⁴¹ , S. Hellman^{43a,43b} , C. Helsens³⁴ , R. C. W. Henderson⁸⁷ , L. Henkelmann³⁰ , A. M. Henriques Correia³⁴ , H. Herde¹⁴⁹ , Y. Hernández Jiménez¹⁵¹ , H. Herr⁹⁷ , M. G. Herrmann¹¹¹ , T. Herrmann⁴⁶ , G. Herten⁵⁰ , R. Hertenberger¹¹¹ , L. Hervas³⁴ , N. P. Hessey^{163a} , H. Hibi⁸⁰ , S. Higashino⁷⁹ , E. Higón-Rodríguez¹⁶⁹ , K. K. Hill²⁷ , K. H. Hiller⁴⁴ , S. J. Hillier¹⁹ , M. Hils⁴⁶ , I. Hinchliffe¹⁶ , F. Hinterkeuser²² , M. Hirose¹²⁸ , S. Hirose¹⁶⁴ , D. Hirschbuehl¹⁷⁷ , B. Hiti⁸⁹ , O. Hladik¹³⁶ , J. Hobbs¹⁵¹ , R. Hobincu^{25c} , N. Hod¹⁷⁵ , M. C. Hodgkinson¹⁴⁵ , B. H. Hodgkinson³⁰ , A. Hoecker³⁴ , J. Hofer⁴⁴ , D. Hohn⁵⁰ , T. Holm²² , T. R. Holmes³⁵ , M. Holzbock¹¹² , L. B. A. H. Hommels³⁰ , B. P. Honan⁹⁸ , J. Hong^{58c} , T. M. Hong¹³⁴ , J. C. Honig⁵⁰ , A. Hönle¹¹² , B. H. Hooberman¹⁶⁸ , W. H. Hopkins⁵ , Y. Horii¹¹³ , L. A. Horyn³⁵ , S. Hou¹⁵⁴ , J. Howarth⁵⁵ , J. Hoya⁸⁶ , M. Hrabovsky¹²⁶ , A. Hrynevich¹⁰⁶ , T. Hryn'ova⁴ , P. J. Hsu⁶¹ , S.-C. Hsu¹⁴⁴ , Q. Hu³⁷ , S. Hu^{58c} , Y. F. Hu^{13a,13d.an} , D. P. Huang⁹² , X. Huang^{13c} , Y. Huang^{58a} , Y. Huang^{13a} , Z. Hubacek¹³⁷ , F. Hubaut⁹⁹ , M. Huebner²² , F. Huegging²² , T. B. Huffman¹³⁰ , M. Huhtinen³⁴ , R. Hulsken⁵⁶ , N. Huseynov^{77.ab} , J. Huston¹⁰⁴ , J. Huth⁵⁷ , R. Hyneman¹⁴⁹ , S. Hyrych^{26a} , G. Iacobucci⁵² , G. Iakovidis²⁷ , I. Ibragimov¹⁴⁷ , L. Iconomidou-Fayard⁶² , P. Iengo³⁴ , R. Iguchi¹⁵⁹ , T. Iizawa⁵² , Y. Ikegami⁷⁹ , A. Ilg¹⁸ , N. Ilic¹⁶² , H. Imam^{33a} , T. Ingebretsen Carlson^{43a,43b} , G. Introzzi^{68a,68b} , M. Iodice^{72a} , V. Ippolito^{70a,70b} , M. Ishino¹⁵⁹ , W. Islam¹²⁵ , C. Issever^{17.44} , S. Istin^{11c.ao} , J. M. Iturbe Ponce^{60a} , R. Iuppa^{73a,73b} , A. Ivina¹⁷⁵ , J. M. Izen⁴¹ , V. Izzo^{67a} , P. Jacka¹³⁶ , P. Jackson¹ , R. M. Jacobs⁴⁴ , B. P. Jaeger¹⁴⁸ , C. S. Jagfeld¹¹¹ , G. Jäkel¹⁷⁷ , K. Jakobs⁵⁰ , T. Jakoubek¹⁷⁵ , J. Jamieson⁵⁵ , K. W. Janas^{81a} , G. Jarlskog⁹⁴ , A. E. Jaspan⁸⁸ , N. Javadov^{77.ab} , T. Javůrek³⁴ , M. Javurkova¹⁰⁰ , F. Jeanneau¹⁴⁰ , L. Jeanty¹²⁷ , J. Jejelava^{155a.ac} , P. Jenni^{50.e} , S. Jézéquel⁴ , J. Jia¹⁵¹ , Z. Jia^{13c} , Y. Jiang^{58a} , S. Jiggins⁵⁰ , J. Jimenez Pena¹¹² , S. Jin^{13c} , A. Jinaru^{25b} , O. Jinnouchi¹⁶⁰ , H. Jivan^{31f} , P. Johansson¹⁴⁵ , K. A. Johns⁶ , C. A. Johnson⁶³ , D. M. Jones³⁰ , E. Jones¹⁷³ , R. W. L. Jones⁸⁷ , T. J. Jones⁸⁸ , J. Jovicevic⁵¹ , X. Ju¹⁶ , J. J. Junggeburth³⁴ , A. Juste Rozas^{12.x} , S. Kabana^{142c} , A. Kaczmarska⁸² , M. Kado^{70a,70b} , H. Kagan¹²³ , M. Kagan¹⁴⁹ , A. Kahn³⁷ , C. Kahra⁹⁷ , T. Kaji¹⁷⁴ , E. Kajomovitz¹⁵⁶ , C. W. Kalderon²⁷ , A. Kamenshchikov¹¹⁹ , M. Kaneda¹⁵⁹ , N. J. Kang¹⁴¹ , S. Kang⁷⁶ , Y. Kano¹¹³ , J. Kanzaki⁷⁹ , D. Kar^{31f} , K. Karava¹³⁰ , M. J. Kareem^{163b} , I. Karkanas¹⁵⁸ , S. N. Karpov⁷⁷ , Z. M. Karpova⁷⁷ , V. Kartvelishvili⁸⁷ , A. N. Karyukhin¹¹⁹ , E. Kasimi¹⁵⁸ , C. Kato^{58d} , J. Katzy⁴⁴ , K. Kawade¹⁴⁶ , K. Kawagoe⁸⁵ , T. Kawaguchi¹¹³ , T. Kawamoto¹⁴⁰ , G. Kawamura⁵¹ , E. F. Kay¹⁷¹ , F. I. Kaya¹⁶⁵ , S. Kazakos¹² , V. F. Kazanin^{118a,118b} , Y. Ke¹⁵¹ , J. M. Keaveney^{31a} , R. Keeler¹⁷¹ , J. S. Keller³² , D. Kelsey¹⁵² , J. J. Kempster¹⁹ , J. Kendrick¹⁹ , K. E. Kennedy³⁷ , O. Kepka¹³⁶ , S. Kersten¹⁷⁷ , B. P. Kerševan⁸⁹ , S. Ketabchi Haghighat¹⁶² , M. Khandoga¹³¹ , A. Khanov¹²⁵ , A. G. Kharlamov^{118a,118b} , T. Kharlamova^{118a,118b} , E. E. Khoda¹⁴⁴ , T. J. Khoo¹⁷ , G. Khoriauli¹⁷² , E. Khramov⁷⁷ , J. Khubua^{155b} , S. Kido⁸⁰ , M. Kiehn³⁴ , A. Kilgallon¹²⁷ , E. Kim¹⁶⁰ , Y. K. Kim³⁵ , N. Kimura⁹² , A. Kirchhoff⁵¹ , D. Kirchmeier⁴⁶ , C. Kirfel²²


J. A. Kremer⁹⁷, J. Kretzschmar⁸⁸, K. Kreul¹⁷, P. Krieger¹⁶², F. Krieter¹¹¹, S. Krishnamurthy¹⁰⁰, A. Krishnan^{59b}, M. Krivos¹³⁸, K. Krizka¹⁶, K. Kroeninge⁴⁵, H. Kroha¹¹², J. Kroll¹³⁶, J. Kroll¹³², K. S. Krowpman¹⁰⁴, U. Kruchonak⁷⁷, H. Krüger²², N. Krumnack⁷⁶, M. C. Kruse⁴⁷, J. A. Krzysiak⁸², A. Kubota¹⁶⁰, O. Kuchinskaia¹⁶¹, S. Kuday^{3b}, D. Kuechler⁴⁴, J. T. Kuechler⁴⁴, S. Kuehn³⁴, T. Kuhl⁴⁴, V. Kukhtin⁷⁷, Y. Kulchitsky^{105.af}, S. Kuleshov^{142b}, M. Kumar^{31f}, N. Kumari⁹⁹, M. Kuna⁵⁶, A. Kupco¹³⁶, T. Kupfer⁴⁵, O. Kuprash⁵⁰, H. Kurashige⁸⁰, L. L. Kurchaninov^{163a}, Y. A. Kurochkin¹⁰⁵, A. Kurova¹⁰⁹, M. G. Kurth^{13a,13d}, E. S. Kuwertz³⁴, M. Kuze¹⁶⁰, A. K. Kvam¹⁴⁴, J. Kvita¹²⁶, T. Kwan¹⁰¹, K. W. Kwok^{60a}, C. Lacasta¹⁶⁹, F. Lacava^{70a,70b}, H. Lacker¹⁷, D. Lacour¹³¹, N. N. Lad⁹², E. Ladygin⁷⁷, R. Lafaye⁴, B. Laforge¹³¹, T. Lagouri^{142c}, S. Lai⁵¹, I. K. Lakomic^{81a}, N. Lalloue⁵⁶, J. E. Lambert¹²⁴, S. Lammers⁶³, W. Lampl⁶, C. Lampoudis¹⁵⁸, E. Lançon²⁷, U. Landgraf⁵⁰, M. P. J. Landon⁹⁰, V. S. Lang⁵⁰, J. C. Lange⁵¹, R. J. Langenberg¹⁰⁰, A. J. Lankford¹⁶⁶, F. Lanni²⁷, K. Lantzsch²², A. Lanza^{68a}, A. Lapertosa^{53a,53b}, J. F. Laporte¹⁴⁰, T. Lari^{66a}, F. Lasagni Manghi^{21b}, M. Lassnig³⁴, V. Latonova¹³⁶, T. S. Lau^{60a}, A. Laudrain⁹⁷, A. Laurier³², M. Lavorgna^{67a,67b}, S. D. Lawlor⁹¹, Z. Lawrence⁹⁸, M. Lazzaroni^{66a,66b}, B. Le⁹⁸, B. Leban⁸⁹, A. Lebedev⁷⁶, M. LeBlanc³⁴, T. LeCompte⁵, F. Ledroit-Guillon⁵⁶, A. C. A. Lee⁹², G. R. Lee¹⁵, L. Lee⁵⁷, S. C. Lee¹⁵⁴, S. Lee⁷⁶, L. L. Leeuw^{31c}, B. Lefebvre^{163a}, H. P. Lefebvre⁹¹, M. Lefebvre¹⁷¹, C. Leggett¹⁶, K. Lehmann¹⁴⁸, N. Lehmann¹⁸, G. Lehmann Miotto³⁴, W. A. Leight⁴⁴, A. Leisos^{158.w}, M. A. L. Leite^{78c}, C. E. Leitgeb⁴⁴, R. Leitner¹³⁸, K. J. C. Leney⁴⁰, T. Lenz²², S. Leone^{69a}, C. Leonidopoulos⁴⁸, A. Leopold¹³¹, C. Leroy¹⁰⁷, R. Les¹⁰⁴, C. G. Lester³⁰, M. Levchenko¹³³, J. Levêque⁴, D. Levin¹⁰³, L. J. Levinson¹⁷⁵, D. J. Lewis¹⁹, B. Li^{13b}, B. Li^{58b}, C. Li^{58a}, C-Q. Li^{58c,58d}, H. Li^{58a}, H. Li^{58b}, H. Li^{58b}, J. Li^{58c}, K. Li¹⁴⁴, L. Li^{58c}, M. Li^{13a,13d}, Q. Y. Li^{58a}, S. Li^{58c,58d,c}, T. Li^{58b}, X. Li⁴⁴, Y. Li⁴⁴, Z. Li^{58b}, Z. Li¹³⁰, Z. Li¹⁰¹, Z. Li⁸⁸, Z. Liang^{13a}, M. Liberatore⁴⁴, B. Liberti^{71a}, K. Lie^{60c}, K. Lin¹⁰⁴, R. A. Linck⁶³, R. E. Lindley⁶, J. H. Lindon², A. Linss⁴⁴, E. Lipeles¹³², A. Lipniacka¹⁵, T. M. Liss^{168.ak}, A. Lister¹⁷⁰, J. D. Little⁷, B. Liu^{13a}, B. X. Liu¹⁴⁸, J. B. Liu^{58a}, J. K. K. Liu³⁵, K. Liu^{58c,58d}, M. Liu^{58a}, M. Y. Liu^{58a}, P. Liu^{13a}, X. Liu^{58a}, Y. Liu⁴⁴, Y. Liu^{13c,13d}, Y. L. Liu¹⁰³, Y. W. Liu^{58a}, M. Livan^{68a,68b}, A. Lleres⁵⁶, J. Llorente Merino¹⁴⁸, S. L. Lloyd⁹⁰, E. M. Lobodzinska⁴⁴, P. Loch⁶, S. Loffredo^{71a,71b}, T. Lohse¹⁷, K. Lohwasser¹⁴⁵, M. Lokajicek¹³⁶, J. D. Long¹⁶⁸, I. Longarini^{70a,70b}, L. Longo³⁴, R. Longo¹⁶⁸, I. Lopez Paz¹², A. Lopez Solis⁴⁴, J. Lorenz¹¹¹, N. Lorenzo Martinez⁴, A. M. Lory¹¹¹, A. Lösle⁵⁰, X. Lou^{43a,43b}, X. Lou^{13a}, A. Lounis⁶², J. Love⁵, P. A. Love⁸⁷, J. J. Lozano Bahilo¹⁶⁹, G. Lu^{13a,13d}, M. Lu^{58a}, S. Lu¹³², Y. J. Lu⁶¹, H. J. Lubatti¹⁴⁴, C. Luci^{70a,70b}, F. L. Lucio Alves^{13c}, A. Lucotte⁵⁶, F. Luehring⁶³, I. Luise¹⁵¹, L. Luminari^{70a}, O. Lundberg¹⁵⁰, B. Lund-Jensen¹⁵⁰, N. A. Luongo¹²⁷, M. S. Lutz¹⁵⁷, D. Lynn²⁷, H. Lyons⁸⁸, R. Lysak¹³⁶, E. Lytken⁹⁴, F. Lyu^{13a}, V. Lyubushkin⁷⁷, T. Lyubushkina⁷⁷, H. Ma²⁷, L. L. Ma^{58b}, Y. Ma⁹², D. M. Mac Donell¹⁷¹, G. Maccarrone⁴⁹, C. M. Macdonald¹⁴⁵, J. C. MacDonald¹⁴⁵, R. Madar³⁶, W. F. Mader⁴⁶, M. Madugoda Ralalage Don¹²⁵, N. Madysa⁴⁶, J. Maeda⁸⁰, T. Maeno²⁷, M. Maerker⁴⁶, V. Magerl⁵⁰, J. Magro^{64a,64c}, D. J. Mahon³⁷, C. Maidantchik^{78b}, A. Maio^{135a,135b,135d}, K. Maj^{81a}, O. Majersky^{26a}, S. Majewski¹²⁷, N. Makovec⁶², B. Malaescu¹³¹, Pa. Malecki⁸², V. P. Maleev¹³³, F. Malek⁵⁶, D. Malito^{39a,39b}, U. Mallik⁷⁵, C. Malone³⁰, S. Maltezos⁹, S. Malyukov⁷⁷, J. Mamuzic¹⁶⁹, G. Mancini⁴⁹, J. P. Mandalia⁹⁰, I. Mandić⁸⁹, L. Manhaes de Andrade Filho^{78a}, I. M. Maniatis¹⁵⁸, M. Manisha¹⁴⁰, J. Manjarres Ramos⁴⁶, K. H. Mankinen⁹⁴, A. Mann¹¹¹, A. Manousos⁷⁴, B. Mansoulie¹⁴⁰, I. Manthos¹⁵⁸, S. Manzoni¹¹⁶, A. Marantis^{158.w}, G. Marchiori¹³¹, M. Marcisovsky¹³⁶, L. Marcoccia^{71a,71b}, C. Marcon⁹⁴, M. Marjanovic¹²⁴, Z. Marshall¹⁶, S. Marti-Garcia¹⁶⁹, T. A. Martin¹⁷³, V. J. Martin⁴⁸, B. Martin dit Latour¹⁵, L. Martinelli^{70a,70b}, M. Martinez^{12.x}, P. Martinez Agullo¹⁶⁹, V. I. Martinez Outschoorn¹⁰⁰, S. Martin-Haugh¹³⁹, V. S. Martoiu^{25b}, A. C. Martyniuk⁹², A. Marzin³⁴, S. R. Maschek¹¹², L. Masetti⁹⁷, T. Mashimo¹⁵⁹, J. Masik⁹⁸, A. L. Maslennikov^{118a,118b}, L. Massa^{21b}, P. Massarotti^{67a,67b}, P. Mastrandrea^{69a,69b}, A. Mastroberardino^{39a,39b}, T. Masubuchi¹⁵⁹, D. Matakias²⁷, T. Mathisen¹⁶⁷, A. Matic¹¹¹, N. Matsuzawa¹⁵⁹, J. Maurer^{25b}, B. Maček⁸⁹, D. A. Maximov^{118a,118b}, R. Mazini¹⁵⁴, I. Maznas¹⁵⁸, S. M. Mazza¹⁴¹, C. Mc Ginn²⁷, J. P. Mc Gowan¹⁰¹, S. P. Mc Kee¹⁰³, T. G. McCarthy¹¹², W. P. McCormack¹⁶, E. F. McDonald¹⁰², A. E. McDougall¹¹⁶, J. A. Mcfayden¹⁵², G. Mchedlidze^{155b}, M. A. McKay⁴⁰, K. D. McLean¹⁷¹, S. J. McMahon¹³⁹, P. C. McNamara¹⁰², R. A. McPherson^{171.aa}, J. E. Mdhuli^{31f}, Z. A. Meadows¹⁰⁰, S. Meehan³⁴, T. Megy³⁶, S. Mehlhase¹¹¹, A. Mehta⁸⁸, B. Meirose⁴¹, D. Melini¹⁵⁶, B. R. Mellado Garcia^{31f}, A. H. Melo⁵¹, F. Meloni⁴⁴, A. Melzer²², E. D. Mendes Gouveia^{135a}, A. M. Mendes Jacques Da Costa¹⁹, H. Y. Meng¹⁶², L. Meng³⁴, S. Menke¹¹², M. Mentink³⁴, E. Meoni^{39a,39b}, C. Merlassino¹³⁰, P. Mermod^{52.*}, L. Merola^{67a,67b}, C. Meroni^{66a}, G. Merz¹⁰³, O. Meshkov^{108,110}, J. K. R. Meshreki¹⁴⁷, J. Metcalfe⁵, A. S. Mete⁵, C. Meyer⁶³,




J-P. Meyer¹⁴⁰, M. Michetti¹⁷, R. P. Middleton¹³⁹, L. Mijović⁴⁸, G. Mikenberg¹⁷⁵, M. Mikestikova¹³⁶, M. Mikuz⁸⁹, H. Mildner¹⁴⁵, A. Milic¹⁶², C. D. Milke⁴⁰, D. W. Miller³⁵, L. S. Miller³², A. Milov¹⁷⁵, D. A. Milstead^{43a,43b}, T. Min^{13c}, A. A. Minaenko¹¹⁹, I. A. Minashvili^{155b}, L. Mince⁵⁵, A. I. Mincer¹²¹, B. Mindur^{81a}, M. Mineev⁷⁷, Y. Minegishi¹⁵⁹, Y. Mino⁸³, L. M. Mir¹², M. Miralles Lopez¹⁶⁹, M. Mironova¹³⁰, T. Mitani¹⁷⁴, V. A. Mitsou¹⁶⁹, M. Mittal^{58c}, O. Miu¹⁶², P. S. Miyagawa⁹⁰, Y. Miyazaki⁸⁵, A. Mizukami⁷⁹, J. U. Mjörnmark⁹⁴, T. Mkrtchyan^{59a}, M. Mlynarikova¹¹⁷, T. Moa^{43a,43b}, S. Mobius⁵¹, K. Mochizuki¹⁰⁷, P. Moder⁴⁴, P. Mogg¹¹¹, A. F. Mohammed^{13a}, S. Mohapatra³⁷, G. Mokgatitswane^{31f}, B. Mondal¹⁴⁷, S. Mondal¹³⁷, K. Mönig⁴⁴, E. Monnier⁹⁹, A. Montalbano¹⁴⁸, J. Montejo Berlingen³⁴, M. Montella¹²³, F. Monticelli⁸⁶, N. Morange⁶², A. L. Moreira De Carvalho^{135a}, M. Moreno Llácer¹⁶⁹, C. Moreno Martinez¹², P. Morettini^{53b}, M. Morgenstern¹⁵⁶, S. Morgenstern¹⁷³, D. Mori¹⁴⁸, M. Morii⁵⁷, M. Morinaga¹⁵⁹, V. Morisbak¹²⁹, A. K. Morley³⁴, A. P. Morris⁹², L. Morvaj³⁴, P. Moschovakos³⁴, B. Moser¹¹⁶, M. Mosidze^{155b}, T. Moskalets⁵⁰, P. Moskvitina¹¹⁵, J. Moss^{29,o}, E. J. W. Moyses¹⁰⁰, S. Muanza⁹⁹, J. Mueller¹³⁴, R. Mueller¹⁸, D. Muenstermann⁸⁷, G. A. Mullier⁹⁴, J. J. Mullin¹³², D. P. Mungo^{66a,66b}, J. L. Munoz Martinez¹², F. J. Munoz Sanchez⁹⁸, M. Murin⁹⁸, P. Murin^{26b}, W. J. Murray^{139,173}, A. Murrone^{66a,66b}, J. M. Muse¹²⁴, M. Muškinja¹⁶, C. Mwewa²⁷, A. G. Myagkov^{119,ag}, A. J. Myers⁷, A. A. Myers¹³⁴, G. Myers⁶³, M. Myska¹³⁷, B. P. Nachman¹⁶, O. Nackenhorst⁴⁵, A. Nag Nag⁴⁶, K. Nagai¹³⁰, K. Nagano⁷⁹, J. L. Nagle²⁷, E. Nagy⁹⁹, A. M. Nairz³⁴, Y. Nakahama¹¹³, K. Nakamura⁷⁹, H. Nanjo¹²⁸, F. Napolitano^{59a}, R. Narayan⁴⁰, I. Naryshkin¹³³, M. Naseri³², C. Nass²², T. Naumann⁴⁴, G. Navarro^{20a}, J. Navarro-Gonzalez¹⁶⁹, R. Nayak¹⁵⁷, P. Y. Nechaeva¹⁰⁸, F. Nechansky⁴⁴, T. J. Neep¹⁹, A. Negri^{68a,68b}, M. Negrini^{21b}, C. Nellist¹¹⁵, C. Nelson¹⁰¹, K. Nelson¹⁰³, S. Nemecek¹³⁶, M. Nessi^{34,g}, M. S. Neubauer¹⁶⁸, F. Neuhaus⁹⁷, J. Neundorff⁴⁴, R. Newhouse¹⁷⁰, P. R. Newman¹⁹, C. W. Ng¹³⁴, Y. S. Ng¹⁷, Y. W. Y. Ng¹⁶⁶, B. Ngair^{33c}, H. D. N. Nguyen⁹⁹, R. B. Nickerson¹³⁰, R. Nicolaidou¹⁴⁰, D. S. Nielsen³⁸, J. Nielsen¹⁴¹, M. Niemeyer⁵¹, N. Nikiforou¹⁰, V. Nikolaenko^{119,ag}, I. Nikolic-Audit¹³¹, K. Nikolopoulos¹⁹, P. Nilsson²⁷, H. R. Nindhito⁵², A. Nisati^{70a}, N. Nishu², R. Nisius¹¹², T. Nitta¹⁷⁴, T. Nobe¹⁵⁹, D. L. Noel³⁰, Y. Noguchi⁸³, I. Nomidis¹³¹, M. A. Nomura²⁷, M. B. Norfolk¹⁴⁵, R. R. B. Norisam⁹², J. Novak⁸⁹, T. Novak⁴⁴, O. Novgorodova⁴⁶, L. Novotny¹³⁷, R. Novotny¹¹⁴, L. Nozka¹²⁶, K. Ntekas¹⁶⁶, E. Nurse⁹², F. G. Oakham^{32,al}, J. Ocariz¹³¹, A. Ochi⁸⁰, I. Ochoa^{135a}, J. P. Ochoa-Ricoux^{142a}, S. Oda⁸⁵, S. Odaka⁷⁹, S. Oerdek¹⁶⁷, A. Ogrodnik^{81a}, A. Oh⁹⁸, C. C. Ohm¹⁵⁰, H. Oide¹⁶⁰, R. Oishi¹⁵⁹, M. L. Ojeda¹⁶², Y. Okazaki⁸³, M. W. O'Keefe⁸⁸, Y. Okumura¹⁵⁹, A. Olariu^{25b}, L. F. Oleiro Seabra^{135a}, S. A. Olivares Pino^{142c}, D. Oliveira Damazio²⁷, D. Oliveira Goncalves^{78a}, J. L. Oliver¹⁶⁶, M. J. R. Olsson¹⁶⁶, A. Olszewski⁸², J. Olszowska⁸², Ö. O. Öncel²², D. C. O'Neil¹⁴⁸, A. P. O'Neill¹³⁰, A. Onofre^{135a,135c}, P. U. E. Onyisi¹⁰, R. G. Oreamuno Madriz¹¹⁷, M. J. Oreglia³⁵, G. E. Orellana⁸⁶, D. Orestano^{72a,72b}, N. Orlando¹², R. S. Orr¹⁶², V. O'Shea⁵⁵, R. Ospanov^{58a}, G. Otero y Garzon²⁸, H. Otono⁸⁵, P. S. Ott^{59a}, G. J. Ottino¹⁶, M. Ouchrif^{33d}, J. Ouellette²⁷, F. Ould-Saada¹²⁹, A. Ouraou^{140,*}, Q. Ouyang^{13a}, M. Owen⁵⁵, R. E. Owen¹³⁹, K. Y. Oyulmaz^{11c}, V. E. Ozcan^{11c}, N. Ozturk⁷, S. Ozturk^{11c}, J. Pacalt¹²⁶, H. A. Pacey³⁰, K. Pachal⁴⁷, A. Pacheco Pages¹², C. Padilla Aranda¹², S. Pagan Griso¹⁶, G. Palacino⁶³, S. Palazzo⁴⁸, S. Palestini³⁴, M. Palka^{81b}, P. Palni^{81a}, D. K. Panchal¹⁰, C. E. Pandini⁵², J. G. Panduro Vazquez⁹¹, P. Pani⁴⁴, G. Panizzo^{64a,64c}, L. Paolozzi⁵², C. Papadatos¹⁰⁷, S. Parajuli⁴⁰, A. Paramonov⁵, C. Paraskevopoulos⁹, D. Paredes Hernandez^{60b}, S. R. Paredes Saenz¹³⁰, B. Parida¹⁷⁵, T. H. Park¹⁶², A. J. Parker²⁹, M. A. Parker³⁰, F. Parodi^{53a,53b}, E. W. Parrish¹¹⁷, J. A. Parsons³⁷, U. Parzefall⁵⁰, L. Pascual Dominguez¹⁵⁷, V. R. Pascuzzi¹⁶, F. Pasquali¹¹⁶, E. Pasqualucci^{70a}, S. Passaggio^{53b}, F. Pastore⁹¹, P. Pasuwan^{43a,43b}, J. R. Pater⁹⁸, A. Pathak¹⁷⁶, J. Patton⁸⁸, T. Pauly³⁴, J. Pearkes¹⁴⁹, M. Pedersen¹²⁹, L. Pedraza Diaz¹¹⁵, R. Pedro^{135a}, T. Peiffer⁵¹, S. V. Peleganchuk^{118a,118b}, O. Penc¹³⁶, C. Peng^{60b}, H. Peng^{58a}, M. Penzin¹⁶¹, B. S. Peralva^{78a}, M. M. Perego⁶², A. P. Pereira Peixoto^{135a}, L. Pereira Sanchez^{43a,43b}, D. V. Perepelitsa²⁷, E. Perez Codina^{163a}, M. Perganti⁹, L. Perini^{66a,66b}, H. Pernegger³⁴, S. Perrella³⁴, A. Perrevoort¹¹⁶, K. Peters⁴⁴, R. F. Y. Peters⁹⁸, B. A. Petersen³⁴, T. C. Petersen³⁸, E. Petit⁹⁹, V. Petousis¹³⁷, C. Petridou¹⁵⁸, P. Petroff⁶², F. Petrucci^{72a,72b}, M. Pettee¹⁷⁸, N. E. Pettersson³⁴, K. Petukhova¹³⁸, A. Peyaud¹⁴⁰, R. Pezoa^{142d}, L. Pezzotti³⁴, G. Pezzullo¹⁷⁸, T. Pham¹⁰², P. W. Phillips¹³⁹, M. W. Phipps¹⁶⁸, G. Piacquadio¹⁵¹, E. Pianori¹⁶, F. Piazza^{66a,66b}, A. Picazio¹⁰⁰, R. Piegai²⁸, D. Pietreanu^{25b}, J. E. Pilcher³⁵, A. D. Pilkington⁹⁸, M. Pinamonti^{64a,64c}, J. L. Pinfold², C. Pitman Donaldson⁹², D. A. Pizzi³², L. Pizzimento^{71a,71b}, A. Pizzini¹¹⁶, M.-A. Pleier²⁷, V. Plesanovs⁵⁰, V. Pleskot¹³⁸, E. Plotnikova⁷⁷, P. Podberczko^{118a,118b}, R. Poettgen⁹⁴, R. Poggi⁵², L. Poggioni¹³¹, I. Pogrebnyak¹⁰⁴, D. Pohl²², I. Pokharel⁵¹, G. Polesello^{68a}, A. Poley^{148,163a}, A. Policicchio^{70a,70b}, R. Polifka¹³⁸, A. Polini^{21b}, C. S. Pollard¹³⁰, Z. B. Pollock¹²³, V. Polychronakos²⁷, D. Ponomarenko¹⁰⁹

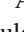
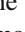



L. Pontecorvo³⁴ , S. Popa^{25a} , G. A. Popeneciu^{25d} , L. Portales⁴ , D. M. Portillo Quintero^{163a} , S. Pospisil¹³⁷ , P. Postolache^{25c} , K. Potamianos¹³⁰ , I. N. Potrap⁷⁷ , C. J. Potter³⁰ , H. Potti¹ , T. Poulsen⁴⁴ , J. Poveda¹⁶⁹ , T. D. Powell¹⁴⁵ , G. Pownall⁴⁴ , M. E. Pozo Astigarraga³⁴ , A. Prades Ibanez¹⁶⁹ , P. Pralavorio⁹⁹ , M. M. Prapa⁴² , S. Prell⁷⁶ , D. Price⁹⁸ , M. Primavera^{65a} , M. A. Principe Martin⁹⁶ , M. L. Proffitt¹⁴⁴ , N. Proklova¹⁰⁹ , K. Prokofiev^{60c} , F. Prokoshin⁷⁷ , S. Protopopescu²⁷ , J. Proudfoot⁵ , M. Przybycien^{81a} , D. Pudzha¹³³ , P. Puzo⁶² , D. Pyatiizbyantseva¹⁰⁹ , J. Qian¹⁰³ , Y. Qin⁹⁸ , T. Qiu⁹⁰ , A. Quadt⁵¹ , M. Queitsch-Maitland³⁴ , G. Rabanal Bolanos⁵⁷ , F. Ragusa^{66a,66b} , G. Rahal⁹⁵ , J. A. Raine⁵² , S. Rajagopalan²⁷ , K. Ran^{13a,13d} , D. F. Rassloff^{59a} , D. M. Rauch⁴⁴ , S. Rave⁹⁷ , B. Ravina⁵⁵ , I. Ravinovich¹⁷⁵ , M. Raymond³⁴ , A. L. Read¹²⁹ , N. P. Readioff¹⁴⁵

, D. M. Rebutti^{68a,68b} , G. Redlinger²⁷ , K. Reeves⁴¹ , D. Reikher¹⁵⁷ , A. Reiss⁹⁷ , A. Rej¹⁴⁷ , C. Rembser³⁴ , A. Renardi⁴⁴ , M. Renda^{25b} , M. B. Rendel¹¹² , A. G. Rennie⁵⁵ , S. Resconi^{66a} , E. D. Resseguie¹⁶ , S. Rettie⁹² , B. Reynolds¹²³ , E. Reynolds¹⁹ , M. Rezaei Estabragh¹⁷⁷ , O. L. Rezanova^{118a,118b} , P. Reznicek¹³⁸ , E. Ricci^{73a,73b} , R. Richter¹¹² , S. Richter⁴⁴ , E. Richter-Was^{81b} , M. Ridel¹³¹ , P. Rieck¹¹² , P. Riedler³⁴ , O. Rifki⁴⁴ , M. Rijssenbeek¹⁵¹ , A. Rimoldi^{68a,68b} , M. Rimoldi⁴⁴ , L. Rinaldi^{21a,21b} , T. T. Rinn¹⁶⁸ , M. P. Rinnagel¹¹¹ , G. Ripellino¹⁵⁰ , I. Riu¹² , P. Rivadeneira⁴⁴ , J. C. Rivera Vergara¹⁷¹ , F. Rizatdinova¹²⁵ , E. Rizvi⁹⁰ , C. Rizzi⁵² , B. A. Roberts¹⁷³ , S. H. Robertson^{101,aa} , M. Robin⁴⁴ , D. Robinson³⁰ , C. M. Robles Gajardo^{142d} , M. Robles Manzano⁹⁷ , A. Robson⁵⁵ , A. Rocchi^{71a,71b} , C. Roda^{69a,69b} , S. Rodriguez Bosca^{59a} , A. Rodriguez Rodriguez⁵⁰ , A. M. Rodríguez Vera^{163b}

, S. Roe³⁴ , A. R. Roepe¹²⁴ , J. Roggel¹⁷⁷ , O. Röhne¹²⁹ , R. A. Rojas^{142d} , B. Roland⁵⁰ , C. P. A. Roland⁶³ , J. Roloff²⁷ , A. Romaniouk¹⁰⁹ , M. Romano^{21b} , A. C. Romero Hernandez¹⁶⁸ , N. Rompotis⁸⁸ , M. Ronzani¹²¹ , L. Roos¹³¹ , S. Rosati^{70a} , B. J. Rosser¹³² , E. Rossi¹⁶² , E. Rossi⁴ , E. Rossi^{67a,67b} , L. P. Rossi^{53b} , L. Rossini⁴⁴ , R. Rosten¹²³ , M. Rotaru^{25b} , B. Rottler⁵⁰ , D. Rousseau⁶² , D. Rouso³⁰ , G. Rovelli^{68a,68b} , A. Roy¹⁰ , A. Rozanov⁹⁹ , Y. Rozen¹⁵⁶ , X. Ruan^{31f} , A. J. Ruby⁸⁸ , T. A. Ruggeri¹ , F. Rühr⁵⁰ , A. Ruiz-Martinez¹⁶⁹ , A. Rummler³⁴ , Z. Rurikova⁵⁰ , N. A. Rusakovich⁷⁷ , H. L. Russell³⁴ , L. Rustige³⁶ , J. P. Rutherford⁶ , E. M. Rüttinger¹⁴⁵ , M. Rybar¹³⁸ , E. B. Rye¹²⁹ , A. Ryzhov¹¹⁹ , J. A. Sabater Iglesias⁴⁴ , P. Sabatini¹⁶⁹ , L. Sabetta^{70a,70b} , H. F-W. Sadrozinski¹⁴¹ , R. Sadykov⁷⁷ , F. Safai Tehrani^{70a} , B. Safarzadeh Samani¹⁵²

, M. Safdari¹⁴⁹ , P. Saha¹¹⁷ , S. Saha¹⁰¹ , M. Sahinsoy¹¹² , A. Sahu¹⁷⁷ , M. Saimpert¹⁴⁰ , M. Saito¹⁵⁹ , T. Saito¹⁵⁹ , D. Salamani³⁴ , G. Salamanna^{72a,72b} , A. Salnikov¹⁴⁹ , J. Salt¹⁶⁹ , A. Salvador Salas¹² , D. Salvatore^{39a,39b} , F. Salvatore¹⁵² , A. Salzburger³⁴ , D. Sammel⁵⁰ , D. Sampsonidis¹⁵⁸ , D. Sampsonidou^{58c,58d} , J. Sánchez¹⁶⁹ , A. Sanchez Pineda⁴ , V. Sanchez Sebastian¹⁶⁹ , H. Sandaker¹²⁹ , C. O. Sander⁴⁴ , I. G. Sanderswood⁸⁷ , J. A. Sandesara¹⁰⁰ , M. Sandhoff¹⁷⁷ , C. Sandoval^{20b} , D. P. C. Sankey¹³⁹ , M. Sannino^{53a,53b} , Y. Sano¹¹³ , A. Sansoni⁴⁹ , C. Santoni³⁶ , H. Santos^{135a,135b} , S. N. Santpur¹⁶ , A. Santra¹⁷⁵ , K. A. Saoucha¹⁴⁵ , A. Sapronov⁷⁷ , J. G. Saraiva^{135a,135d} , J. Sardain⁹⁹ , O. Sasaki⁷⁹ , K. Sato¹⁶⁴ , C. Sauer^{59b} , F. Sauerburger⁵⁰ , E. Sauvan⁴ , P. Savard^{162,al} , R. Sawada¹⁵⁹ , C. Sawyer¹³⁹ , L. Sawyer⁹³ , I. Sayago Galvan¹⁶⁹ , C. Sbarra^{21b} , A. Sbrizzi^{64a,64c}

, T. Scanlon⁹² , J. Schaarschmidt¹⁴⁴ , P. Schacht¹¹² , D. Schaefer³⁵ , U. Schäfer⁹⁷ , A. C. Schaffer⁶² , D. Schaile¹¹¹ , R. D. Schamberger¹⁵¹ , E. Schanet¹¹¹ , C. Scharf¹⁷ , N. Scharmberg⁹⁸ , V. A. Schegelsky¹³³ , D. Scheirich¹³⁸ , F. Schenck¹⁷ , M. Schernau¹⁶⁶ , C. Schiavi^{53a,53b} , L. K. Schildgen²² , Z. M. Schillaci²⁴ , E. J. Schioppa^{65a,65b} , M. Schioppa^{39a,39b} , B. Schlag⁹⁷ , K. E. Schleicher⁵⁰ , S. Schlenker³⁴ , K. Schmieden⁹⁷ , C. Schmitt⁹⁷ , S. Schmitt⁴⁴ , L. Schoeffel¹⁴⁰ , A. Schoening^{59b} , P. G. Scholer⁵⁰ , E. Schopf¹³⁰ , M. Schott⁹⁷ , J. Schovancova³⁴ , S. Schramm⁵² , F. Schroeder¹⁷⁷ , H-C. Schultz-Coulon^{59a} , M. Schumacher⁵⁰ , B. A. Schumm¹⁴¹ , Ph. Schune¹⁴⁰ , A. Schwartzman¹⁴⁹ , T. A. Schwarz¹⁰³ , Ph. Schwemling¹⁴⁰ , R. Schwienhorst¹⁰⁴ , A. Sciandra¹⁴¹ , G. Sciolla²⁴ , F. Scuri^{69a} , F. Scutti¹⁰² , C. D. Sebastiani⁸⁸ , K. Sedlaczek⁴⁵ , P. Seema¹⁷ , S. C. Seidel¹¹⁴ , A. Seiden¹⁴¹ , B. D. Seidlitz²⁷

, T. Seiss³⁵ , C. Seitz⁴⁴ , J. M. Seixas^{78b} , G. Sekhniaidze^{67a} , S. J. Sekula⁴⁰ , L. Selem⁴ , N. Semprini-Cesari^{21a,21b} , S. Sen⁴⁷ , C. Serfon²⁷ , L. Serin⁶² , L. Serkin^{64a,64b} , M. Sessa^{72a,72b} , H. Severini¹²⁴ , S. Sevova¹⁴⁹ , F. Sforza^{53a,53b} , A. Sfyrla⁵² , E. Shabalina⁵¹ , R. Shaheen¹⁵⁰ , J. D. Shahinian¹³² , N. W. Shaikh^{43a,43b} , D. Shaked Renous¹⁷⁵ , L. Y. Shan^{13a} , M. Shapiro¹⁶ , A. Sharma³⁴ , A. S. Sharma¹ , S.

J. Smiesko¹³⁸ , S. Yu. Smirnov¹⁰⁹ , Y. Smirnov¹⁰⁹ , L. N. Smirnova^{110,s} , O. Smirnova⁹⁴ , E. A. Smith³⁵ , H. A. Smith¹³⁰ , M. Smizanska⁸⁷ , K. Smolek¹³⁷ , A. Smykiewicz⁸² , A. A. Snesarev¹⁰⁸ , H. L. Snoek¹¹⁶ , S. Snyder²⁷ , R. Sobie^{171,aa} , A. Soffer¹⁵⁷ , F. Sohns⁵¹ , C. A. Solans Sanchez³⁴ , E. Yu. Soldatov¹⁰⁹ , U. Soldevila¹⁶⁹ , A. A. Solodkov¹¹⁹ , S. Solomon⁵⁰ , A. Soloshenko⁷⁷ , O. V. Solovyanov¹¹⁹ , V. Solovyev¹³³ , P. Sommer¹⁴⁵ , H. Son¹⁶⁵ , A. Sonay¹² , W. Y. Song^{163b} , A. Sopczak¹³⁷ , A. L. Sapiro⁹² , F. Sopkova^{26b} , S. Sottocornola^{68a,68b} , R. Soualah^{64a,64c} , A. M. Soukharev^{118a,118b} , Z. Soumami^{33e} , D. South⁴⁴ , S. Spagnolo^{65a,65b} , M. Spalla¹¹² , M. Spangenberg¹⁷³ , F. Spanò⁹¹ , D. Sperlich⁵⁰ , T. M. Spieker^{59a} , G. Spigo³⁴ , M. Spina¹⁵² , D. P. Spiteri⁵⁵ , M. Spousta¹³⁸ , A. Stabile^{66a,66b} , R. Stamen^{59a} , M. Stamenkovic¹¹⁶ , A. Stampekis¹⁹ , M. Standke²² , E. Stanecka⁸²

, B. Stanislaus³⁴ , M. M. Stanitzki⁴⁴ , M. Stankaityte¹³⁰ , B. Stapf⁴⁴ , E. A. Starchenko¹¹⁹ , G. H. Stark¹⁴¹ , J. Stark⁹⁹ , D. M. Starko^{163b} , P. Staroba¹³⁶ , P. Starovoitov^{59a} , S. Stärz¹⁰¹ , R. Staszewski⁸² , G. Stavropoulos⁴² , P. Steinberg²⁷ , A. L. Steinhebel¹²⁷ , B. Stelzer^{148,163a} , H. J. Stelzer¹³⁴ , O. Stelzer-Chilton^{163a} , H. Stenzel⁵⁴ , T. J. Stevenson¹⁵² , G. A. Stewart³⁴ , M. C. Stockton³⁴ , G. Stoica^{25b} , M. Stolarski^{135a} , S. Stonjek¹¹² , A. Straessner⁴⁶ , J. Strandberg¹⁵⁰ , S. Strandberg^{43a,43b} , M. Strauss¹²⁴ , T. Streblor⁹⁹ , P. Strizenc^{26b} , R. Ströhmer¹⁷² , D. M. Strom¹²⁷ , L. R. Strom⁴⁴ , R. Stroynowski⁴⁰ , A. Strubig^{43a,43b} , S. A. Stucci²⁷ , B. Stugu¹⁵ , J. Stupak¹²⁴ , N. A. Styles⁴⁴ , D. Su¹⁴⁹ , S. Su^{58a} , W. Su^{58c,58d,144} , X. Su^{58a} , N. B. Suarez¹³⁴ , K. Sugizaki¹⁵⁹ , V. V. Sulim¹⁰⁸ , M. J. Sullivan⁸⁸ , D. M. S. Sultan⁵² , S. Sultansoy^{3c} , T. Sumida⁸³ , S. Sun¹⁰³

, S. Sun¹⁷⁶ , X. Sun⁹⁸ , O. Sunneborn Guadagnoli¹⁶⁷ , C. J. E. Suster¹⁵³ , M. R. Sutton¹⁵² , M. Svatos¹³⁶ , M. Swiatkowski^{163a} , T. Swirski¹⁷² , I. Sykora^{26a} , M. Sykora¹³⁸ , T. Sykora¹³⁸ , D. Ta⁹⁷ , K. Tackmann^{44,y} , A. Taffard¹⁶⁶ , R. Tafirout^{163a} , E. Tagiev¹¹⁹ , R. H. M. Taibah¹³¹ , R. Takashima⁸⁴ , K. Takeda⁸⁰ , T. Takeshita¹⁴⁶ , E. P. Takeva⁴⁸ , Y. Takubo⁷⁹ , M. Talby⁹⁹ , A. A. Talyshv^{118a,118b} , K. C. Tam^{60b} , N. M. Tamir¹⁵⁷ , A. Tanaka¹⁵⁹ , J. Tanaka¹⁵⁹ , R. Tanaka⁶² , Z. Tao¹⁷⁰ , S. Tapia Araya⁷⁶ , S. Tapprogge⁹⁷ , A. Tarek Abouelfadl Mohamed¹⁰⁴ , S. Tarem¹⁵⁶ , K. Tariq^{58b} , G. Tarna^{25b,f} , G. F. Tartarelli^{66a} , P. Tas¹³⁸ , M. Tasevsky¹³⁶ , E. Tassi^{39a,39b} , G. Tateno¹⁵⁹ , Y. Tayalati^{33e} , G. N. Taylor¹⁰² , W. Taylor^{163b} , H. Teagle⁸⁸ , A. S. Tee¹⁷⁶ , R. Teixeira De Lima¹⁴⁹ , P. Teixeira-Dias⁹¹ , H. Ten Kate³⁴ , J. J. Teoh¹¹⁶ , K. Terashi¹⁵⁹ , J. Terron⁹⁶

, S. Terzo¹² , M. Testa⁴⁹ , R. J. Teuscher^{162,aa} , N. Themistokleous⁴⁸ , T. Theveneaux-Pelzer¹⁷ , O. Thielmann¹⁷⁷ , D. W. Thomas⁹¹ , J. P. Thomas¹⁹ , E. A. Thompson⁴⁴ , P. D. Thompson¹⁹ , E. Thomson¹³² , E. J. Thorpe⁹⁰ , Y. Tian⁵¹ , V. Tikhomirov^{108,ah} , Yu. A. Tikhonov^{118a,118b} , S. Timoshenko¹⁰⁹ , P. Tipton¹⁷⁸ , S. Tisserant⁹⁹ , S. H. Tlou^{31f} , A. Tnourji³⁶ , K. Todome^{21a,21b} , S. Todorova-Nova¹³⁸ , S. Todt⁴⁶ , M. Togawa⁷⁹ , J. Tojo⁸⁵ , S. Tokár^{26a} , K. Tokushuku⁷⁹ , E. Tolley¹²³ , R. Tombs³⁰ , M. Tomoto^{79,113} , L. Tompkins¹⁴⁹ , P. Tornambe¹⁰⁰ , E. Torrence¹²⁷ , H. Torres⁴⁶ , E. Torró Pastor¹⁶⁹ , M. Toscani²⁸ , C. Tosciri³⁵ , J. Toth^{99,z} , D. R. Tovey¹⁴⁵ , A. Traet¹⁵ , C. J. Treado¹²¹ , T. Trefzger¹⁷² , A. Tricoli²⁷ , I. M. Trigger^{163a} , S. Trincaz-Duvoid¹³¹ , D. A. Trischuk¹⁷⁰ , W. Trischuk¹⁶² , B. Trocmé⁵⁶ , A. Trofymov⁶² , C. Troncon^{66a} , F. Trovato¹⁵² , L. Truong^{31c}

, M. Trzebinski⁸² , A. Trzupek⁸² , F. Tsai¹⁵¹ , A. Tsiamis¹⁵⁸ , P. V. Tsiarehka^{105,af} , A. Tsirigotis^{158,w} , V. Tsiskaridze¹⁵¹ , E. G. Tskhadadze^{155a} , M. Tsopoulou¹⁵⁸ , I. I. Tsukerman¹²⁰ , V. Tsulaia¹⁶ , S. Tsuno⁷⁹ , O. Tsur¹⁵⁶ , D. Tsybychev¹⁵¹ , Y. Tu^{60b} , A. Tudorache^{25b} , V. Tudorache^{25b} , A. N. Tuna³⁴ , S. Turchikhin⁷⁷ , I. Turk Cakir^{3b,u} , R. J. Turner¹⁹ , R. Turra^{66a} , P. M. Tuts³⁷ , S. Tzamarias¹⁵⁸ , P. Tzanis⁹ , E. Tzovara⁹⁷ , K. Uchida¹⁵⁹ , F. Ukegawa¹⁶⁴ , G. Unal³⁴ , M. Unal¹⁰ , A. Undrus²⁷ , G. Unel¹⁶⁶ , F. C. Ungaro¹⁰² , K. Uno¹⁵⁹ , J. Urban^{26b} , P. Urquijo¹⁰² , G. Usai⁷ , R. Ushioda¹⁶⁰ , M. Usman¹⁰⁷ , Z. Uysal^{11d} , V. Vacek¹³⁷ , B. Vachon¹⁰¹ , K. O. H. Vadla¹²⁹ , T. Vafeiadis³⁴ , C. Valderanis¹¹¹ , E. Valdes Santurio^{43a,43b} , M. Valente^{163a} , S. Valentinetti^{21a,21b} , A. Valero¹⁶⁹ , L. Valéry⁴⁴ , R. A. Vallance¹⁹ , A. Vallier⁹⁹ , J.
A. Valls Ferrer¹⁶⁹ , T. R. Van Daalen¹⁴⁴ , P. Van Gemmeren⁵ , S. Van Stroud⁹² , I. Van Vulpen¹¹⁶ , M. Vanadia^{71a,71b} , W. Vandelli³⁴ , M. Vandenbroucke¹⁴⁰ , E. R. Vandewall¹²⁵ , D. Vannicola¹⁵⁷ , L. Vannoli^{53a,53b} , R. Vari^{70a} , E. W. Varnes⁶ , C. Varni¹⁶ , T. Varol¹⁵⁴ , D. Varouchas⁶² , K. E. Varvell¹⁵³ , M. E. Vasile^{25b} , L. Vaslin³⁶ , G. A. Vasquez¹⁷¹ , F. Vazeille³⁶ , D. Vazquez Furelos¹² , T. Vazquez Schroeder³⁴ , J. Veatch⁵¹ , V. Vecchio⁹⁸

M. Vranjes Milosavljevic¹⁴, V. Vrba^{137,*}, M. Vreeswijk¹¹⁶, N. K. Vu⁹⁹, R. Vuillermet³⁴, O. V. Vujinovic⁹⁷, I. Vukotic³⁵, S. Wada¹⁶⁴, C. Wagner¹⁰⁰, W. Wagner¹⁷⁷, S. Wahdan¹⁷⁷, H. Wahlberg⁸⁶, R. Wakasa¹⁶⁴, M. Wakida¹¹³, V. M. Walbrecht¹¹², J. Walder¹³⁹, R. Walker¹¹¹, S. D. Walker⁹¹, W. Walkowiak¹⁴⁷, A. M. Wang⁵⁷, A. Z. Wang¹⁷⁶, C. Wang^{58a}, C. Wang^{58c}, H. Wang¹⁶, J. Wang^{60a}, P. Wang⁴⁰, R.-J. Wang⁹⁷, R. Wang⁵⁷, R. Wang¹¹⁷, S. M. Wang¹⁵⁴, S. Wang^{58b}, T. Wang^{58a}, W. T. Wang^{58a}, W. X. Wang^{58a}, X. Wang^{13c}, X. Wang¹⁶⁸, Y. Wang^{58a}, Z. Wang¹⁰³, C. Wanotayaroj³⁴, A. Warburton¹⁰¹, C. P. Ward³⁰, R. J. Ward¹⁹, N. Warrack⁵⁵, A. T. Watson¹⁹, M. F. Watson¹⁹, G. Watts¹⁴⁴, B. M. Waugh⁹², A. F. Webb¹⁰, C. Weber²⁷, M. S. Weber¹⁸, S. A. Weber³², S. M. Weber^{59a}, C. Wei^{58a}, Y. Wei¹³⁰, A. R. Weidberg¹³⁰, J. Weingarten⁴⁵, M. Weirich⁹⁷, C. Weiser⁵⁰, T. Wenaus²⁷, B. Wendland⁴⁵, T. Wengler³⁴, S. Wenig³⁴, N. Vermes²², M. Wessels^{59a}, K. Whalen¹²⁷, A. M. Wharton⁸⁷, A. S. White⁵⁷, A. White⁷, M. J. White¹, D. Whiteson¹⁶⁶, L. Wickremasinghe¹²⁸, W. Wiedenmann¹⁷⁶, C. Wiel⁴⁶, M. Wielers¹³⁹, N. Wieseotte⁹⁷, C. Wiglesworth³⁸, L. A. M. Wiik-Fuchs⁵⁰, D. J. Wilbern¹²⁴, H. G. Wilkens³⁴, L. J. Wilkins⁹¹, D. M. Williams³⁷, H. H. Williams¹³², S. Williams³⁰, S. Willocq¹⁰⁰, P. J. Windischhofer¹³⁰, I. Wingerter-Seez⁴, F. Winklmeier¹²⁷, B. T. Winter⁵⁰, M. Wittgen¹⁴⁹, M. Wobisch⁹³, A. Wolf⁹⁷, R. Wölker¹³⁰, J. Wollrath¹⁶⁶, M. W. Wolter⁸², H. Wolters^{135a,135c}, V. W. S. Wong¹⁷⁰, A. F. Wongel⁴⁴, S. D. Worm⁴⁴, B. K. Wosiek⁸², K. W. Woźniak⁸², K. Wraight⁵⁵, J. Wu^{13a,13d}, S. L. Wu¹⁷⁶, X. Wu⁵², Y. Wu^{58a}, Z. Wu^{58a,140}, J. Wuerzinger¹³⁰, T. R. Wyatt⁹⁸, B. M. Wynne⁴⁸, S. Xella³⁸, M. Xia^{13b}, J. Xiang^{60c}, X. Xiao¹⁰³, M. Xie^{58a}, X. Xie^{58a}, I. Xioidis¹⁵², D. Xu^{13a}, H. Xu^{58a}, H. Xu^{58a}, L. Xu^{58a}, R. Xu¹³², T. Xu^{58a}, W. Xu¹⁰³, Y. Xu^{13b}, Z. Xu^{58b}, Z. Xu¹⁴⁹, B. Yabsley¹⁵³, S. Yacoub^{31a}, N. Yamaguchi⁸⁵, Y. Yamaguchi¹⁶⁰, M. Yamatani¹⁵⁹, H. Yamauchi¹⁶⁴, T. Yamazaki¹⁶, Y. Yamazaki⁸⁰, J. Yan^{58c}, S. Yan¹³⁰, Z. Yan²³, H. J. Yang^{58c,58d}, H. T. Yang¹⁶, S. Yang^{58a}, T. Yang^{60c}, X. Yang^{58a}, X. Yang^{13a}, Y. Yang¹⁵⁹, Z. Yang^{58a,103}, W.-M. Yao¹⁶, Y. C. Yap⁴⁴, H. Ye^{13c}, J. Ye⁴⁰, S. Ye²⁷, I. Yeletsikh⁷⁷, M. R. Yexley⁸⁷, P. Yin³⁷, K. Yorita¹⁷⁴, K. Yoshihara⁷⁶, C. J. S. Young⁵⁰, C. Young¹⁴⁹, R. Yuan^{58b,j}, X. Yue^{59a}, M. Zaazoua^{33e}, B. Zabinski⁸², G. Zacharis⁹, E. Zaid⁴⁸, A. M. Zaitsev^{119,ag}, T. Zakareishvili^{155b}, N. Zakharchuk³², S. Zambito³⁴, D. Zanzi⁵⁰, S. V. Zeibner⁴⁵, C. Zeitnitz¹⁷⁷, J. C. Zeng¹⁶⁸, O. Zenin¹¹⁹, T. Ženiš^{26a}, S. Zenz⁹⁰, S. Zerradi^{33a}, D. Zerwas⁶², M. Zgubič¹³⁰, B. Zhang^{13c}, D. F. Zhang^{13b}, G. Zhang^{13b}, J. Zhang⁵, K. Zhang^{13a}, L. Zhang^{13c}, M. Zhang¹⁶⁸, R. Zhang¹⁷⁶, S. Zhang¹⁰³, X. Zhang^{58c}, X. Zhang^{58b}, Z. Zhang⁶², P. Zhao⁴⁷, Y. Zhao¹⁴¹, Z. Zhao^{58a}, A. Zhemchugov⁷⁷, Z. Zheng¹⁴⁹, D. Zhong¹⁶⁸, B. Zhou¹⁰³, C. Zhou¹⁷⁶, H. Zhou⁶, N. Zhou^{58c}, Y. Zhou⁶, C. G. Zhu^{58b}, C. Zhu^{13a,13d}, H. L. Zhu^{58a}, H. Zhu^{13a}, J. Zhu¹⁰³, Y. Zhu^{58a}, X. Zhuang^{13a}, K. Zhukov¹⁰⁸, V. Zhulanov^{118a,118b}, D. Zieminska⁶³, N. I. Zimine⁷⁷, S. Zimmermann^{50,*}, J. Zinsser^{59b}, M. Ziolkowski¹⁴⁷, L. Živković¹⁴, A. Zoccoli^{21a,21b}, K. Zoch⁵², T. G. Zorbas¹⁴⁵, O. Zormpa⁴², W. Zou³⁷, L. Zwalinski³⁴

¹ Department of Physics, University of Adelaide, Adelaide, Australia

² Department of Physics, University of Alberta, Edmonton, AB, Canada

³ (a) Department of Physics, Ankara University, Ankara, Turkey; (b) Application and Research Center for Advanced Studies, Istanbul Aydin University, Istanbul, Turkey; (c) Division of Physics, TOBB University of Economics and Technology, Ankara, Turkey

⁴ LAPP, Univ. Savoie Mont Blanc, CNRS/IN2P3, Annecy, France

⁵ High Energy Physics Division, Argonne National Laboratory, Argonne, IL, USA

⁶ Department of Physics, University of Arizona, Tucson, AZ, USA

⁷ Department of Physics, University of Texas at Arlington, Arlington, TX, USA

⁸ Physics Department, National and Kapodistrian University of Athens, Athens, Greece

⁹ Physics Department, National Technical University of Athens, Zografou, Greece

¹⁰ Department of Physics, University of Texas at Austin, Austin, TX, USA

¹¹ (a) Faculty of Engineering and Natural Sciences, Bahcesehir University, Istanbul, Turkey; (b) Faculty of Engineering and Natural Sciences, Istanbul Bilgi University, Istanbul, Turkey; (c) Department of Physics, Bogazici University, Istanbul, Turkey; (d) Department of Physics Engineering, Gaziantep University, Gaziantep, Turkey

¹² Institut de Física d'Altes Energies (IFAE), Barcelona Institute of Science and Technology, Barcelona, Spain

¹³ (a) Institute of High Energy Physics, Chinese Academy of Sciences, Beijing, China; (b) Physics Department, Tsinghua University, Beijing, China; (c) Department of Physics, Nanjing University, Nanjing, China; (d) University of Chinese Academy of Science (UCAS), Beijing, China

¹⁴ Institute of Physics, University of Belgrade, Belgrade, Serbia

¹⁵ Department for Physics and Technology, University of Bergen, Bergen, Norway

- ¹⁶ Physics Division, Lawrence Berkeley National Laboratory and University of California, Berkeley, CA, USA
- ¹⁷ Institut für Physik, Humboldt Universität zu Berlin, Berlin, Germany
- ¹⁸ Albert Einstein Center for Fundamental Physics and Laboratory for High Energy Physics, University of Bern, Bern, Switzerland
- ¹⁹ School of Physics and Astronomy, University of Birmingham, Birmingham, UK
- ²⁰ ^(a)Facultad de Ciencias y Centro de Investigaciones, Universidad Antonio Nariño, Bogotá, Colombia; ^(b)Departamento de Física, Universidad Nacional de Colombia, Bogotá, Colombia
- ²¹ ^(a)Dipartimento di Fisica e Astronomia A. Righi, Università di Bologna, Bologna, Italy; ^(b)INFN Sezione di Bologna, Bologna, Italy
- ²² Physikalisches Institut, Universität Bonn, Bonn, Germany
- ²³ Department of Physics, Boston University, Boston, MA, USA
- ²⁴ Department of Physics, Brandeis University, Waltham, MA, USA
- ²⁵ ^(a)Transilvania University of Brasov, Brasov, Romania; ^(b)Horia Hulubei National Institute of Physics and Nuclear Engineering, Bucharest, Romania; ^(c)Department of Physics, Alexandru Ioan Cuza University of Iasi, Iasi, Romania; ^(d)National Institute for Research and Development of Isotopic and Molecular Technologies, Physics Department, Cluj-Napoca, Romania; ^(e)University Politehnica Bucharest, Bucharest, Romania; ^(f)West University in Timisoara, Timisoara, Romania
- ²⁶ ^(a)Faculty of Mathematics, Physics and Informatics, Comenius University, Bratislava, Slovak Republic; ^(b)Department of Subnuclear Physics, Institute of Experimental Physics of the Slovak Academy of Sciences, Kosice, Slovak Republic
- ²⁷ Physics Department, Brookhaven National Laboratory, Upton, NY, USA
- ²⁸ Universidad de Buenos Aires, Facultad de Ciencias Exactas y Naturales, Departamento de Física, y CONICET, Instituto de Física de Buenos Aires (IFIBA), Buenos Aires, Argentina
- ²⁹ California State University, Long Beach, CA, USA
- ³⁰ Cavendish Laboratory, University of Cambridge, Cambridge, UK
- ³¹ ^(a)Department of Physics, University of Cape Town, Cape Town, South Africa; ^(b)iThemba Labs, Western Cape, South Africa; ^(c)Department of Mechanical Engineering Science, University of Johannesburg, Johannesburg, South Africa; ^(d)National Institute of Physics, University of the Philippines Diliman (Philippines), Quezon City, Philippines; ^(e)University of South Africa, Department of Physics, Pretoria, South Africa; ^(f)School of Physics, University of the Witwatersrand, Johannesburg, South Africa
- ³² Department of Physics, Carleton University, Ottawa, ON, Canada
- ³³ ^(a)Faculté des Sciences Ain Chock, Réseau Universitaire de Physique des Hautes Energies-Université Hassan II, Casablanca, Morocco; ^(b)Faculté des Sciences, Université Ibn-Tofail, Kénitra, Morocco; ^(c)Faculté des Sciences Semlalia, Université Cadi Ayyad, LPHEA-Marrakech, Marrakech, Morocco; ^(d)LPMR, Faculté des Sciences, Université Mohamed Premier, Oujda, Morocco; ^(e)Faculté des sciences, Université Mohammed V, Rabat, Morocco
- ³⁴ CERN, Geneva, Switzerland
- ³⁵ Enrico Fermi Institute, University of Chicago, Chicago, IL, USA
- ³⁶ LPC, Université Clermont Auvergne, CNRS/IN2P3, Clermont-Ferrand, France
- ³⁷ Nevis Laboratory, Columbia University, Irvington, NY, USA
- ³⁸ Niels Bohr Institute, University of Copenhagen, Copenhagen, Denmark
- ³⁹ ^(a)Dipartimento di Fisica, Università della Calabria, Rende, Italy; ^(b)INFN Gruppo Collegato di Cosenza, Laboratori Nazionali di Frascati, Frascati, Italy
- ⁴⁰ Physics Department, Southern Methodist University, Dallas, TX, USA
- ⁴¹ Physics Department, University of Texas at Dallas, Richardson, TX, USA
- ⁴² National Centre for Scientific Research “Demokritos”, Agia Paraskevi, Greece
- ⁴³ ^(a)Department of Physics, Stockholm University, Stockholm, Sweden; ^(b)Oskar Klein Centre, Stockholm, Sweden
- ⁴⁴ Deutsches Elektronen-Synchrotron DESY, Hamburg and Zeuthen, Germany
- ⁴⁵ Fakultät Physik, Technische Universität Dortmund, Dortmund, Germany
- ⁴⁶ Institut für Kern- und Teilchenphysik, Technische Universität Dresden, Dresden, Germany
- ⁴⁷ Department of Physics, Duke University, Durham, NC, USA
- ⁴⁸ SUPA-School of Physics and Astronomy, University of Edinburgh, Edinburgh, UK
- ⁴⁹ INFN e Laboratori Nazionali di Frascati, Frascati, Italy
- ⁵⁰ Physikalisches Institut, Albert-Ludwigs-Universität Freiburg, Freiburg, Germany
- ⁵¹ II. Physikalisches Institut, Georg-August-Universität Göttingen, Göttingen, Germany

- 52 Département de Physique Nucléaire et Corpusculaire, Université de Genève, Geneva, Switzerland
- 53 (a)Dipartimento di Fisica, Università di Genova, Genoa, Italy; (b)INFN Sezione di Genova, Genoa, Italy
- 54 II. Physikalisches Institut, Justus-Liebig-Universität Giessen, Giessen, Germany
- 55 SUPA-School of Physics and Astronomy, University of Glasgow, Glasgow, UK
- 56 LPSC, Université Grenoble Alpes, CNRS/IN2P3, Grenoble INP, Grenoble, France
- 57 Laboratory for Particle Physics and Cosmology, Harvard University, Cambridge, MA, USA
- 58 (a)Department of Modern Physics and State Key Laboratory of Particle Detection and Electronics, University of Science and Technology of China, Hefei, China; (b)Institute of Frontier and Interdisciplinary Science and Key Laboratory of Particle Physics and Particle Irradiation (MOE), Shandong University, Qingdao, China; (c)School of Physics and Astronomy, Shanghai Jiao Tong University, Key Laboratory for Particle Astrophysics and Cosmology (MOE), SKLPPC, Shanghai, China; (d)Tsung-Dao Lee Institute, Shanghai, China
- 59 (a)Kirchhoff-Institut für Physik, Ruprecht-Karls-Universität Heidelberg, Heidelberg, Germany; (b)Physikalisches Institut, Ruprecht-Karls-Universität Heidelberg, Heidelberg, Germany
- 60 (a)Department of Physics, Chinese University of Hong Kong, Shatin, N.T., Hong Kong, China; (b)Department of Physics, University of Hong Kong, Hong Kong, China; (c)Department of Physics and Institute for Advanced Study, Hong Kong University of Science and Technology, Clear Water Bay, Kowloon, Hong Kong, China
- 61 Department of Physics, National Tsing Hua University, Hsinchu, Taiwan
- 62 IJCLab, Université Paris-Saclay, CNRS/IN2P3, 91405 Orsay, France
- 63 Department of Physics, Indiana University, Bloomington, IN, USA
- 64 (a)INFN Gruppo Collegato di Udine, Sezione di Trieste, Udine, Italy; (b)ICTP, Trieste, Italy; (c)Dipartimento Politecnico di Ingegneria e Architettura, Università di Udine, Udine, Italy
- 65 (a)INFN Sezione di Lecce, Lecce, Italy; (b)Dipartimento di Matematica e Fisica, Università del Salento, Lecce, Italy
- 66 (a)INFN Sezione di Milano, Milan, Italy; (b)Dipartimento di Fisica, Università di Milano, Milan, Italy
- 67 (a)INFN Sezione di Napoli, Naples, Italy; (b)Dipartimento di Fisica, Università di Napoli, Naples, Italy
- 68 (a)INFN Sezione di Pavia, Pavia, Italy; (b)Dipartimento di Fisica, Università di Pavia, Pavia, Italy
- 69 (a)INFN Sezione di Pisa, Pisa, Italy; (b)Dipartimento di Fisica E. Fermi, Università di Pisa, Pisa, Italy
- 70 (a)INFN Sezione di Roma, Rome, Italy; (b)Dipartimento di Fisica, Sapienza Università di Roma, Rome, Italy
- 71 (a)INFN Sezione di Roma Tor Vergata, Rome, Italy; (b)Dipartimento di Fisica, Università di Roma Tor Vergata, Rome, Italy
- 72 (a)INFN Sezione di Roma Tre, Rome, Italy; (b)Dipartimento di Matematica e Fisica, Università Roma Tre, Rome, Italy
- 73 (a)INFN-TIFPA, Povo, Italy; (b)Università degli Studi di Trento, Trento, Italy
- 74 Institut für Astro- und Teilchenphysik, Leopold-Franzens-Universität, Innsbruck, Austria
- 75 University of Iowa, Iowa City, IA, USA
- 76 Department of Physics and Astronomy, Iowa State University, Ames, IA, USA
- 77 Joint Institute for Nuclear Research, Dubna, Russia
- 78 (a)Departamento de Engenharia Elétrica, Universidade Federal de Juiz de Fora (UFJF), Juiz de Fora, Brazil; (b)Universidade Federal do Rio De Janeiro COPPE/EE/IF, Rio de Janeiro, Brazil; (c)Instituto de Física, Universidade de São Paulo, São Paulo, Brazil
- 79 KEK, High Energy Accelerator Research Organization, Tsukuba, Japan
- 80 Graduate School of Science, Kobe University, Kobe, Japan
- 81 (a)AGH University of Science and Technology, Faculty of Physics and Applied Computer Science, Krakow, Poland; (b)Marian Smoluchowski Institute of Physics, Jagiellonian University, Kraków, Poland
- 82 Institute of Nuclear Physics Polish Academy of Sciences, Kraków, Poland
- 83 Faculty of Science, Kyoto University, Kyoto, Japan
- 84 Kyoto University of Education, Kyoto, Japan
- 85 Research Center for Advanced Particle Physics and Department of Physics, Kyushu University, Fukuoka, Japan
- 86 Instituto de Física La Plata, Universidad Nacional de La Plata and CONICET, La Plata, Argentina
- 87 Physics Department, Lancaster University, Lancaster, UK
- 88 Oliver Lodge Laboratory, University of Liverpool, Liverpool, UK
- 89 Department of Experimental Particle Physics, Jožef Stefan Institute and Department of Physics, University of Ljubljana, Ljubljana, Slovenia
- 90 School of Physics and Astronomy, Queen Mary University of London, London, UK
- 91 Department of Physics, Royal Holloway University of London, Egham, UK

- ⁹² Department of Physics and Astronomy, University College London, London, UK
- ⁹³ Louisiana Tech University, Ruston, LA, USA
- ⁹⁴ Fysiska Institutionen, Lunds Universitet, Lund, Sweden
- ⁹⁵ Centre de Calcul de l'Institut National de Physique Nucléaire et de Physique des Particules (IN2P3), Villeurbanne, France
- ⁹⁶ Departamento de Física Teórica C-15 and CIAFF, Universidad Autónoma de Madrid, Madrid, Spain
- ⁹⁷ Institut für Physik, Universität Mainz, Mainz, Germany
- ⁹⁸ School of Physics and Astronomy, University of Manchester, Manchester, UK
- ⁹⁹ CPPM, Aix-Marseille Université, CNRS/IN2P3, Marseille, France
- ¹⁰⁰ Department of Physics, University of Massachusetts, Amherst, MA, USA
- ¹⁰¹ Department of Physics, McGill University, Montreal, QC, Canada
- ¹⁰² School of Physics, University of Melbourne, Melbourne, VIC, Australia
- ¹⁰³ Department of Physics, University of Michigan, Ann Arbor, MI, USA
- ¹⁰⁴ Department of Physics and Astronomy, Michigan State University, East Lansing, MI, USA
- ¹⁰⁵ B.I. Stepanov Institute of Physics, National Academy of Sciences of Belarus, Minsk, Belarus
- ¹⁰⁶ Research Institute for Nuclear Problems of Byelorussian State University, Minsk, Belarus
- ¹⁰⁷ Group of Particle Physics, University of Montreal, Montreal, QC, Canada
- ¹⁰⁸ P.N. Lebedev Physical Institute of the Russian Academy of Sciences, Moscow, Russia
- ¹⁰⁹ National Research Nuclear University MEPhI, Moscow, Russia
- ¹¹⁰ D.V. Skobeltsyn Institute of Nuclear Physics, M.V. Lomonosov Moscow State University, Moscow, Russia
- ¹¹¹ Fakultät für Physik, Ludwig-Maximilians-Universität München, Munich, Germany
- ¹¹² Max-Planck-Institut für Physik (Werner-Heisenberg-Institut), Munich, Germany
- ¹¹³ Graduate School of Science and Kobayashi-Maskawa Institute, Nagoya University, Nagoya, Japan
- ¹¹⁴ Department of Physics and Astronomy, University of New Mexico, Albuquerque, NM, USA
- ¹¹⁵ Institute for Mathematics, Astrophysics and Particle Physics, Radboud University/Nikhef, Nijmegen, The Netherlands
- ¹¹⁶ Nikhef National Institute for Subatomic Physics and University of Amsterdam, Amsterdam, The Netherlands
- ¹¹⁷ Department of Physics, Northern Illinois University, De Kalb, IL, USA
- ¹¹⁸ ^(a)Budker Institute of Nuclear Physics and NSU, SB RAS, Novosibirsk, Russia; ^(b)Novosibirsk State University, Novosibirsk, Russia
- ¹¹⁹ Institute for High Energy Physics of the National Research Centre Kurchatov Institute, Protvino, Russia
- ¹²⁰ Institute for Theoretical and Experimental Physics named by A.I. Alikhanov of National Research Centre "Kurchatov Institute", Moscow, Russia
- ¹²¹ Department of Physics, New York University, New York, NY, USA
- ¹²² Ochanomizu University, Otsuka, Bunkyo-ku, Tokyo, Japan
- ¹²³ Ohio State University, Columbus, OH, USA
- ¹²⁴ Homer L. Dodge Department of Physics and Astronomy, University of Oklahoma, Norman, OK, USA
- ¹²⁵ Department of Physics, Oklahoma State University, Stillwater, OK, USA
- ¹²⁶ Joint Laboratory of Optics, Palacký University, Olomouc, Czech Republic
- ¹²⁷ Institute for Fundamental Science, University of Oregon, Eugene, OR, USA
- ¹²⁸ Graduate School of Science, Osaka University, Osaka, Japan
- ¹²⁹ Department of Physics, University of Oslo, Oslo, Norway
- ¹³⁰ Department of Physics, Oxford University, Oxford, UK
- ¹³¹ LPNHE, Sorbonne Université, Université Paris Cité, CNRS/IN2P3, Paris, France
- ¹³² Department of Physics, University of Pennsylvania, Philadelphia, PA, USA
- ¹³³ Konstantinov Nuclear Physics Institute of National Research Centre "Kurchatov Institute", PNPI, St. Petersburg, Russia
- ¹³⁴ Department of Physics and Astronomy, University of Pittsburgh, Pittsburgh, PA, USA
- ¹³⁵ ^(a)Laboratório de Instrumentação e Física Experimental de Partículas-LIP, Lisbon, Portugal; ^(b)Departamento de Física, Faculdade de Ciências, Universidade de Lisboa, Lisbon, Portugal; ^(c)Departamento de Física, Universidade de Coimbra, Coimbra, Portugal; ^(d)Centro de Física Nuclear da Universidade de Lisboa, Lisbon, Portugal; ^(e)Departamento de Física, Universidade do Minho, Braga, Portugal; ^(f)Departamento de Física Teórica y del Cosmos, Universidad de Granada, Granada, Spain; ^(g)Dep Física and CEFITEC of Faculdade de Ciências e Tecnologia, Universidade Nova de Lisboa, Caparica, Portugal; ^(h)Instituto Superior Técnico, Universidade de Lisboa, Lisbon, Portugal
- ¹³⁶ Institute of Physics of the Czech Academy of Sciences, Prague, Czech Republic

- 137 Czech Technical University in Prague, Prague, Czech Republic
- 138 Faculty of Mathematics and Physics, Charles University, Prague, Czech Republic
- 139 Particle Physics Department, Rutherford Appleton Laboratory, Didcot, UK
- 140 IRFU, CEA, Université Paris-Saclay, Gif-sur-Yvette, France
- 141 Santa Cruz Institute for Particle Physics, University of California Santa Cruz, Santa Cruz, CA, USA
- 142 ^(a)Departamento de Física, Pontificia Universidad Católica de Chile, Santiago, Chile; ^(b)Department of Physics, Universidad Andres Bello, Santiago, Chile; ^(c)Instituto de Alta Investigación, Universidad de Tarapacá, Arica, Chile ; ^(d)Departamento de Física, Universidad Técnica Federico Santa María, Valparaíso, Chile
- 143 Universidade Federal de São João del Rei (UFSJ), São João del Rei, Brazil
- 144 Department of Physics, University of Washington, Seattle, WA, USA
- 145 Department of Physics and Astronomy, University of Sheffield, Sheffield, UK
- 146 Department of Physics, Shinshu University, Nagano, Japan
- 147 Department Physik, Universität Siegen, Siegen, Germany
- 148 Department of Physics, Simon Fraser University, Burnaby, BC, Canada
- 149 SLAC National Accelerator Laboratory, Stanford, CA, USA
- 150 Department of Physics, Royal Institute of Technology, Stockholm, Sweden
- 151 Departments of Physics and Astronomy, Stony Brook University, Stony Brook, NY, USA
- 152 Department of Physics and Astronomy, University of Sussex, Brighton, UK
- 153 School of Physics, University of Sydney, Sydney, Australia
- 154 Institute of Physics, Academia Sinica, Taipei, Taiwan
- 155 ^(a)E. Andronikashvili Institute of Physics, Iv. Javakhishvili Tbilisi State University, Tbilisi, Georgia; ^(b)High Energy Physics Institute, Tbilisi State University, Tbilisi, Georgia
- 156 Department of Physics, Technion, Israel Institute of Technology, Haifa, Israel
- 157 Raymond and Beverly Sackler School of Physics and Astronomy, Tel Aviv University, Tel Aviv, Israel
- 158 Department of Physics, Aristotle University of Thessaloniki, Thessaloniki, Greece
- 159 International Center for Elementary Particle Physics and Department of Physics, University of Tokyo, Tokyo, Japan
- 160 Department of Physics, Tokyo Institute of Technology, Tokyo, Japan
- 161 Tomsk State University, Tomsk, Russia
- 162 Department of Physics, University of Toronto, Toronto, ON, Canada
- 163 ^(a)TRIUMF, Vancouver, BC, Canada; ^(b)Department of Physics and Astronomy, York University, Toronto, ON, Canada
- 164 Division of Physics and Tomonaga Center for the History of the Universe, Faculty of Pure and Applied Sciences, University of Tsukuba, Tsukuba, Japan
- 165 Department of Physics and Astronomy, Tufts University, Medford, MA, USA
- 166 Department of Physics and Astronomy, University of California Irvine, Irvine, CA, USA
- 167 Department of Physics and Astronomy, University of Uppsala, Uppsala, Sweden
- 168 Department of Physics, University of Illinois, Urbana, IL, USA
- 169 Instituto de Física Corpuscular (IFIC), Centro Mixto Universidad de Valencia-CSIC, Valencia, Spain
- 170 Department of Physics, University of British Columbia, Vancouver, BC, Canada
- 171 Department of Physics and Astronomy, University of Victoria, Victoria, BC, Canada
- 172 Fakultät für Physik und Astronomie, Julius-Maximilians-Universität Würzburg, Würzburg, Germany
- 173 Department of Physics, University of Warwick, Coventry, UK
- 174 Waseda University, Tokyo, Japan
- 175 Department of Particle Physics and Astrophysics, Weizmann Institute of Science, Rehovot, Israel
- 176 Department of Physics, University of Wisconsin, Madison, WI, USA
- 177 Fakultät für Mathematik und Naturwissenschaften, Fachgruppe Physik, Bergische Universität Wuppertal, Wuppertal, Germany
- 178 Department of Physics, Yale University, New Haven, CT, USA
- ^a Also at Borough of Manhattan Community College, City University of New York, New York, NY, USA
- ^b Also at Bruno Kessler Foundation, Trento, Italy
- ^c Also at Center for High Energy Physics, Peking University, Beijing, China
- ^d Also at Centro Studi e Ricerche Enrico Fermi, Rome, Italy
- ^e Also at CERN, Geneva, Switzerland

- ^f Also at CPPM, Aix-Marseille Université, CNRS/IN2P3, Marseille, France
- ^g Also at Département de Physique Nucléaire et Corpusculaire, Université de Genève, Geneva, Switzerland
- ^h Also at Departament de Física de la Universitat Autònoma de Barcelona, Barcelona, Spain
- ⁱ Also at Department of Financial and Management Engineering, University of the Aegean, Chios, Greece
- ^j Also at Department of Physics and Astronomy, Michigan State University, East Lansing, MI, USA
- ^k Also at Department of Physics and Astronomy, University of Louisville, Louisville, KY, USA
- ^l Also at Department of Physics, Ben Gurion University of the Negev, Beersheba, Israel
- ^m Also at Department of Physics, California State University, East Bay, USA
- ⁿ Also at Department of Physics, California State University, Fresno, USA
- ^o Also at Department of Physics, California State University, Sacramento, USA
- ^p Also at Department of Physics, King's College London, London, UK
- ^q Also at Department of Physics, St. Petersburg State Polytechnical University, St. Petersburg, Russia
- ^r Also at Department of Physics, University of Fribourg, Fribourg, Switzerland
- ^s Also at Faculty of Physics, M.V. Lomonosov Moscow State University, Moscow, Russia
- ^t Also at Faculty of Physics, Sofia University, 'St. Kliment Ohridski', Sofia, Bulgaria
- ^u Also at Faculty of Engineering, Giresun University, Giresun, Turkey
- ^v Also at Graduate School of Science, Osaka University, Osaka, Japan
- ^w Also at Hellenic Open University, Patras, Greece
- ^x Also at Institutio Catalana de Recerca i Estudis Avancats, ICREA, Barcelona, Spain
- ^y Also at Institut für Experimentalphysik, Universität Hamburg, Hamburg, Germany
- ^z Also at Institute for Particle and Nuclear Physics, Wigner Research Centre for Physics, Budapest, Hungary
- ^{aa} Also at Institute of Particle Physics (IPP), Ottawa, Canada
- ^{ab} Also at Institute of Physics, Azerbaijan Academy of Sciences, Baku, Azerbaijan
- ^{ac} Also at Institute of Theoretical Physics, Ilia State University, Tbilisi, Georgia
- ^{ad} Also at Instituto de Física Teórica, IFT-UAM/CSIC, Madrid, Spain
- ^{ae} Also at Istanbul University, Dept. of Physics, Istanbul, Turkey
- ^{af} Also at Joint Institute for Nuclear Research, Dubna, Russia
- ^{ag} Also at Moscow Institute of Physics and Technology State University, Dolgoprudny, Russia
- ^{ah} Also at National Research Nuclear University MEPhI, Moscow, Russia
- ^{ai} Also at Physics Department, An-Najah National University, Nablus, Palestine
- ^{aj} Also at Physikalisches Institut, Albert-Ludwigs-Universität Freiburg, Freiburg, Germany
- ^{ak} Also at The City College of New York, New York, NY, USA
- ^{al} Also at TRIUMF, Vancouver, BC, Canada
- ^{am} Also at Università di Napoli Parthenope, Naples, Italy
- ^{an} Also at University of Chinese Academy of Sciences (UCAS), Beijing, China
- ^{ao} Also at Physics Department, Yeditepe University, Istanbul, Turkey
- * Deceased